DYNAMIC ANALYSIS OF A MATHEMATICAL MODEL FOR HEPATITIS B VIRUS INFECTION WITH IMMUNE RESPONSE AND DRUG THERAPIES

PENSIRI YOSYINGYONG

A Thesis Submitted to the Graduate School of Naresuan University
in Partial Fulfillment of the Requirements
for the Doctor of Philosophy Degree in Mathematics
March 2024

This thesis entitled "DYNAMIC ANALYSIS OF A MATHEMATICAL MODEL FOR HEPATITIS B VIRUS INFECTION WITH IMMUNE RESPONSE AND DRUG THERAPIES "

by Pensiri Yosyingyong

has been approved by the Graduate School as partial fulfillment of the requirements for the Doctor of Philosophy Degree in Mathematics of Naresuan University

Oral Defense Committee

..... Chair

(Associate Professor Sayan Kaennakham, Ph.D.)

..... Advisor

(Associate Professor Ratchada Viriyapong, Ph.D.)

..... Internal Examiner

(Associate Professor Supaporn Suksern, Ph.D.)

..... Internal Examiner

(Associate Professor Chairat Modnak, Ph.D.)

..... External Examiner

(Assistant Professor Benjawan Rodjanadid, Ph.D.)

Approved

.....

(Associate Professor Krongkarn Chootip, Ph.D.)

Dean of the Graduate School

13 MAR 2024

ACKNOWLEDGEMENT

I express my deepest appreciation to my thesis advisor, Associate Professor Dr.Ratchada Viriyapong, for invaluable guidance, perfect supervision, and motivation. Her teachings and insightful advice have been instrumental, and without her unwavering support, this thesis would not have reached its successful completion. Additionally, I express my gratitude to Dr.Elvin James Moore from the Department of Mathematics at King Mongkut's University of Technology North Bangkok for his guidance and support in the numerical analysis and English language aspects of the research work.

In addition, I express my sincere gratitude to the Development and Promotion of Science and Technology Talents Project (DPST) for their financial support throughout my graduate study. Their assistance plays a crucial role in the successful completion of my research.

Lastly, I express my heartfelt appreciation to my family, friends, and cats for their unwavering love, insightful suggestions, steadfast support, and constant encouragement throughout my Ph.D. journey. Their collective presence has been a source of strength and inspiration, enriching both my academic and personal experiences.

Pensiri Yosyingyong

Title	DYNAMIC ANALYSIS OF A MATHEMATICAL MODEL FOR HEPATITIS B VIRUS INFECTION WITH IMMUNE RESPONSE AND DRUG THERAPIES
Author	Pensiri Yosyingyong
Advisor	Associate Professor Ratchada Viriyapong, Ph.D.
Academic Paper	Ph.D. Dissertation in Mathematics, Naresuan University, 2023
Keywords	Delay model, Hepatitis B virus, Diffusive, Optimal control, Immune response, Cytotoxic T-lymphocyte (CTLs).

ABSTRACT

In this thesis, we have formulated three mathematical models to study Hepatitis B virus (HBV) infection. Our initial model explains hepatitis B virus (HBV) infection within hepatocytes, incorporating intracellular HBV DNA-containing capsids, antibodies, and cytotoxic T-lymphocytes (CTLs). Further, two drug therapies (blocking new infection and inhibiting viral production) are included in the model. This model accounts for two time delays: one for the productively infected hepatocytes and another for the antigenic stimulation that generates CTLs. We compute the basic reproduction number by the next-generation method and verify the positivity and boundedness of the solutions. Further, the stability analysis is performed. The numerical simulation results demonstrate that the method of preventing new infections give more efficient in reducing the number of infected hepatocytes in comparison to the method of inhibiting viral production. Moreover, both time delays exert an influence on the infection number and duration of infection, meaning that a long delay results in a more severe HBV infection. The second model is an optimal control model of HBV infection, we consider both drug types as control variables to seek a optimal control treatment strategy to reduce infection. We establish the existence, uniqueness, non-negativity, and boundedness of model solutions. Further, we derive the basic reproduction number for stability analysis of the infection-free equilibrium and conduct sensitivity analysis to identify the most influential parameters for disease control. Then,

optimal control and Pontryagin's Maximum Principle (PMP) are utilised to maximize concentrations of uninfected hepatocytes, antibodies, and cytotoxic T-lymphocytes at minimum cost. Our numerical results indicate that intracellular delays play a crucial role in decelerating the rate of infection. Furthermore, both optimal control strategies significantly reduce the concentrations of infected hepatocytes, intracellular HBV DNA-containing capsids, free viruses, antibodies, and cytotoxic T-lymphocytes. These control therapies prove to be effective measures for mitigating HBV infection. To enhance the realism of the model for hepatitis B virus (HBV) infection in the third model, we have broadened the scope of our research with spatial diffusion. We have considered the assumption that hepatocytes remain stationary, while viruses and cytotoxic T lymphocytes (CTLs) can move within the liver. In our analysis, we compute the basic reproduction number and the CTL immune response reproduction number, which are critical thresholds for equilibrium stability. We analyze both local and global stability for each equilibrium point. Our numerical results demonstrate that spatial diffusion does not significantly impact the global dynamics of HBV infection, however, it affects the speed of time for the free virus to reach its equilibrium state.

LIST OF CONTENTS

Chapter **Page**

LIST OF TABLES

Table **Page**

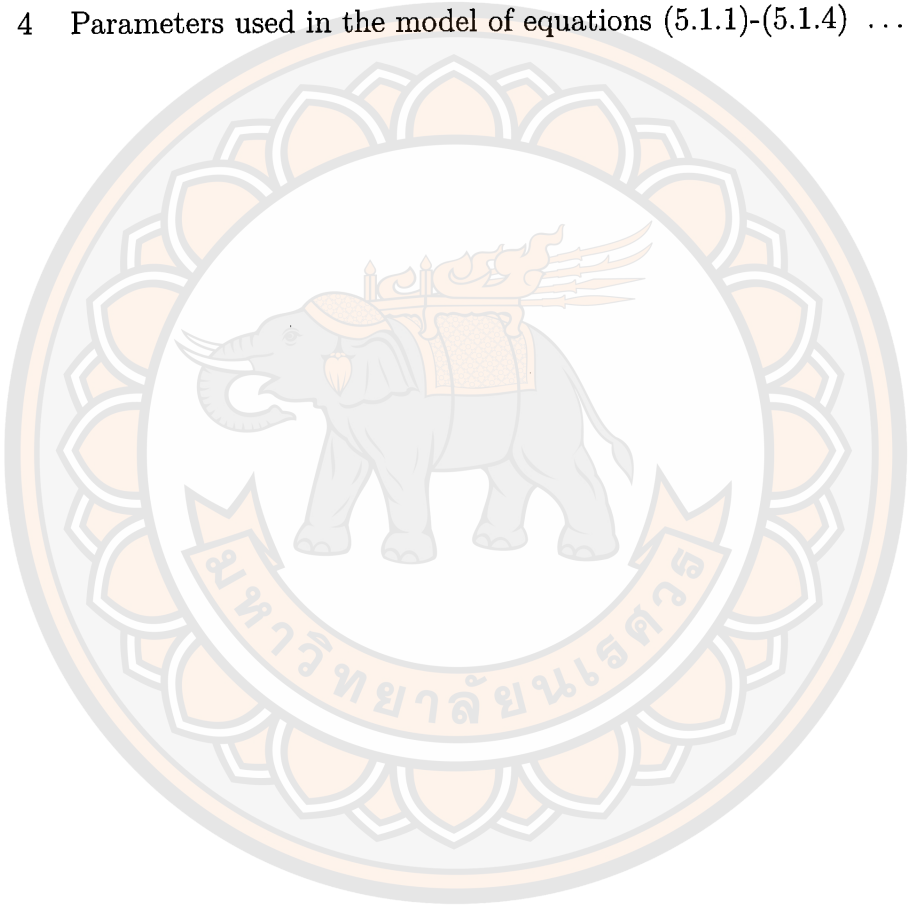

LIST OF FIGURES

Figure **Page**

CHAPTER I

INTRODUCTION

1.1 Background information

Hepatitis B virus (HBV) infection is a significant worldwide health issue. It is a liver infection caused by the hepatitis B virus. Generally, the infection is classified as either acute or chronic and can lead to more serious long-term complications, such as liver inflammation, cirrhosis or liver cancer [1]. According to World Health Organization (WHO) reports, HBV infection is predominantly reported in Africa, Southern Europe, Asia, and Latin America. In 2019, there were 298 million people living with chronic HBV infection, with 1.5 million new infections each year, resulting in approximately 820,000 deaths [2]. In extremely endemic areas, hepatitis B is most spread from mother to child at birth or transmitted through contact with the blood or other body fluids of an infected person. From the global epidemic situation, it is essential to have some effective prevention and treatment measures for hepatitis B infection.

HBV can replicate within hepatocytes without causing direct cell damage, this can be seen by those who are asymptomatic HBV carriers. Approximately 5-10% of HBV-infected adults may progress to a chronic state. The immune responses to HBV antigens are responsible for both disease pathogenesis and viral clearance. The adaptive immune response, particularly virus-specific cytotoxic T lymphocytes (CTLs), is important for eliminating infected hepatocytes and inhibiting viral replication [3–11]. Another part of the adaptive immune response affects antibodies produced by B cells, which neutralize virus particles and prevent cell reinfection [10, 12]. Furthermore, the body's immune response requires time from the viral attack to productive cell infection, emphasizing the importance of considering time delays in such circumstances [13–20]. Additionally, HBV infections have exhibited time delays in virus amplification and spreading throughout the liver [21].

According to WHO recommendations, the most effective prevention against hepatitis B virus infection is vaccination. Vaccination is suitable for all age groups and is administered to infants in some countries. The efficacy of vaccination in providing protection is estimated to last for at least 20 years [2]. People with chronic hepatitis B infection are often recommended to undergo medication to reduce the risk of disease progression, prevent transmission to others, and decrease the possibility of complications associated with hepatitis B. The two main types of drugs used for this purpose are standard PEGylated interferon (IFN-) and nucleoside analogues (NAs). IFN plays a role in suppressing viral protein synthesis, preventing viral infection of cells, and degrading viral mRNA. On the other hand, NAs function by elongating DNA to inhibit HBV replication [21–23]. In addition, in some cases, treatment may include antiviral medications such as lamivudine, adefovir, entecavir, and interferon alfa-2b injection [24]. However, these drugs often have a role to eliminate the viral covalently closed circular DNA (cccDNA), which is responsible for the persistence of HBV [25, 26]. Recently, alternative therapies have been proposed and are under clinical trials, focusing on viral gene silencing through the control of the RNA interference (RNAi) pathway. This approach aims to suppress HBV replication and may lead to the inactivation of cccDNA during chronic infection [25, 26]. However, the mentioned drugs can hardly clear the viral covalently closed circular DNA (cDNA) which is responsible for the persistence of HBV [25,26]. The alternative therapies have been recently in clinical trials and proposed, they are based on viral gene silencing by controlling the RNA interference (RNAi) pathway which suppresses HBV replication and may result in disabling cDNA during chronic infection [25,26]. With the fact mentioned above, although the HBV vaccines are widely used, safe and effective and some drugs could cure and greatly reduce the viral burden [27,28], there are limitations against chronic infection. Hence, HBV infection is still a major health problem around the world.

Mathematical models have been shown to greatly contribute to a better understanding of HBV infection. The work by Nowak et al. [29] is one of the earliest models using simple ordinary differential equations (ODEs) for the HBV infection of hepatocytes, consisting of three variables: the concentration of

uninfected hepatocytes, infected hepatocytes, and free virus particles. Several mathematical models have been proposed after that (e.g., [30–38]). Some of these models incorporate treatments or drug efficacy (e.g., [38–40]).

In some studies, the time delay has been considered. The models which involve the time delay from being infected to the release of free virus particles and free movement of virus particles in the liver are of the works by Gourley et al., 2008 [41]; Xie et al., 2010 [42]; Guo and Cai, 2011 [16]; Wang et al., 2008 [43]. Further, some studies involve the effect of humoral immunity or CTL-mediated cellular immunity e.g. the work by Yousfi et al., 2011 [34] and Fisicaro et al., 2009 [44]. Recently, Sun et al., 2017 [45] proposed a delay model with 6 variables including uninfected cells, exposed cells, infected cells, free viruses, CTLs and alanine aminotransferases (ALT), where the delay was put on the CTLs process.

In 2015, Manna and Chakrabarty, 2015 [46] proposed a model which included the intracellular HBV DNA-containing capsids and a delay in the production of the infected hepatocytes. Later on, Guo et al., 2018 [47] extended the work of Manna and Chakrabarty, 2015 [46] by adding a delay when the infected cells created new intracellular HBV DNA-containing capsids due to the penetration by a virus. Furthermore, Aniji et al., 2020 [48] proposed the model involves a delay as a time between antigenic stimulation and the production of CTLs including a delay during the decay of CTLs. With the important role of antibodies against HBV infection, Meskaf et al., 2017 [18], Sun et al., 2017 [45] and Allali et al., 2018 [49] added antibodies as a variable into their models. Among the above studies, in some studies drug therapies have also been applied in the models e.g the work by Hattaf et al., 2009 [50], Manna and Chakrabarty, 2018 [51] and in particular Danane et al., 2018 [20] had included the drug therapies in their delay model.

Optimal control theory has been applied to devise effective strategies for controlling the transmission or infection of diseases, including HBV infection. This approach enables the formulation of strategies that optimize specific objectives, such as minimizing the spread of the virus, improving treatment efficacy, or reducing the overall treatment cost. Some examples of optimal control of delayed HBV infection models are as follows. In 2016, Forde et al. [52]

proposed a model which included immune effector cells and a time delay that accounted for the lag between the antigen encounter and the effector cell expansion. In 2017, Meskef et al. [18] developed a model that included an adaptive immune response with CTLs, antibodies and a time delay for virus production in the infected cells after viral entry. In the same year, Sun and Liu [45] proposed a new time delay HBV model with an incubation period and time delay for both virus production and immune response after viral entry into healthy cells. Sun and Liu also added a time delay into a drug therapy term which represented the effect of the drugs in reducing the infection rate from free viruses. In 2018, Allali et al. [49] further improved the model of Meskef et al. [18] by modifying the growth term of both healthy and infected hepatocyte cells to be logistic growth. In 2018, Danane et al. [53] proposed a new optimal control delay model which included HBV DNA-containing capsids and a single time delay with the same meaning as in the above models. This model was further improved by Danane et al. [20] who added antibodies to the model. In 2019, Meskef [54] further extended the work of Danane and Allali [20] because during therapy a fraction of infected hepatocytes could be cured and could revert to healthy hepatocytes. In 2020, Khatun and Biswas [55] developed optimal control strategies for preventing HBV infection and reducing chronic liver cirrhosis incidence.

To become more realistic, many researchers have incorporated spatial diffusion into their models. One of the earliest models that considered this aspect is the work by Wang and Wang [56]. They investigated HBV infection and assumed that under ordinary conditions, both susceptible and infected hepatocytes cannot move, while viruses can freely diffuse within the liver. They assumed that the virus undergoes motion following Fickian diffusion. Later, several researchers extended Wang and Wang's model to further their understanding in a more biological way. In 2011, Shaoli et al. [57] proposed a model which included cytotoxic T lymphocyte (CTL) where they mainly considered the spatial mobility of the virus, whereas Manna et al. [58] considered the spatial mobility of intracellular HBV DNA-containing capsids and virus in their model. Elaiw et al. [59] in 2019 proposed a diffusive model that included viral capsids and two types of immune responses where the diffusion terms were added in viral capsids and HBV particles. In 2020, Huang

et al. [60] added two more variables to their model which were free antibody and virus-antibody complexes, where they added diffusion terms to reflect the spatial variations of free antibodies, virus-antibody complexes, and free virus. To the authors' knowledge, there is no research on the diffusive HBV infection model which includes the spatial mobility of CTL cells. However, a diffusive term of CTL cells is included in the HIV infection model, as demonstrated in the work by Elaiw et al. [61] and Alshamrani et al. [62]. Moreover, some studies have explored both diffusion and time delay for the HBV model, such as the works by Guo et al. [47], Xu et al. [63], Chan et al. [64], Zhang et al. [65], Hattaf et al. [66], Hattaf et al. [67], and Manna et al. [68].

In this thesis, we study the dynamics of HBV infection of hepatocytes by developing three mathematical models which are a time-delay model, an optimal control model of time-delay model and a diffusive model. The structure of the thesis is organized as follows. An introduction of hepatitis B virus infection and the scope of the study is in Chapter 1, whereas the theories and literature reviews are in Chapter 2. Chapter 3 is of our first model which we extend the work of Danane, J., et al. [20] by developing a model for HBV infection which incorporates the intracellular HBV DNA-containing capsids, CTLs and antibodies with a time delay from being attacked by the virus to being infected hepatocytes and a time delay in the antigenic stimulation generating CTLs. Further, two drug therapies, i.e., blocking new infection and inhibiting viral production have been applied in the model. In our analysis, we examine the positivity and boundary of the solution, investigated the basic reproduction number (R_0), and explore local and global stability. We support our results with numerical simulations and discussions. In Chapter 4, we report our second model which is an optimal control model of two-time delays, namely a virus production delay and an antigenic stimulation generating CTLs delay. The two controls in the model are drug therapy in blocking new infections and drug therapy in inhibiting viral production. Additionally, we introduce a treatment process developed to facilitate the recovery of infected cells, transitioning them from the infected state to the uninfected state. This inclusion improves the model's realism by accounting for the potential recovery and restoration of previously

infected cells. This model has been analyzed using sensitivity analysis and Pontryagin's Maximum Principle to identify suitable strategies for controlling hepatitis B virus infection. Chapter 5 shows our third model which is diffusive model, we include random mobility for both viruses and CTL cells in our model. We also assume that their motion follows the Fickian diffusion. We modify the work of Shaoli et al. [57] by adding the spatial mobility for CTL immune response, this is because we take into account that immune cells diffuse in the organs under the condition of bounded resources and space. We compute the basic reproduction number (R_0) and use it as a criterion for analyzing the local and global stability of this model. Additionally, we perform a numerical analysis and provide a discussion. Finally, we conclude this thesis by summarizing our work in Chapter 6.

1.2 Research objectives

1. To formulate and analyze time delay model of hepatitis B virus infection.
2. To formulate and analyze optimal control of time delay model of hepatitis B virus infection.
3. To formulate and analyze a diffusive model of hepatitis B virus infection.

1.3 Usefulness of the research

1. To obtain and understand time delay model of hepatitis B virus infection.
2. To obtain and understand optimal control of time delay model of hepatitis B virus infection.
3. To obtain and understand a diffusive model of hepatitis B virus infection.

CHAPTER II

PRELIMIARIES

2.1 Relevant theories

2.1.1 Delay-differential equations (DDEs)

Delay-differential equations (DDEs) are a type of dynamical system that includes delays in the evolution of the system's variables. When concerning the endemic state within the framework of infectious disease modeling, Delay Differential Equations (DDEs) can be formulated to analyze the dynamics of the disease. These equations study delays in critical processes such as transmission, incubation, or recovery. Here is a general formulation of DDEs for an infectious disease model. Let's consider a population divided into different compartments:
- $S(t)$: Susceptible individuals at time t,
- $I(t)$: Infected individuals at time t,
- $R(t)$: Recovered individuals at time t.

The DDEs for an infectious disease model can be expressed as follows:

$$\frac{dS(t)}{dt} = -\beta I(t-\tau)S(t), \tag{2.1.1}$$

$$\frac{dI(t)}{dt} = \beta I(t-\tau)S(t) - \gamma I(t), \tag{2.1.2}$$

$$\frac{dR(t)}{dt} = \gamma I(t). \tag{2.1.3}$$

The equations represent the rates of change of the susceptible, infected, and recovered individuals over time. Relevant parameters include β as the rate of infection, γ as the rate of recovery from infection, and τ as the time delay representing the incubation period or the time it takes for an infected individual to become infectious. The delay term τ allows for a more realistic representation of the disease dynamics, considering the time lag between infection and the potential to infect others.

By linearizing a DDE system around its equilibrium point, we can derive the

characteristic equation. This involves examining the eigenvalues of the resulting linear system. Analyzing the characteristic equation is crucial for understanding the stability and dynamics of the system, offering valuable insights into its behavior. Let's denote the vector of state variables as $X(t) = [S(t), I(t), R(t)]^T$. The linearized system is given by:

$$\frac{dX(t)}{dt} = AX(t) - e^{-\lambda\tau}BX(t-\tau), \tag{2.1.4}$$

where

$$A = \begin{bmatrix} -\beta I(t) & 0 & 0 \\ \beta I(t) & -\gamma & 0 \\ 0 & \gamma & 0 \end{bmatrix},$$

and

$$B = \begin{bmatrix} 0 & \beta S(t) & 0 \\ 0 & -\beta S(t) & 0 \\ 0 & 0 & 0 \end{bmatrix}.$$

The characteristic equation is obtained by finding the eigenvalues of the matrix $\lambda I - A + e^{-\lambda\tau}B$, where I is the identity matrix. Therefore, the characteristic equation is:

$$\det(\lambda I - A + e^{-\lambda\tau}B) = 0.$$

This equation, when solved for λ, gives the characteristic roots (eigenvalues) of the linearized system, and the stability of the equilibrium point can be analyzed based on the real parts of these eigenvalues. If all eigenvalues of the system have negative real parts, then the system will be stable. Conversely, if any eigenvalue has a positive real part, then the system will be unstable.

2.1.2 The stability of continuous systems by Routh-Hurwitz criteria

With more than two equations in the system of ordinary differential equations, it will take longer time or be more difficult to find eigenvalues. Routh-Hurwitz criteria is the criteria to guarantee all eigenvalues of Jacobian matrix at equilibrium point have negative real parts. Therefore, a Routh-Hurwitz criterion is necessary to ease this difficulty [69].

Given the characteristic equation of Jacobian matrix at steady state as

$$P(\lambda) = \lambda^n + a_1\lambda^{n-1} + \cdots + a_{n-1}\lambda + a_n,$$

where the coefficients a_i are real constants, $i = 1, 2, ..., n$.

For characteristic equation of degree $n = 2, 3, 4$ and 5, the Routh-Hurwitz criteria are summarized below.

Routh-Hurwitz criteria for $n = 2, 3, 4$ and 5.

$n = 2$; $a_1 > 0$ and $a_2 > 0$

$n = 3$; $a_1 > 0, a_3 > 0$ and $a_1a_2 > a_3$

$n = 4$; $a_1 > 0, a_3 > 0, a_4 > 0$ and $a_1a_2a_3 > a_3^2 + a_1^2a_4$

$n = 5$; $a_1a_2a_3 > a_3^2 + a_1^2a_4$ and

$(a_1a_4 - a_5)(a_1a_2a_3 - a_3^2 - a_1^2a_4) > a_5(a_1a_2 - a_3)^2 + a_1a_5^2$.

2.1.3 The stability of continuous systems with a single time delay

In this thesis, we consider the stability switches of a high dimensional [70–72], linear dynamic system with a single time delay governed by the following characteristic equation

$$D(\lambda, \tau) = P(\lambda) + Q(\lambda)e^{-\lambda\tau} = 0, \tag{2.1.5}$$

where $\tau \geq 0$ is the time delay, $P(\lambda)$ and $Q(\lambda)$ are two polynomials of real coefficients with $\deg(P) = n > \deg(Q)$. Without loss of generality, we assume that both polynomials $P(\lambda)$ and $Q(\lambda)$ have a purely imaginary root $\lambda = i\omega$ $(\omega > 0)$. So, we have $D(i\omega, \tau) = 0$, let

$$\begin{aligned} P_R(\omega) \equiv Re[P(i\omega)], P_I(\omega) \equiv Im[P(i\omega)], \\ Q_R(\omega) \equiv Re[Q(i\omega)], Q_I(\omega) \equiv Im[Q(i\omega)], \end{aligned} \tag{2.1.6}$$

where $P_R(\omega)$ and $Q_R(\omega)$ are even functions, whereas $P_I(\omega)$ and $Q_I(\omega)$ are odd functions. Hence, the equivalent form of $D(i\omega, \tau) = 0$ reads

$$\begin{cases} Q_R(\omega)\cos\omega\tau + Q_I(\omega\tau)\sin\omega\tau = -P_R(\omega), \\ Q_I(\omega)\cos\omega\tau - Q_R(\omega\tau)\sin\omega\tau = -P_I(\omega). \end{cases} \tag{2.1.7}$$

In order for Eq.(2.1.5) to have a pair of pure imaginary roots $\pm i\omega$ for $\tau \geq 0$, it is necessary that $|P(i\omega)| = |Q(i\omega)|$, that is,

$$P_R^2(\omega) + P_I^2(\omega) - [Q_R^2(\omega) + Q_I^2(\omega)] = 0 \tag{2.1.8}$$

has a positive root ω. The left side of above equation can simply be recast in an explicit form

$$F(\omega) \equiv \omega^{2n} + b_1\omega^{2(n-1)} + b_2\omega^{2(n-2)} + ... + b_{n-1}\omega^2 + b_n. \tag{2.1.9}$$

Thus, we have the following theorem.

Assume that Eq.(2.1.5) has no pure imaginary characteristic roots $i\omega$ such that $Q(i\omega) = 0$.

Theorem 2.1.1. *If the polynomial $F(\omega)$ has no positive root, the system is delay independent stable or unstable for any given time delay, depending on whether or not the system free of time delay is stable.*

Theorem 2.1.2. *Suppose that $F(\omega)$ has only one simple positive root ω. If the system free of time delay is asymptotically stable, there exists exactly one critical time delay $\tau_0 > 0$ such that the system remains asymptotically stable when $\tau \in [0, \tau_0)$, and becomes unstable when $\tau \geq \tau_0$. If the system is unstable for $\tau = 0$, it is unstable for an arbitrary time delay τ.*

Theorem 2.1.3. *If $F(\omega)$ has at least two positive roots $\omega_1 > \omega_2 > ... > \omega_p > 0$ and the roots are simple, a finite number of stability switches may occur as the time delay τ increases from zero to the positive infinity, and the system becomes unstable at last.*

2.1.4 Basic reproduction number (R_0)

Definition 2.1.4. The basic reproduction number, denoted by R_0, is defined as the average number of secondary infections that occurs when one infective is introduced into a completely susceptible population.

If $R_0 < 1$, then the disease cannot invade the population and the infection will die out over a period of time. The amount of time this will take generally depends on how small R_0 is. If $R_0 > 1$, then an invasion is possible and infection can spread through the population. Generally, the larger the value of R_0, the more severe, and possibly widespread, the epidemic will be.

2.1.4.1 Computing R_0 by the next generation method

For the next generation method [73], R_0 is defined as the spectral radius of the next operation operator. The formation of the operator involves determining two compartments, infected and non-infected from the model. In this section, we outline the steps needed to find the next generation operator in matrix notation (assuming only finitely many types).

Let us assume that there are n compartments of which m are infected. We define the vector $\bar{x} = x_i, i = 1, 2, ..., n$, where x_i denotes the number or proportion of individuals in the i th compartment. Let $F_i(\bar{x})$ be the rate of appearance of new infections in compartment i and $V_i(\bar{x}) = V_i^-(\bar{x}) - V_i^+(\bar{x})$, where V_i^+ is the rate of transfer of individuals into compartment i by all other means and V_i^- is the rate of transfer of individuals out of the i th compartment. The difference $F_i(\bar{x}) - V_i(\bar{x})$, gives the rate of change of x_i. Note that F_i should include only infectious that are newly arising, but does not include terms which describe the transfer of infectious individuals from one infected compartment to another.

Assuming that F_i and V_i meet the conditions, we can form the next generation matrix (operator) FV^{-1} from matrices of partial derivatives of F_i and V_i. Specifically,

$$F = \left[\frac{\partial F_i(x_0)}{\partial x_j} \right], V = \left[\frac{\partial V_i(x_0)}{\partial x_j} \right],$$

where $i, j = 1, 2, ..., m$ and where x_0 is the disease-free equilibrium point. The entries of FV^{-1} give the rate at which infected individuals in x_j produce new infectious in x_i, times the average length of time an individual spends in a single visit to compartment j. R_0 is given by the spectral radius (dominant eigenvalue) of the matrix FV^{-1}.

2.1.5 Sensitivity analysis (SA) of the basic reproduction number with respect to the model parameters

The basic reproduction number, R_0 serves as a critical indicator for understanding the potential spread of infectious diseases within a population. It measures the typical amount of new infections caused by an infected person entering a vulnerable group without immunity. If $R_0 < 1$, it signifies that an infected individual typically generates fewer infections during its infectious phase, which could lead to the infection dying out. Conversely, if $R_0 > 1$, each infected individual often produces more than one new infection, indicating the potential for the infection to spread throughout the population. To assess the impact of various factors on disease transmission and prevalence, a sensitivity analysis (SA) of R_0 was conducted concerning model parameters. This analysis helps identify the relative importance of different factors contributing to disease transmission. The goal is to inform intervention strategies and control measures, ultimately aiding in the reduction of disease transmission.

We use the method of normalized forward sensitivity index (see, e.g., Samsuzzoha et al. [74] and Ngoteya et al. [75]), where the normalized forward sensitivity index of the basic reproduction number R_0 with respect to a parameter value h is given by :

$$S_h^{R_0} = \frac{h}{R_0}\frac{\partial R_0}{\partial h} = h\frac{\partial \log(R_0)}{\partial h}. \tag{2.1.10}$$

2.1.6 Optimal control

Optimal control is an effective method for solving problems in various domains, aiming for the most suitable control strategy. In this research, we utilized the optimal control problems with time-delay. We have followed the Pontryagin maximum principle, as studied in various books (see, e.g., [76–78]). The state of dynamical system is determined by the following delay differential equation system with time-delay

$$\frac{dx}{dt} = g(x(t), x(t-\tau), u(t)), \tag{2.1.11}$$

where $x(t)$ is a state of dynamical system, $u(t)$ is a control of dynamical system, τ is a constant time-delay.

The primary objective of optimal control problems is to maximize a specified performance criterion, typically expressed as an objective function. We look at the special case of a fixed-time discrete time-delay optimal contol proplem with $t \in [t_0, T], t_0, T$ fixed. We define a set of discrete time points on the interval $[t_0, T]$ by $t_{j+1} = t_j + h, j = 0, 1, 2, \ldots, N, h = \frac{T-t_0}{N}$, where N is number of interval. Then $t_0 = t_0, t_N = T$ and we define $x_0 = x(t_0), x_N = x(T)$. We assume a time delay $\tau = Mh$, where M is a positive integer. We consider the following problem

$$J(u_{t_j}) = \max_{u \in R^m} \int_{t_0}^{T} f(t_j, x(t_j), x(t_{j-M}), u(t_j))dt, \qquad (2.1.12)$$
$$u_{min}(t_j) \leq u(t_j) \leq u_{max}(t_j)$$

subject to state equations:

$$x(t_{j+1}) = g(t_j, x(t_j), x(t_{j-M}), u(t_j)), x(t_j) \geq 0, x(t_j) \in \mathbb{R}^n,$$
$$\text{and } x(t_{-r}), r = 0, 1, 2, ..., M, \text{ given, } x_N \text{ free.} \qquad (2.1.13)$$

Next, we introduce a costate vector $\lambda(t_j) \in \mathbb{R}^n$ and a Hamiltonian function defined by:

$$H(t_j, x(t_j), x(t_{j-M}), u(t_j), \lambda(t_{j+1})) = f_0(t_j, x(t_j), x(t_{j-M}), u(t_j)) + \lambda(t_{j+1})^T g(t_j, x(t_j), x(t_{j-M}), u(t_j)). \qquad (2.1.14)$$

We are maximizing H with respect to u at u^*, and the above conditions can be written in terms of the Hamiltonian:

$$\frac{\partial H}{\partial u} = 0 \text{ at } \Rightarrow f_u + \lambda g_u = 0 \text{ (optimality condition)},$$
$$\lambda' = -\frac{\partial H}{\partial x} \Rightarrow \lambda' = -(f_x + \lambda g_x) \ (adjointequation),$$
$$\lambda(T) = 0 \text{ (transversality condition)}.$$

We can view our optimal control problem as having two unknowns, u^* and x^*, at the start. We have introduced an adjoint variable λ, which is similar to a Lagrange multiplier. It attaches the differential equation information onto the maximization of the objective functional. The following is an outline of how this theory can be applied to solve the simplest problems.

Summary of Pontryagin Maximum Principle for Discrete Time-Delay Problems

1. Formulation of the Hamiltonian:
   - Begin by constructing the Hamiltonian, denoted as H, for the given discrete time-delay problem. The Hamiltonian is typically a function of the state variable x, the control variable u, and the costate variable λ.

2. Adjoint Differential Equation and Boundary Conditions:
   - Derive the adjoint differential equation along with the associated transversality boundary condition and the optimality condition. This introduces three unknowns: the optimal control u^*, the optimal state x^*, and the costate variable λ.

3. Solving for u^* interms of x^* and λ:
   - Solving the optimality equation $H_u = 0$ to express u^* as a function of x^* and λ.

4. Solving Differential Equations for x^* and λ:
   - Solve the two coupled differential equations for x^* and λ, incorporating two boundary conditions. Substitute the expression for u^* obtained in the previous step into these differential equations.

5. Optimal Control Determination:
   - Once x^* and λ are found, solve for the optimal control u^*. This completes the determination of the optimal state, adjoint, and control for the given discrete time-delay problem.

This systematic approach helps in navigating through the steps of the Pontryagin Maximum Principle, providing a structured methodology for solving discrete time-delay optimal control problems.

2.1.7 The diffusion equations

The one-dimensional diffusion equation is linear second order partial differential equation

$$u_t - Du_{xx} = f \tag{2.1.15}$$

where $u = u(x,t)$, x is a real space variable, t a time variable and D a positive constant, celled diffusion coefficient.
In space dimension $n > 1$, that is when $x \in \mathbb{R}^n$, the diffusion equation reads

$$u_t - D\Delta u = f \tag{2.1.16}$$

where Δ denotes the Laplace operator:

$$\Delta = \sum_{k=1}^{n} \frac{\partial^2}{\partial x_k^2}. \tag{2.1.17}$$

Model in population genetics, combustion and population dynamics lead to non-linear diffusion equations

$$u_t = D\Delta u + f(u) \tag{2.1.18}$$

2.1.8 The stability analysis of diffusion system

Let $0 = \mu_0 < \mu_1 < \cdots < \mu_n < \ldots$ be the complete set of eigenvalues of operator $-\Delta$ with homogeneous Neumann boundary condition.

Definition 2.1.5. The stability of a diffusion system at its homogeneous equilibrium state can be studied by calculating the eigenvalues of

$$\det(J - \widetilde{D}\mu_i I - \lambda I) = 0 \tag{2.1.19}$$

where J is the Jacobian matrix of the system, $\widetilde{D}$ is the diagonal matrix made of diffusion constants, μ is the eigenvalues of the boundary value problem, and λ is the eigenvalues of system.

Next, we will verify that all eigenvalues have negative real parts, as indicated in section 2.1.2 Routh-Hurwitz criteria.

2.1.9 Global stability of the equilibrium point

2.1.9.1 Lyapunov stability theorem

Theorem 2.1.6. *Let E be an open subset of $\mathbb{R}^n$ be a domain containing x_0. Suppose $f \in C^1(E)$ and that $f(x_0) = 0$. Suppose further that there exists a real valued function $V \in C^1(E)$ satisfying $V(x_0) = 0$ and $V(x) > 0$ if $x \neq x_0$. If*

1. *$\dot{V}(x) \leq 0$ for all $x \in E, x_0$ is globally stable,*
2. *$\dot{V}(x) < 0$ for all $x \in E \backslash x_0$ is globally asymptotically stable,*
3. *$\dot{V}(x) > 0$ for all $x \in E \backslash x_0$ is globally unstable.*

2.2 Literature review

In 2018, we presented a nonlinear mathematical model as part of our master's degree research work, studying the dynamics of hepatitis B virus (HBV) infection within hepatocytes [38]. This model explores the relationships among the virus, the immune response, and the impact of drug therapy. It comprises of four components: uninfected hepatocytes $x(t)$, infected hepatocytes $y(t)$, free viruses $v(t)$, and cytotoxic T lymphocyte (CTL) cells $z(t)$. Furthermore, the model incorporates the adaptive immune response and introduces two treatment regimens. These treatments specifically manage the efficacy of drug therapy in blocking new infections and inhibiting viral production. The flowchart of our model in 2018 is shown in Figure 1.

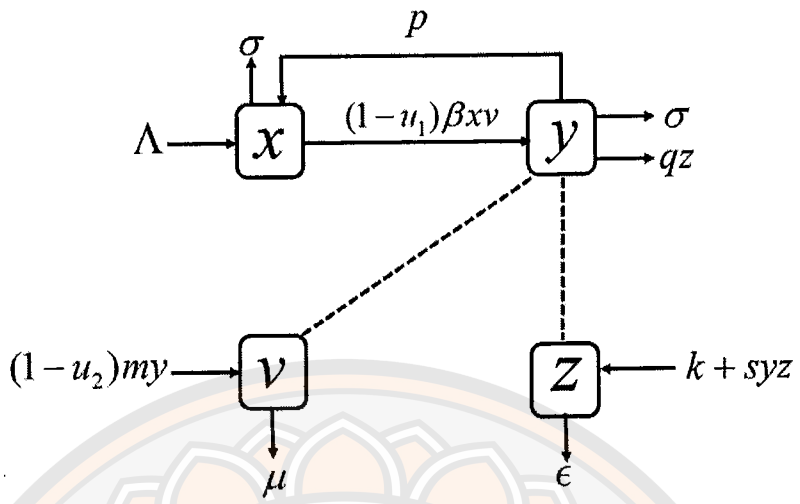

Figure 1 The flow chart of the HBV infection with immune response and drug therapy [38].

We proposed the following system of differential equations:

$$\frac{dx}{dt} = \Lambda - (1-u_1)\beta x(t)v(t) + py(t) - \sigma x(t) \tag{2.2.1}$$

$$\frac{dy}{dt} = (1-u_1)\beta x(t)v(t) - py(t) - \sigma y(t) - qy(t)z(t) \tag{2.2.2}$$

$$\frac{dv}{dt} = (1-u_2)my(t) - \mu v(t) \tag{2.2.3}$$

$$\frac{dz}{dt} = k + sy(t)z(t) - \epsilon z(t), \tag{2.2.4}$$

with initial condition

$$x(0) \geq 0, y(0) \geq 0, v(0) \geq 0, z(0) \geq 0. \tag{2.2.5}$$

Notation:

- Λ is the constant production rate of the uninfected hepatocytes.
- β is the rate of infection of uninfected hepatocytes by free virus.
- p is the cure rate of infected hepatocytes by non-cytolytic cure process.
- σ is the natural death rate of hepatocytes.
- q is the death rate of infected hepatocytes due to immune-mediated killing.
- m is the rate of free virus particles production by infected hepatocytes.

μ is the death rate of free virus.

k is the production rate of CTL cells.

s is the activation rate of CTL cells by infected hepatocytes.

ϵ is the death rate of CTL cells.

u_1 is the efficiency of drug therapy in blocking new infection.

u_2 is the efficiency of drug therapy in inhibiting viral production.

At the Doctor of Philosophy level, we have studied interesting research about time delays and the diffusion of HBV infection incorporating immune response and drug therapies. This is to enhance the above model and achieve a more profound and realistic understanding of the field of biology and/or biomedical science.

2.2.1 The HBV model with a time delay

In 2007, Gourley et al. [41] studied, formulated and investigated the global dynamics of a simple model of hepatitis B virus using delay differential equations. Firstly, the model employs a more realistic standard incidence function, providing a more accurate representation of the infection dynamics. Secondly, the model explicitly integrates a time delay in virus production, acknowledging the temporal aspect of the viral life cycle. They analyzed the system's stability, both locally and globally, using theoretical methods and confirming those insights through practical numerical simulations. The flow chart of this model is shown in Figure 2.

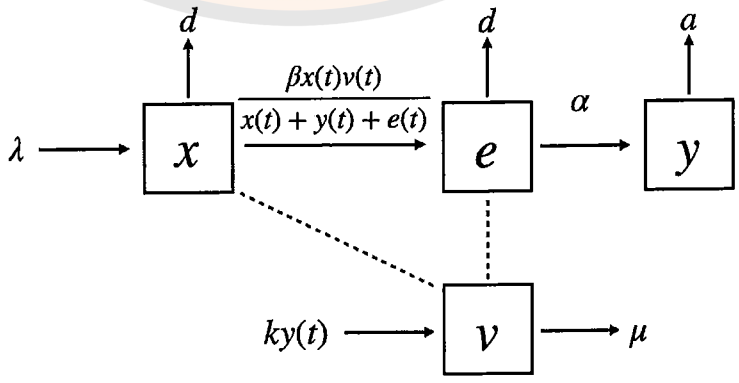

Figure 2 The flow chart of a delayed differential equation model of HBV infection [41].

They proposed the following one-delay model:

$$\frac{dx}{dt} = \lambda - dx(t) - \frac{\beta x(t)v(t)}{x(t)+y(t)+e(t)}, \tag{2.2.6}$$

$$\frac{de}{dt} = \frac{\beta x(t)v(t)}{x(t)+y(t)+e(t)} - \frac{\beta e^{-d\tau}v(t-\tau)x(t-\tau)}{x(t-\tau)+y(t-\tau)+e(t-\tau)} - de(t), \tag{2.2.7}$$

$$\frac{dy}{dt} = \frac{\beta e^{-}d\tau v(t-\tau)x(t-\tau)}{x(t-\tau)+y(t-\tau)+e(t-\tau)} - ay(t), \tag{2.2.8}$$

$$\frac{dv}{dt} = ky(t) - \mu v(t), \tag{2.2.9}$$

where x, e, y, and v denote the number of uninfected cells, exposed cells, infected cells, and free virions, respectively. The parameter τ represents the time delay for virion production.

Notation:

λ is the production rate of liver cell.

d is the death rate of liver cell.

β is the maximum infection rate.

a is the death rate of infected liver cells.

k is the production rate of virion.

μ is the death rate of virion.

In 2010, Xie et al. [42] studied the dynamic characteristics of a viral infection model considering a delayed immune response. The research emphasizes the crucial role of the immune response in either eliminating or controlling diseases once the human body is infected by a virus. The study specifically explores the impact of time delay on the stability of system equilibria. The results contribute to a deeper understanding of the dynamics of viral infections with delayed immune responses. The findings not only enhance theoretical insights into stability conditions but also provide practical implications for explaining the complexities observed in the immune states of infected individuals. The flow chart of this model is shown in Figure 3.

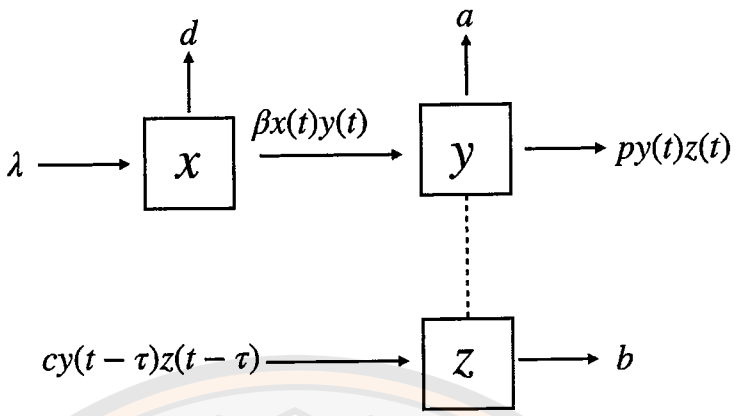

Figure 3 The flow chart of a viral infection model with delayed immune response [42].

They proposed the following one-delay model:

$$\frac{dx}{dt} = \lambda - dx(t) - \beta x(t)y(t), \tag{2.2.10}$$

$$\frac{dy}{dt} = \beta x(t)y(t) - ay(t) - py(t)z(t), \tag{2.2.11}$$

$$\frac{dz}{dt} = cy(t-\tau)z(t-\tau) - bz(t), \tag{2.2.12}$$

where x, y, and z denote the number of susceptible cells, infected cells, and CTLs, respectively. The parameter τ represents the time delay of CTL response.
Notation:

λ is the production rate of susceptible cell.

d is the death rate of susceptible cells.

β is the infection rate by the virus.

a is the death rate of infected cells.

p is the death rate of infected cells are killed by the CTL response.

c is the expansion rate of CTLs in response to viral antigen derived from infected cells.

b is the decay rate of CTLs.

In 2016, Forde et al. [52] studied and determined an optimal control strategy by developing a system of delay differential equations of the immune response caused by HBV infection. This mathematical approach helps investigate the optimal interplay between the virological and immunomodulatory

effects of therapy. The control variables include the management of viremia (virus presence in the blood) and the administration of minimal drug dosages over a short period. Numerical results show that the high drug levels that induce immune modulation rather than suppression of virological factors are essential for the clearance of hepatitis B virus. The flow chart of this model is shown in Figure 4, where $\Lambda_T = rT\left(1 - \frac{T+I+R}{K}\right), \Lambda_I = rI\left(1 - \frac{T+I+R}{K}\right), \Lambda_R = rT\left(1 - \frac{T+I+R}{K}\right), d_2 = ((1+a_1\epsilon)\mu + \rho)IE, \pi_1 = \pi(1 - fa_2\epsilon - (1-f)b_2\eta)I.$

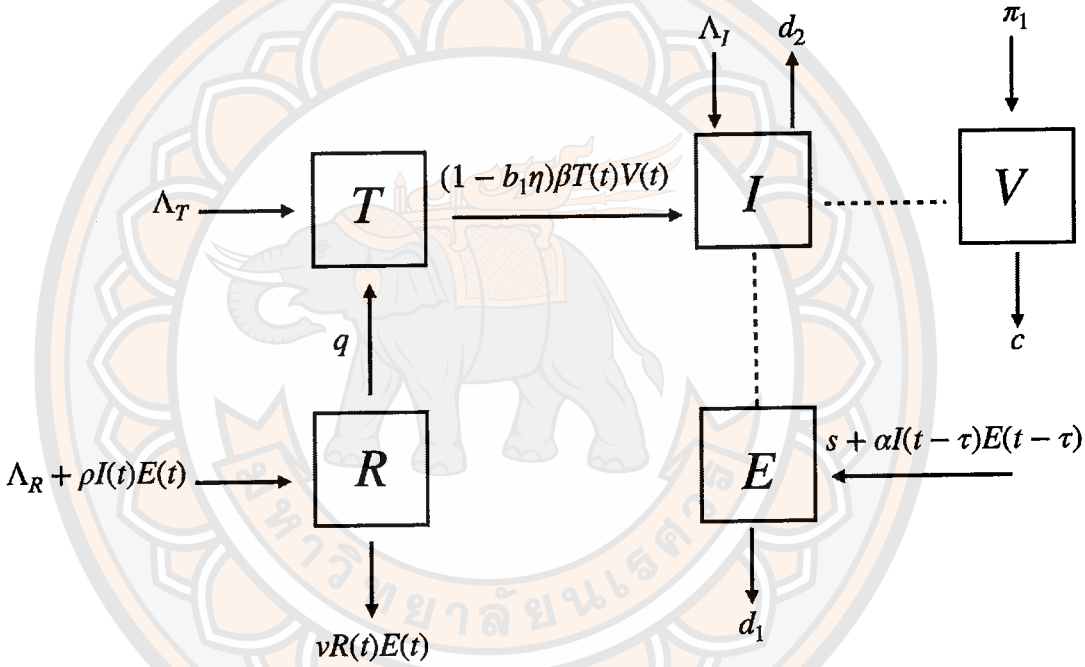

Figure 4 The flow chart of optimal control of drug therapy in a hepatitis B model [52].

They proposed the following one-delay model:

$$\frac{dT}{dt} = rT\left(1 - \frac{T+I+R}{K}\right) - (1-b_1\eta)\beta TV + qR(t), \tag{2.2.13}$$

$$\frac{dI}{dt} = rI\left(1 - \frac{T+I+R}{K}\right) + (1-b_1\eta)\beta TV - ((1+a_1\epsilon)\mu + \rho)IE, \tag{2.2.14}$$

$$\frac{dV}{dt} = \pi(1 - fa_2\epsilon - (1-f)b_2\eta)I - cV, \tag{2.2.15}$$

$$\frac{dE}{dt} = s + \alpha I(t-\tau)E(t-\tau) - d(1-a_3\epsilon)E, \tag{2.2.16}$$

$$\frac{dR}{dt} = \rho IE + rR\left(1 - \frac{T+I+R}{K}\right) - qR - vRE, \tag{2.2.17}$$

where T, I, V, E and R denote the number of uninfected hepatocytes, infected hepatocytes, free virus, immune effector, and refractory hepatocytes, respectively. The parameter τ represents the time delay of the lag between antigen encounter and effector cell expansion.

Notation:

r	is the rate of hepatocytes maximum proliferation.
K	is the hepatocytes carrying capacity.
β	is the infectivity rate constant.
μ	is the death rate of infected cells are killed the effector cell.
υ	is the death rate of refractory cells are killed by the effector cell.
ρ	is the cure rate with the non-cytolytic process.
q	is the rate of waning of refractory cell immunity.
π	is the production rate of free virus.
c	is the clearance rate of free virus.
s	is the production rate of effector cell.
α	is the rate of immune effector expansion.
d	is the clearance rate of the effector cell.
ϵ	is the efficacy of IFN-α.
a_i	are scalar parameters representing the strength of the corresponding effect of interferon.
η	is the efficacy of NAs.
b_i	are scalar parameters representing the relative strength of the corresponding effect of NAs.
f	is the relative contribution of interferon-α.
$1-f$	is the relative contribution of NAs.

In 2017, Manna, K., and Chakrabarty, S.P. [19] formulated a mathematical model to describe the dynamics of hepatitis B virus (HBV) infection. This model contains the interaction between infected hepatocytes, the quantity of intracellular HBV DNA-containing capsids, and the virions. They considered the time delay, denoted as τ, signifying the duration between the instance when uninfected hepatocytes are initially infected by HBV and

productively infected hepatocytes. The flow chart of this model is shown in Figure 5.

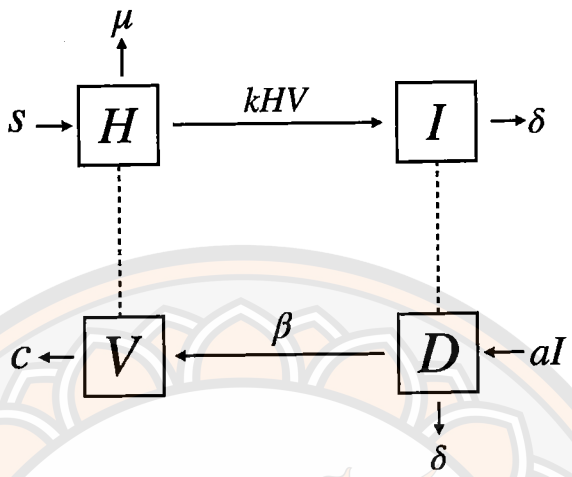

Figure 5 The flow chart of the hepatitis B viral infection model with capsid and time delay [19].

They proposed the following one-delay model:

$$\frac{dH}{dt} = s - kH(t)V(t) - \mu H(t), \tag{2.2.18}$$

$$\frac{dI}{dt} = kH(t-\tau)V(t-\tau) - \delta I(t), \tag{2.2.19}$$

$$\frac{dD}{dt} = aI(t) - \beta D(t) - \delta D(t), \tag{2.2.20}$$

$$\frac{dV}{dt} = \beta D(t) - cV(t), \tag{2.2.21}$$

where H, I, D, and V denote the number of uninfected hepatocytes, infected hepatocytes, intracellular HBV DNA-containing capsids, and hepatitis B virions, respectively. The parameter τ represents the time delay during the process of infection of uninfected hepatocytes to productively infected hepatocytes.

Notation:

s is the production at a constant rate of the uninfected hepatocytes.

μ is the death rate of uninfected hepatocytes.

k is the conversion rate of uninfected to infected hepatocytes by HBV infection.

δ is the clearance rate of infected hepatocytes and capsids.

a is the conversion rate to intracellular HBV DNA-containing capsids by infected hepatocytes.

β is the replication rate of viral by capsids.

c is the natural death rate for the HBV.

In 2017, Sun, D., and Liu, F. [45] presented a hepatitis B virus (HBV) model that integrates immune responses, specifically cytotoxic T lymphocyte (CTL) and alanine aminotransferases (ALT), targeting both infected cells and viruses. This model also incorporates a time delay parameter, signifying the period during which the immune system effectively eliminates viruses. Furthermore, the model includes an exposed state and accounts for the proliferation of hepatocytes. The flow chart of this model is shown in Figure 6.

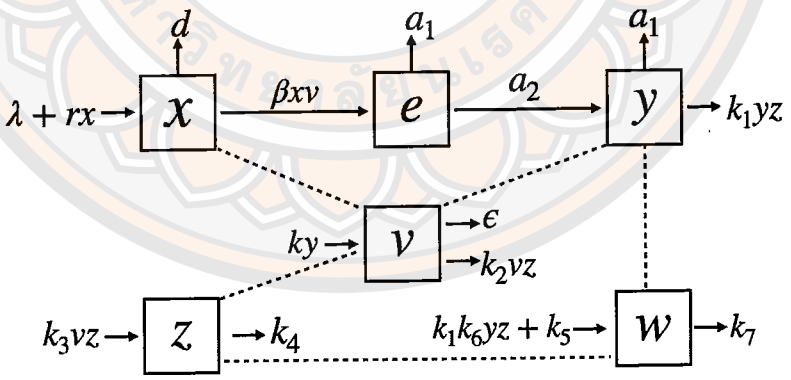

Figure 6 The flow chart of a new delayed HBV model with exposed state and immune response to infected cells and viruses [45].

Their model can be written in the system of delay equation as below:

$$\frac{dx}{dt} = \lambda + rx(t) - dx(t) - \beta v(t)x(t), \tag{2.2.22}$$

$$\frac{de}{dt} = \beta x(t)v(t) - a_1 e(t) - a_2 e(t), \tag{2.2.23}$$

$$\frac{dy}{dt} = a_2 e(t) - a_1 y(t) - k_1 y(t) z(t), \tag{2.2.24}$$

$$\frac{dv}{dt} = k y(t) - \epsilon v(t) - k_2 v(t) z(t), \tag{2.2.25}$$

$$\frac{dz}{dt} = k_3 v(t-\tau) z(t-\tau) - k_4 z(t), \tag{2.2.26}$$

$$\frac{dw}{dt} = k_5 + k_1 k_6 y(t) z(t) - k_7 w(t), \tag{2.2.27}$$

where x, e, y, v, z and w denote the number of uninfected cells, exposed cells, infected cells, free viruses, CTLs, and alanine aminotransferases (ALT), respectively. The parameter τ represents the time delay of the antigen to generate CTLs, i.e. the CTL response at time $t - \tau$ may depend on the population of antigen at a previous time t.

Notation:

λ is the natural production rate of uninfected cells.

r is the proliferation rate.

d is the natural death rate of uninfected cells.

β is the infection rate from uninfected cells to exposed cells.

a_1 is the natural death rate of exposed cells.

a_2 is the transfer rate from expose cells to infected cells.

ϵ is the natural death rate of free virus.

k_1 is the clearance rate of infected cells.

k_2 is the clearance rate of free viruses.

k_3 is the production rate of CTLs.

k_4 is the natural death rate of CTLs.

k_5 is the production rate of ALT from the extrahepatic tissue.

k_6 is the production rate of ALT when the infected hepatocytes are killed by CTL.

k_7 is the natural death rate of ALT.

In 2018, Danane et al. [20] proposed the hepatitis B virus (HBV) infection model with six differential equations. They enhanced the model deeper to study the dynamics of hepatitis B virus (HBV) by representing the reactions between HBV with DNA-containD ing capsids, hepatocytes, antibodies, and cytotoxic T-lymphocyte (CTL) cells. Furthermore, this model involves the time delay for

infected cells to generate new viruses following viral entry. The existence of the optimal control pair is supported and the characterization of this pair is given by Pontryagin's minimum principle. Note that one of them describes the effectiveness of medical treatment in restraining viral production, while the second stands for the success of drug treatment in blocking new infections. The flow chart of this model is shown in Figure 7.

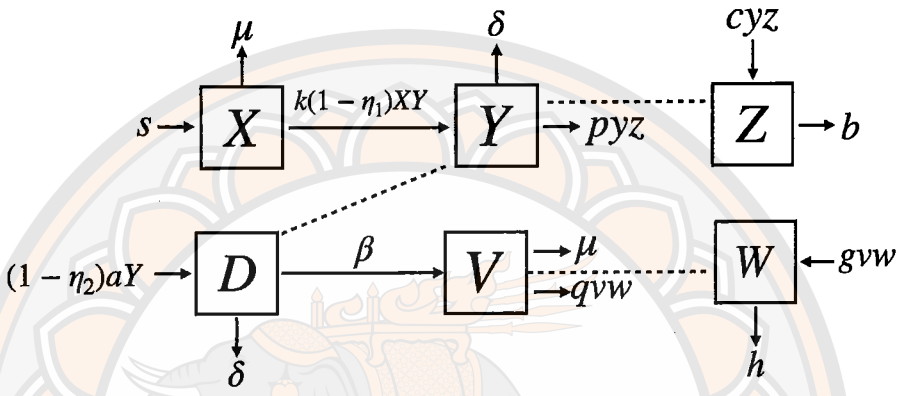

Figure 7 The flow chart of the treatment for a delayed hepatitis B viral infection model with the adaptive immune response and DNA-containing capsids [20].

The model is given by the following nonlinear differential equations:

$$\frac{dX}{dt} = s - \mu X(t) - k(1-\eta_1)X(t)Y(t), \tag{2.2.28}$$

$$\frac{dY}{dt} = e^{-\lambda\tau}k(1-\eta_1)X(t-\tau)V(t-\tau) - \delta Y(t) - pY(t)Z(t), \tag{2.2.29}$$

$$\frac{dD}{dt} = (1-\eta_2)aY(t) - \beta D(t) - \delta D(t), \tag{2.2.30}$$

$$\frac{dV}{dt} = \beta D(t) - uV(t) - qV(t)W(t), \tag{2.2.31}$$

$$\frac{dW}{dt} = gV(t)W(t) - hW(t), \tag{2.2.32}$$

$$\frac{dZ}{dt} = cY(t)Z(t) - bZ(t), \tag{2.2.33}$$

where X, Y, D, V, W and Z denote the number of uninfected cells, infected cells, intracellular HBV DNA-containing capsids, free viruses, antibodies, and CTLs, respectively. The parameter τ represents the time needed for infected hepatocytes to produce new viruses after viral entry.

Notation:

s is the natural production rate of uninfected cells.

μ is the natural death rate of susceptible host cells.

η_1 is the efficiency of pegylated interferon.

η_2 is the efficiency of lamivudine drugs.

k is the rate of uninfected cells become infected cells by HBV.

λ is the average death of infected cells but still not virus-producing cells.

$e^{-\lambda\tau}$ is the probability of surviving from $t-\tau$ to time t.

δ is the clearance rate of infected hepatocytes and capsids.

p is the rate of infected cells that are killed by CTL immune response.

a is the production rate of intracellular HBV DNA-containing capsids.

β is the growth rate of virions in blood.

u is the natural death rate of virus.

q is the rate of free virus are neutralized by antibodies.

g is the expansion rate of antibodies in response to free virus.

h is the decay rate of antibodies.

c is the expansion rate of CTLs in response to viral antigen derived from infected cells.

b is the natural death rate of CTLs.

In the following year, Meskaf, A. [54] presented a delayed differential equation model of hepatitis B virus (HBV) infection which is similar to the work of Danane et al. in 2018 [20]. They added a treatment term $rI(t)$ that facilitates the recovery of infected cells to the uninfected state. The optimal controls representing the efficiency of drug treatment in inhibiting viral production and the preventing new infections are included in the model. The results show a remarkable increase in the number of healthy hepatocytes and a significant decrease in the number of infected hepatocytes with the implementation of the two optimal treatments, this therefore improves the patient's life quality. The flow chart of this model is shown in Figure 8.

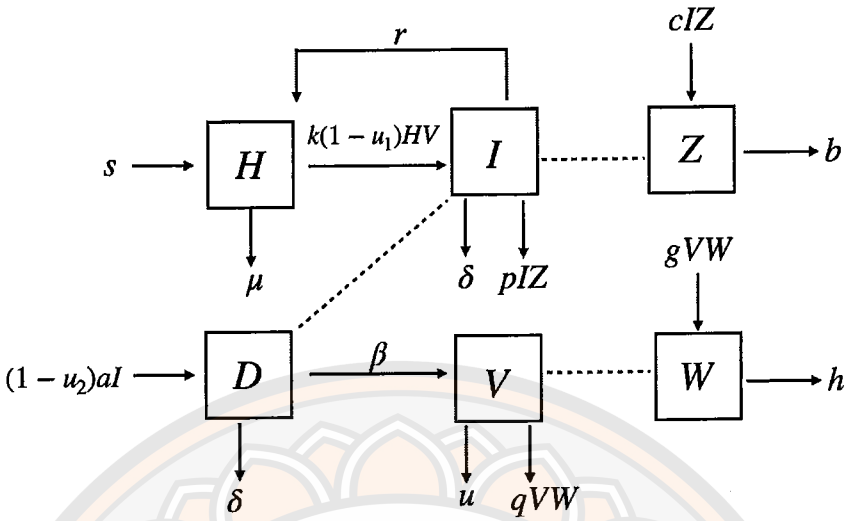

Figure 8 The flow chart of the optimal control of a delayed hepatitis B viral infection model with DNA-containing capsids, the adaptive immune response and cure rate [54].

The model is given by the following nonlinear differential equations:

$$\frac{dH}{dt} = s - \mu H(t) - k(1-u_1)H(t)V(t) + rI(t), \tag{2.2.34}$$

$$\frac{dI}{dt} = ke^{-\lambda\tau}(1-u_1)H(t-\tau)V(t-\tau) - (\delta + r)I(t) - pI(t)Z(t), \tag{2.2.35}$$

$$\frac{dD}{dt} = (1-u_2)aI(t) - \beta D(t) - \delta D(t), \tag{2.2.36}$$

$$\frac{dV}{dt} = \beta D(t) - uV(t) - qV(t)W(t), \tag{2.2.37}$$

$$\frac{dW}{dt} = gV(t)W(t) - hW(t), \tag{2.2.38}$$

$$\frac{dZ}{dt} = cI(t)Z(t) - bZ(t), \tag{2.2.39}$$

where H, I, D, V, W and Z denote the number of uninfected cells, infected cells, intracellular HBV DNA-containing capsids, free viruses, antibodies, and CTLs, respectively. The parameter τ represents the time needed for infected hepatocytes to produce new viruses after viral entry.

Notation:

s is the natural production rate of uninfected cells.

μ is the natural death rate of uninfected cells.

u_1 is the efficiency of pegylated interferon.

u_2 is the efficiency of lamivudine drugs.

k is the rate of uninfected cells become infected cells by HBV.

λ is the average death of infected cells but still not virus-producing cells.

$e^{-\lambda\tau}$ is the probability of surviving from $t-\tau$ to time t.

δ is the clearance rate of infected hepatocytes and capsids.

p is the rate of infected cells that are killed by CTL immune response.

a is the production rate of intracellular HBV DNA-containing capsids.

β is the growth rate of virions in blood.

u is the natural death rate of virus.

q is the rate of free virus are neutralized by antibodies.

g is the expansion rate of antibodies in response to free virus.

h is the decay rate of antibodies.

c is the expansion rate of CTLs in response to viral antigen derived from infected cells.

b is the natural death rate of CTLs.

r is the recovery rate of infected cells which return to the uninfected state.

2.2.2 The HBV model with diffusion

In 2008, Wang, K., Wang, W., and Song, S. [43] proposed a diffusion model of the hepatitis B virus (HBV) infection which confines to a finite domain, induced by intracellular time delay between infection of a cell and production of new virus particles. The equilibrium solutions are obtained and the stability is analyzed if the space is assumed as homogeneous. When the space is inhomogeneous, the effects of diffusion and intracellular time delay are obtained by computer simulations. The flow chart of this model is shown in Figure 9.

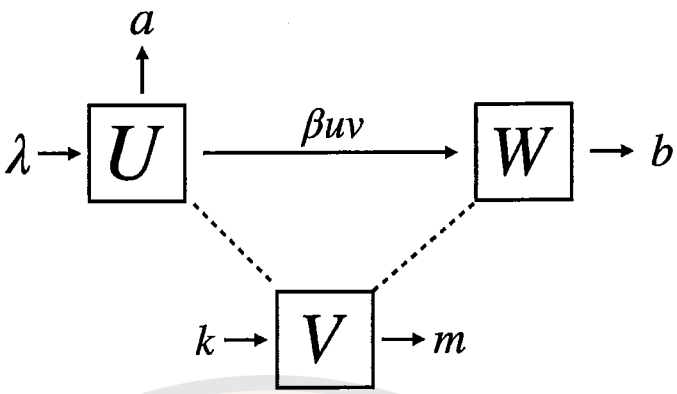

Figure 9 The flow chart of HBV model with spatial dependence [43].

They also disregard the mobility of susceptible cells and infected cells to derive the following model:

$$\begin{aligned}
\frac{\partial U}{\partial t} &= \lambda - U - UV, \\
\frac{\partial W}{\partial t} &= U(t-\tau, x)V(t-\tau, x) - \rho_1 W, \\
\frac{\partial V}{\partial t} &= D\Delta V + \rho_2 W - \rho_3 V,
\end{aligned}$$

where U, W, and V denote the densities of uninfected hepatocytes, infected hepatocytes, and free viruses at location x and time t, respectively. Here, $U = (\frac{a}{\lambda})w$, $W = (\frac{a}{\lambda})w$, $V = (\frac{\beta}{a})v$, $D = \frac{d}{a}$, $\rho_1 = \frac{b}{a}$, $\rho_2 = \frac{k\beta\lambda}{a^3}$, $\rho_3 = \frac{m}{a}$. The parameter τ represents the delay in HBV production following the infection of a hepatocyte. Δ is the Laplacian operator.

Notation:

- λ is the natural production rate of uninfected hepatocytes.
- a is the natural death rate of susceptible host cells.
- β is the rate of uninfected hepatocytes become infected hepatocytes by HBV.
- b is natural death rate of infected hepatocytes.
- k is the production virions rate from being infected.
- m is the natural death rate of virus.
- D is the diffusion coefficients of virions.

In 2011, Shaoli, W. et al. [57] developed a model of Wang, K. et al. [43] by considering a diffused hepatitis B virus (HBV) model with CTL immune

response and nonlinear incidence for the control of viral infections. This paper considered global asymptotical properties of the viral free equilibrium and immune free equilibrium of model system. The results show that the free diffusion of the virus has no effect on the global stability of such HBV infection problem with Neumann homogeneous boundary conditions. The flow chart of this model is shown in Figure 10.

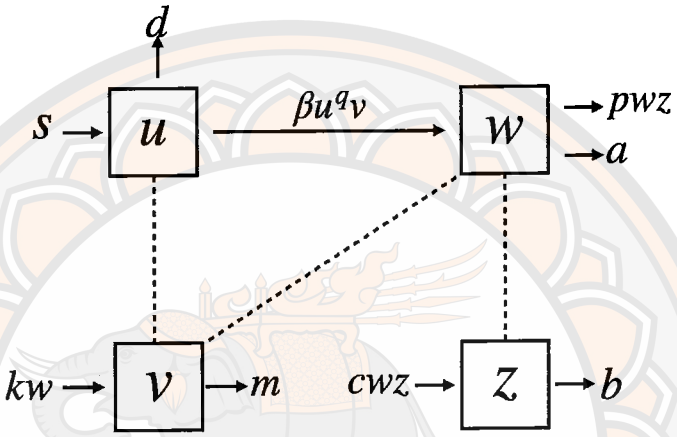

Figure 10 The flow chart of diffused hepatitis B virus (HBV) model with CTL immune response and nonlinear incidence [57].

They consider the following diffused HBV model with CTL immune response and nonlinear incidence:

$$\frac{\partial u}{\partial t} = s - du(x,t) - \beta u^q(x,t)v(x,t), \tag{2.2.40}$$

$$\frac{\partial w}{\partial t} = \beta u^q(x,t)v(x,t) - aw(x,t) - pw(x,t)z(x,t), \tag{2.2.41}$$

$$\frac{\partial v}{\partial t} = D\Delta v + kw(x,t) - mv(x,t), \tag{2.2.42}$$

$$\frac{\partial z}{\partial t} = cw(x,t)z(x,t) - bz(x,t), \tag{2.2.43}$$

where $u(x,t)$, $w(x,t)$, $v(x,t)$ and $z(x,t)$ represent uninfected hepatocytes, infected hepatocytes, free virus, and CTL cells at location x and time t, respectively. Δ is the Laplacian operator.

Notation:

s is the natural production rate of uninfected hepatocytes.

d is the natural death rate of uninfected hepatocytes.

β is a constant rate of the infection process.

a is the natural death rate of infected cells.

p is the death rate of infected cells due to the CTL responses.

k is the rate of free virions being produce from infected cells.

m is the natural death rate of virus.

c is the expansion rate of CTLs in response to viral antigen derived from infected cells.

b is the death rate of CTLs.

D is the diffusion coefficients of virions.

Δ is the Laplacian operator.

In 2015, Manna and Chakrabarty [58] studied a diffusion-driven model for hepatitis B virus (HBV) infection, incorporating the spatial mobility of both HBV and HBV DNA-containing capsids. The global stability of the continuous model is analyzed with a focus on the basic reproduction number. To extend the analysis to a discretized version of the model, a non-standard finite difference (NSFD) scheme is employed to address potential numerical instabilities associated with the standard finite difference (SFD) approximation. The flow chart of this model is shown in Figure 11.

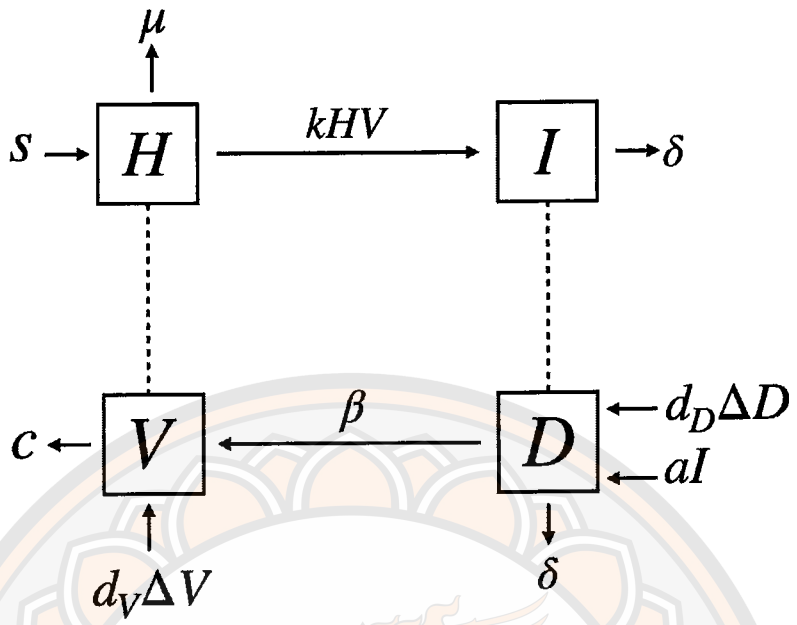

Figure 11 The flow chart of a diffusion driven HBV model with capsids [58].

They proposed the following PDEs model:

$$\frac{\partial H}{dt} = s - kH(x,t)V(x,t) - \mu H(x,t), \tag{2.2.44}$$

$$\frac{\partial I}{dt} = kH(x,t)V(x,t) - \delta I(x,t), \tag{2.2.45}$$

$$\frac{\partial D}{dt} = d_D\Delta D + aI(x,t) - \beta D(x,t) - \delta D(x,t), \tag{2.2.46}$$

$$\frac{\partial V}{dt} = d_V\Delta V + \beta D(x,t) - cV(x,t), \tag{2.2.47}$$

where H, I, D, and V denote the number of uninfected hepatocytes, infected hepatocytes, intracellular HBV DNA-containing capsids, and hepatitis B virions, respectively. Δ is the Laplacian operator.

Notation:

s is the production at a constant rate of the uninfected hepatocytes.

μ is the death rate of uninfected hepatocytes.

k is the conversion rate of uninfected to infected hepatocytes by HBV infection.

δ is the clearance rate of infected hepatocytes and capsids.

a is the conversion rate to intracellular HBV DNA-containing capsids by infected hepatocytes.

β is the replication rate of viral by capsids.

c is the natural death rate for the HBV.

d_D is the diffusion coefficients of capsids.

d_V is the diffusion coefficients of virions.

In 2017, Wang, W., and Ma, W.B. [104] conducted a study focusing on the global dynamics of a reaction-diffusion model for HTLV-I infection. The model incorporates mitotic division of actively infected cells and the immune response of Cytotoxic T lymphocytes (CTL). The research aims to provide insights into the spatial dynamics and interactions involved in HTLV-I infection. They calculated the basic reproduction number (R_0) to use as a condition for analyzing global stability using the Lyapunov method. The analysis concludes that the global asymptotic properties of the steady states for the spatially homogeneous model have been studied. In the case of an unbounded spatial domain, there are no travelling wave solutions connecting the infection-free steady state with itself when $R_0 < 1$.

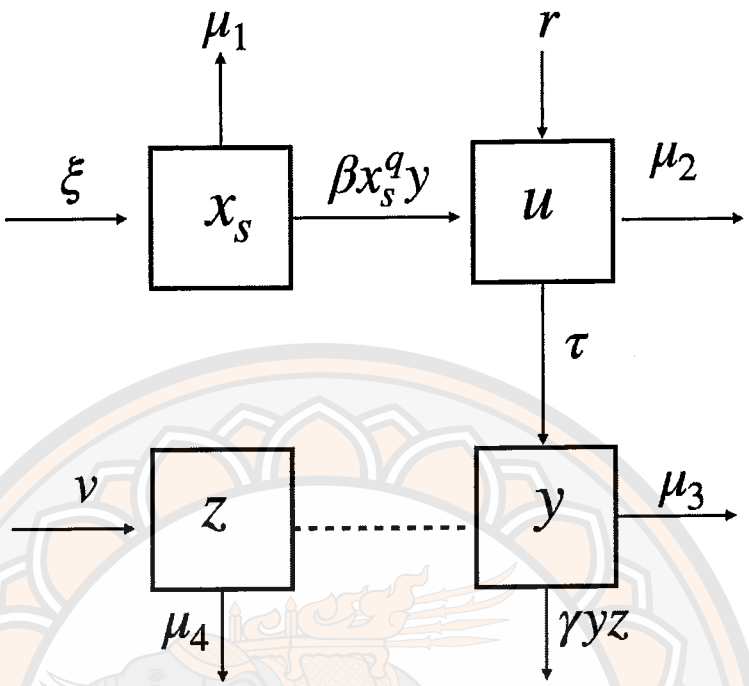

Figure 12 The flow chart of a reaction-diffusion model for HTLV-I infection with the immune response of Cytotoxic T lymphocytes [104].

They proposed the following PDEs model:

$$\frac{\partial x_s(x,t)}{\partial t} = D_1 \Delta x_s(x,t) + \xi - \mu_1 x_s(x,t) - \beta x_s^q(x,t) y(x,t), \tag{2.2.48}$$

$$\frac{\partial u(x,t)}{\partial t} = D_1 \Delta u(x,t) + \beta x_s^q(x,t) y(x,t) + r y(x,t) - (\tau + \mu_2) u(x,t), \tag{2.2.49}$$

$$\frac{\partial y(x,t)}{\partial t} = D_1 \Delta y(x,t) + \tau u(x,t) - \gamma y(x,t) z(x,t) - \mu_3 y(x,t), \tag{2.2.50}$$

$$\frac{\partial z(x,t)}{\partial t} = D_2 \Delta z(x,t) + v y(x,t) - \mu_4 z(x,t), \tag{2.2.51}$$

where $x_s(x,t)$, $u(x,t)$, $y(x,t)$ and $z(x,t)$ represent density of healthy $CD4^+$ helper T-cells, latently infected $CD4^+$ helper T-cells, actively infected $CD4^+$ helper T-cells, and HTLV-I-specific $CD8^+$ CTLs at location x and time t, respectively. Δ is the Laplacian operator.

Notation:

ξ is the rate of production of $CD4^+$ helper T-cells.

μ_1 is the natural death rate of healthy cells.

μ_2 is the natural death rate of latently infected $CD4^+$ helper T-cells.

μ_3 is the natural death rate of actively infected $CD4^+$ helper T-cells.

μ_4 is the natural death rate of HTLV-I-specific $CD8^+$ CTLs.

r is a selective proliferation rate of actively infected $CD4^+$ helper T-cells.

γ is the rate of CTL-mediated lysis of actively infected $CD4^+$ helper T-cells.

τ is the rate of spontaneous Tax expression.

υ is the proliferation rate of CTLs.

D_1 is the diffusion coefficients of $CD4^+$ helper T-cells.

D_2 is the diffusion coefficients of HTLV-I-specific $CD8^+$ CTLs.

In 2018, Kalyan Manna [68] introduces and investigates a delayed reaction diffusion model for hepatitis B virus (HBV) infection, incorporating the spatial mobility of HBV DNA-containing capsids and cytotoxic T lymphocyte (CTL) immune response. Additionally, discrete time delays in the production of productively infected hepatocytes and matured capsids are considered in the model. Overall, the study contributes to a deeper understanding of the dynamics of HBV infection, considering spatial mobility, time delays, and immune response. The established stability conditions provide valuable insights for assessing the effectiveness of immune responses in different scenarios, contributing to the development of strategies for managing HBV infections. The flow chart of this model is shown in Figure 13.

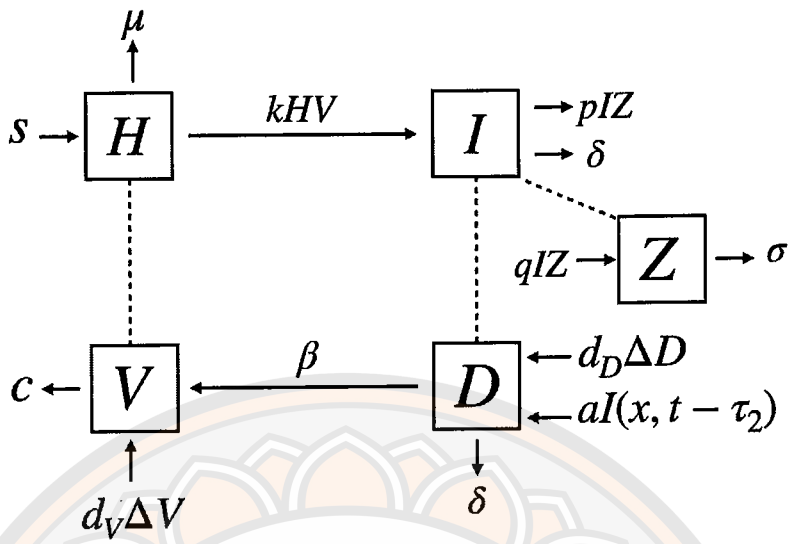

Figure 13 The flow chart of a diffusion driven HBV model with capsids [68].

They proposed the following PDEs model:

$$\frac{\partial H}{dt} = s - kH(x,t)V(t) - \mu H(x,t), \tag{2.2.52}$$

$$\frac{\partial I}{dt} = kH(x,t-\tau_1)V(t-\tau_1) - \delta I(x,t) - pI(x,t)Z(x,t), \tag{2.2.53}$$

$$\frac{\partial D}{dt} = d_D\Delta D + aI(x,t-\tau_2) - \beta D(x,t) - \delta D(x,t), \tag{2.2.54}$$

$$\frac{\partial V}{dt} = d_V\Delta V + \beta D(x,t) - cV(x,t), \tag{2.2.55}$$

$$\frac{\partial Z}{dt} = qI(x,t)Z(x,t) - \sigma Z(x,t), \tag{2.2.56}$$

where H, I, D, V and Z denote the number of uninfected hepatocytes, infected hepatocytes, intracellular HBV DNA-containing capsids, and hepatitis B virions, respectively. Δ is the Laplacian operator.

Notation:

s is the production at a constant rate of the uninfected hepatocytes.

μ is the death rate of uninfected hepatocytes.

k is the conversion rate of uninfected to infected hepatocytes by HBV infection.

δ is the clearance rate of infected hepatocytes and capsids.

a is the conversion rate to intracellular HBV DNA-containing capsids by infected hepatocytes.

β is the replication rate of viral by capsids.

c is the natural death rate for the HBV.

p is the rate of infected cells that are killed by CTL immune response.

q is the expansion rate of CTLs in response to viral antigen derived from infected cells.

τ_1 is he delays in the production of productively infected hepatocytes.

τ_2 is the delays in the production of matured capsids.

d_D is the diffusion coefficients of capsids.

d_V is the diffusion coefficients of virions.

CHAPTER III

TIME DELAY MODEL OF HEPATITIS B VIRUS INFECTION

3.1 Model description and formulation

We have developed a delay model describing the hepatitis B virus (HBV) dynamics involving immune response and drug therapy by extending the work of Danane, J., et al. [20] by adding the delay time that an antigenic stimulation generating CTLs, which is τ_2 in our model. This model is described by a system of delay differential equations (3.1.1)-(3.1.6), it includes six variables: the concentration of uninfected hepatocytes $x(t)$, infected hepatocytes $y(t)$, intracellular HBV DNA-containing capsids $c(t)$, free viruses $v(t)$, antibodies $w(t)$, and CTLs $z(t)$. The uninfected hepatocytes $x(t)$ are produced at a constant rate Λ and die with a rate σ. The infection of hepatocytes in this model incorporates the uninfectes become infected hepatocytes by the free virus with a rate β with an involvement of the efficiency of drug therapy in blocking new infection u_1. The $e^{-m\tau_1}$ is the probability of surviving of hepatocytes in the time period from $t-\tau_1$ to t, where m is a constant rate of the death average of infected hepatocytes which are still not virus-producing cells. Time τ_1 is the delay time in the productively infected hepatocytes. This infection term is represented by the nonlinear term $(1-u_1)e^{-m\tau_1}\beta x(t)v(t)$. The infected hepatocytes $y(t)$ are eliminated by the CTLs, $z(t)$, with a rate q and die at a rate σ. The production of intracellular HBV DNA-containing capsids $c(t)$ incorporates the efficiency of drug therapy in inhibiting viral production u_2 with a production rate a, described by the term $(1-u_2)ay(t)$. The intracellular HBV DNA-containing capsids are transmitted into the bloodstream to become free viruses with a rate α and are decomposed with a rate δ. The free viruses are reduced by the neutralization rate of antibodies γ and die at a rate μ. The antibodies are enhanced in response to the free viruses at a rate g and decay at a rate h. Further, the second time delay in this model cannot be ignored for the immune response, that is the activation of CTLs producing antigens may require

a period of time τ_2. Therefore, we propose the form $ky(t-\tau_2)z(t-\tau_2)$ and the CTLs decay at the rate ϵ. The flow chart of the model is presented in Figure 14.

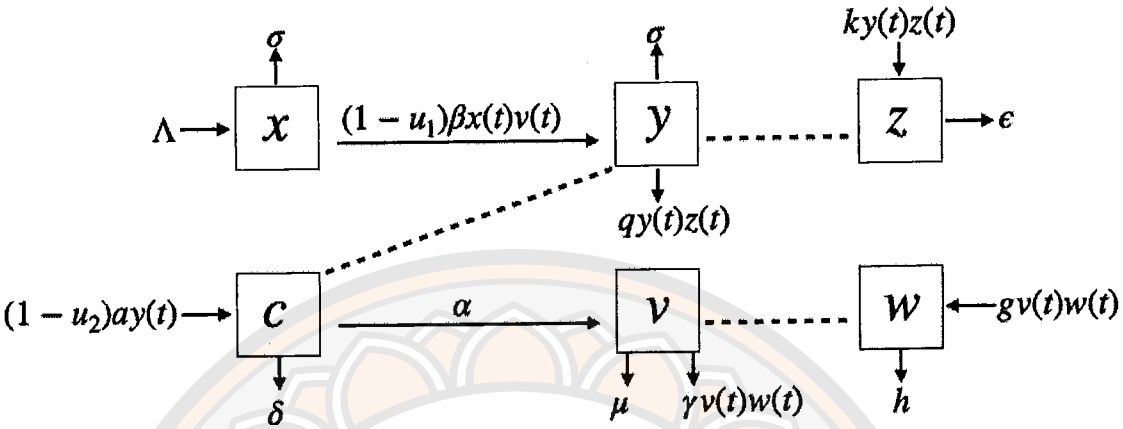

Figure 14 The flow chart of our proposed delays model of HBV infection with immune response and drug therapy.

This model can be written into a form of system of delay differential equations as follows:

$$\frac{dx}{dt} = \Lambda - \sigma x(t) - (1-u_1)\beta x(t)v(t) \tag{3.1.1}$$

$$\frac{dy}{dt} = (1-u_1)\beta e^{-m\tau_1} x(t-\tau_1)v(t-\tau_1) - \sigma y(t) - qy(t)z(t) \tag{3.1.2}$$

$$\frac{dc}{dt} = (1-u_2)ay(t) - \alpha c(t) - \delta c(t) \tag{3.1.3}$$

$$\frac{dv}{dt} = \alpha c(t) - \gamma v(t)w(t) - \mu v(t) \tag{3.1.4}$$

$$\frac{dw}{dt} = gv(t)w(t) - hw(t) \tag{3.1.5}$$

$$\frac{dz}{dt} = ky(t-\tau_2)z(t-\tau_2) - \epsilon z(t), \tag{3.1.6}$$

with initial condition

$$x(0) \geq 0, y(0) \geq 0, c(0) \geq 0, v(0) \geq 0, w(0) \geq 0, z(0) \geq 0,$$

for $\tau_1 > 0$ and $\tau_2 > 0$. Here, $0 < u_1 < 1$ and $0 < u_2 < 1$.

Table 1 Parameters used in the modeln of equations (3.1.1) -(3.1.6).

Parameter	Description	Value	Units	Source
Λ	the production rate of the uninfected hepatocytes.	4.0551	$day^{-1}mm^{-3}$	[45]
σ	the death rate of hepatocytes.	0.011	day^{-1}	[41]
u_1	the efficiency of drug therapy in blocking new infection.	0.5	-	assume
u_2	the efficiency of drug therapy in inhibiting viral production.	0.5	-	assume
β	the infection rate of uninfected hepatocytes by the free virus.	0.0014	$mm^3virion^{-1}$ day^{-1}	[33]
$e^{-m\tau_1}$	the probaility of surviving of hepatocytes in the time period from $t-\tau_1$ to t			
τ_1	the delay in the productively infected hepatocytes.	5	day	assume
τ_2	the delay in an antigenic stimulation generating CTLs.	5	day	assume
m	the constant rate of the death average of infected hepatocytes which still not virus-producing cells.	0.011	day^{-1}	[18]
q	the death rate of infected hepatocytes by the CTLs response.	0.001	mm^3day^{-1}	[18]
a	the production rate of intracellular HBV DNA-containing capsids.	0.15	day^{-1}	assume
α	the growth rate of virions in blood.	0.0693	day^{-1}	[29]
δ	the clearance rate of intracellular	0.053	day^{-1}	[19]
γ	the rate that viruses are neutralized by antibodies.	0.01	mm^3day^{-1}	[18]
μ	the death rate of free viruses.	0.693	day^{-1}	[41]
g	the expansion rate of antibodies in response to free viruses.	0.008	$mm^3virion^{-1}$ day^{-1}	[111]
h	the decay rate of antibodies.	0.15	day^{-1}	[18]
k	the expansion rate of CTLs in response to viral antigen derived from infected hepatocytes.	0.001	mm^3day^{-1}	assume
ϵ	the decay rate of CTLs in the absence of antigenic stimulation.	0.5	day^{-1}	[112]

3.2 Nonnegativity and boundedness of solutions

For equation (3.1.1)-(3.1.6) to be epidemiologically meaningful, we prove that all state variables are non-negative. Since it is irrational to have a negative hepatocytes density and equation (3.1.1)-(3.1.6) describes the dynamics of HBV infection of hepatocytes, we show that all state variables are non-negative and the solutions of equation (3.1.1)-(3.1.6) with non-negative initial conditions will remain non-negative for all $t > 0$. The following lemma is applied.

Lemma 3.2.1. *Given that the initial solutions and parameters of equation* (3.1.1)-(3.1.6) *are non-negative, the solutions* $x(t), y(t), c(t), v(t), w(t)$ *and* $z(t)$ *are non-negative for all* $t > 0$.

Proof. Consider the equation (3.1.1) we have,

$$\frac{dx}{dt} = \Lambda - \sigma x - (1-u_1)\beta xv$$

$$\frac{dx}{dt} + (\sigma + (1-u_1)\beta v)x = \Lambda. \tag{3.2.1}$$

We multiply both sides of the differential equation by the integrating factor which is defined as

$$I = e^{\int_0^t (\sigma+(1-u_1)\beta v(s))ds}, \tag{3.2.2}$$

we have

$$(e^{\int_0^t (\sigma+(1-u_1)\beta v(s))ds})\frac{dx}{dt} + (e^{\int_0^t (\sigma+(1-u_1)\beta v(s))ds})(\sigma+(1-u_1)\beta v)x = (e^{\int_0^t (\sigma+(1-u_1)\beta v(s))ds})\Lambda. \tag{3.2.3}$$

We integrate both side between 0 and t, then

$$\int_0^t (e^{\int_0^t (\sigma+(1-u_1)\beta v(s))\ ds})\left(\frac{dx(s)}{dt} + (\sigma + (1-u_1)\beta v(s))x(s)\right)ds = \int_0^t (e^{\int_0^t (\sigma+(1-u_1)\beta v(s))\ ds})\Lambda ds.$$

Thus, $x(t) = (e^{-\int_0^t (\sigma+(1-u_1)\beta v(s))\ ds})(x(0) + \int_0^t (e^{\int_0^t (\sigma+(1-u_1)\beta v(s))\ ds})\Lambda ds)$, leads to $x(t) \geq 0$. Similarly, we obtain

$$y(t) = e^{-\int_0^t (\sigma+qz(s))ds}(y(0) + \int_0^t e^{\int_0^t (\sigma+qz(s))ds}(1-u_1)\beta e^{-m\tau_1}x(s-\tau_1)v(s-\tau_1)ds) \geq 0$$

$$c(t) = e^{-(\alpha+\delta)t}(c(0) + \int_0^t (1-u_2)ay(s)e^{(\alpha+\delta)}ds) \geq 0$$

$$v(t) = e^{-\int_0^t (\gamma w(s)+\mu)ds}(v(0) + \int_0^t e^{\int_0^t (\gamma w(s)+\mu)ds}\alpha c(s)ds) \geq 0$$

$$w(t) = w(0)e^{\int_0^t (gv(s)-h)\ ds} \geq 0$$

$$z(t) = e^{-\epsilon t}(z(0) + \int_0^t ky(s-\tau_2)z(s-\tau_2)e^{\epsilon t}ds) \geq 0. \tag{3.2.4}$$

Therefore, $x(t) \geq 0,\ y(t) \geq 0,\ c(t) \geq 0,\ v(t) \geq 0,\ w(t) \geq 0,\ z(t) \geq 0$ for all $t > 0$ given that $x(0) \geq 0,\ y(0) \geq 0,\ c(0) \geq 0,\ v(0) \geq 0,\ w(0) \geq 0,\ z(0) \geq 0$. □

Theorem 3.2.2. *Under the given initial conditions, all solutions of equation* (3.1.1)-(3.1.6) *are non-negative and bounded for all* $t \geq 0$.

Proof. We obtain from Lemma 3.2.1 that all solutions of equation (3.1.1)-(3.1.6) are non-negative for all $t \geq 0$, next we use the following function to help determining the boundness of the solutions of equation (3.1.1)-(3.1.6):

$$N(t) = e^{-m\tau_1}x(t-\tau_1)+y(t)+\frac{q}{k}z(t+\tau_2)+\frac{\sigma}{2(1-u_2)a}c(t)+\frac{\sigma}{2(1-u_2)a}v(t)+\frac{\sigma\gamma}{2(1-u_2)ag}w(t). \tag{3.2.5}$$

By differentiating (3.2.5) with respect to t and with equation (3.1.1)-(3.1.6), we have

$$\begin{aligned}
\frac{dN(t)}{dt} &= e^{-m\tau_1}\frac{dx(t-\tau_1)}{dt} + \frac{dy}{dt} + \frac{qd}{k}\frac{z(t+\tau_2)}{dt} + \frac{\sigma}{2(1-u_2)a}\frac{dc(t)}{dt} \\
&\quad + \frac{\sigma}{2(1-u_2)a}\frac{dv(t)}{dt} + \frac{\sigma\gamma}{2(1-u_2)ga}\frac{dw(t)}{dt} \\
&= \Lambda e^{-m\tau_1} - \sigma e^{-m\tau_1}x(t-\tau_1) - (1-u_1)\beta e^{-m\tau_1}x(t-\tau_1)v(t-\tau_1) \\
&\quad + (1-u_1)\beta e^{-m\tau_1}x(t-\tau_1)v(t-\tau_1) - (\sigma - \frac{\sigma}{2})y(t) \\
&\quad - qy(t)z(t) + qy(t)z(t) - \frac{q\epsilon}{k}z(t+\tau_2) - \frac{\sigma\alpha}{2(1-u_2)a}c(t) \\
&\quad - \frac{\sigma\delta}{2(1-u_2)a}c(t) + \frac{\sigma\alpha}{2(1-u_2)a}c(t) - \frac{\sigma\gamma}{2(1-u_2)a}v(t)w(t) \\
&\quad - \frac{\sigma\mu}{2(1-u_2)a}v(t) + \frac{\sigma\gamma}{2(1-u_2)a}v(t)w(t) - \frac{\sigma\gamma h}{2(1-u_2)ga}w(t) \\
&= \Lambda e^{-m\tau_1} - \sigma e^{-m\tau_1}x(t-\tau_1) - \frac{\sigma}{2}y(t) - \frac{q\epsilon}{k}z(t+\tau_2) \\
&\quad - \frac{\sigma\delta}{2(1-u_2)a}c(t) - \frac{\sigma\mu}{2(1-u_2)a}v(t) - \frac{\sigma\gamma h}{2(1-u_2)ga}w(t) \\
&= \Lambda e^{-m\tau_1} - \min(\sigma, \frac{\sigma}{2}, \epsilon, \delta, \mu, h)(e^{-m\tau_1}x(t-\tau_1) + y(t) + \frac{q}{k}z(t+\tau_2) \\
&\quad + \frac{\sigma}{2(1-u_1)a}c(t) + \frac{\sigma}{2(1-u_1)a}v(t) + \frac{\sigma\gamma}{2(1-u_2)ga}w(t)) \\
&\leq \Lambda e^{-m\tau_1} - \min(\sigma, \frac{\sigma}{2}, \epsilon, \delta, \mu, h)N(t).
\end{aligned}$$

Let $Q = \min(\sigma, \frac{\sigma}{2}, \epsilon, \delta, \mu, h)$. Thus, we have

$$\frac{dN(t)}{dt} \leq \Lambda e^{-m\tau_1} - QN(t). \tag{3.2.6}$$

By integrating both sides,

$$\int_0^t \frac{dN(t)}{\Lambda e^{-m\tau_1} - QN(t)} \leq \int_0^t dt$$

we obtain $$N_t \leq \frac{\Lambda e^{-m\tau_1} - e^{-Qt}(\Lambda e^{-m\tau_1} - QN_0)}{Q}.$$

By taking $t \to \infty$, we have

$$N_t \leq \frac{\Lambda e^{-m\tau_1}}{Q}. \tag{3.2.7}$$

Hence, we have that $N(t)$ is bounded, which leads to the variables $x(t), y(t), c(t)$, $v(t), w(t)$ and $z(t)$ are bounded. □

3.3 Equilibrium points

In this model we calculate three equilibrium points: infection-free (E_0), immune-free (E_1), and immune-activated (E_2) equilibrium points. First, we seek to find the infection-free equilibrium point, where the HBV infection is eradicated. This is achieved by setting the right-hand side of the equations in equation (3.1.1)-(3.1.6) to zero and letting $y = v = 0$. Consequently, we obtain $c = 0, w = 0, z = 0$. And

$$\begin{aligned} \Lambda - \sigma x - (1-u_1)\beta x v &= 0 \\ \Lambda - \sigma x - (1-u_1)\beta x(0) &= 0 \\ \Lambda - \sigma x &= 0 \\ x &= \frac{\Lambda}{\sigma}. \end{aligned} \tag{3.3.1}$$

Thus, we obtain the infection-free equilibrium point as follows:

$$E_0 = (x_0, y_0, c_0, v_0, w_0, z_0) = \left(\frac{\Lambda}{\sigma}, 0, 0, 0, 0, 0\right). \tag{3.3.2}$$

Next, we determine the immune-free equilibrium point E_1 which is the steady state when there is a persistence of the infection without the immune responses (i.e. $w_1 = z_1 = 0$). With calculation, we have, E_1 as $(x_1, y_1, c_1, v_1, 0, 0)$ where

$$x_1 = \frac{\sigma\mu(\alpha+\delta)}{(1-u_1)(1-u_2)\beta e^{-m\tau_1}a\alpha}, y_1 = \frac{(\alpha+\delta)c_1}{(1-u_2)a}, c_1 = \frac{\sigma\mu}{(1-u_1)\beta\alpha}(R_0 - 1), v_1 = \frac{\alpha c_1}{\mu}. \tag{3.3.3}$$

Next, we will determine the immune-activated equilibrium point, denoted as $E_2 = (x_2, y_2, c_2, v_2, w_2, z_2)$, where

$$x_2 = \frac{\Lambda g}{\sigma g + (1-u_1)\beta h}, \quad y_2 = \frac{\varepsilon}{k}, \quad c_2 = \frac{(1-u_2)a\varepsilon}{k(\alpha+\delta)}, \quad v_2 = \frac{h}{g},$$
$$w_2 = \frac{(1-u_2)a\varepsilon\alpha g}{(\alpha+\delta)\gamma hk} - \frac{\mu}{\gamma}, \quad z_2 = \frac{(1-u_1)\beta e^{-m\tau_1} khx_2}{qg\varepsilon} - \frac{\sigma}{q}. \tag{3.3.4}$$

Note that the immune-activated equilibrium point exists if and only if the antibody population w_2 and cytotoxic T-lymphocytes population z_2 are positive.

3.4 The basic reproduction number (R_0)

The basic reproduction number is defined as an average number of secondary infections caused by a single infectious individual in a fully susceptible population. It corresponds to the spectral radius of a matrix FV^{-1} where F is Jacobian of $\mathcal{F}$, where $\mathcal{F}$ is the rate of appearance of new infections in compartment and V is the Jacobian of $\mathcal{V}$ which is the rate of transfer of individuals into and out of compartment. To calculate FV^{-1}, we used the next-generation matrix method by van den Driessche et al., 2002 [73]. In this model, define $\mathcal{F}$ as

$$\mathcal{F} = \begin{bmatrix} (1-u_1)\beta e^{-m\tau_1} xv \\ 0 \\ 0 \end{bmatrix} \text{ and } \mathcal{V} = \begin{bmatrix} \sigma y + qzy \\ \alpha c + \delta c - (1-u_2)ay \\ \gamma vw + \mu v - \alpha c \end{bmatrix}.$$

Then we have

$$F = \begin{bmatrix} 0 & 0 & (1-u_1)\beta e^{-m\tau_1} x \\ 0 & 0 & 0 \\ 0 & 0 & 0 \end{bmatrix} \text{ and } V = \begin{bmatrix} \sigma + qz & 0 & 0 \\ -(1-u_2)a & \alpha+\delta & 0 \\ 0 & -\alpha & \gamma w + \mu \end{bmatrix}.$$

By substituting $E_0 = \left(\frac{\Lambda}{\sigma}, 0, 0, 0, 0, 0\right)$ in the Jacobian matrices above, we get

$$F = \begin{bmatrix} 0 & 0 & (1-u_1)\beta e^{-m\tau_1}\frac{\Lambda}{\sigma} \\ 0 & 0 & 0 \\ 0 & 0 & 0 \end{bmatrix} \text{ and } V = \begin{bmatrix} \sigma & 0 & 0 \\ -(1-u_2)a & \alpha+\delta & 0 \\ 0 & -\alpha & \mu \end{bmatrix}.$$

Next,

$$V^{-1} = \frac{1}{\mu\sigma(\alpha+\delta)} \begin{bmatrix} \mu(\alpha+\delta) & 0 & 0 \\ \mu(1-u_2)a & \mu\sigma & 0 \\ (1-u_2)a\alpha & \alpha\sigma & \sigma(\alpha+\delta) \end{bmatrix}.$$

The next generation matrix is

$$FV^{-1} = \begin{bmatrix} \frac{(1-u_1)(1-u_2)\beta e^{-m\tau_1}\Lambda a\alpha}{\sigma^2\mu(\alpha+\delta)} & \frac{(1-u_1)\beta e^{-m\tau_1}\Lambda\alpha}{\sigma^2\mu(\alpha+\delta)} & \frac{(1-u_1)\beta e^{-m\tau_1}\Lambda}{\sigma^2\mu} \\ 0 & 0 & 0 \\ 0 & 0 & 0 \end{bmatrix}.$$

The basic reproduction number is given by $\rho(FV^{-1})$, thus

$$R_0 = \frac{(1-u_1)(1-u_2)\beta e^{-m\tau_1}\Lambda a\alpha}{\sigma^2\mu(\alpha+\delta)}. \tag{3.4.1}$$

3.5 Stability analysis

We analyze the model concerning the local and global stability of the three steady states: infection-free (E_0), immune-free (E_1), and immune-activated (E_2) equilibrium points. For the analysis of local stability, we study through the Jacobian matrices, while for global stability, we use the Lyapunov method.

3.5.1 Local stability of infection-free equilibrium point

Theorem 3.5.1. *If $R_0 < 1$, then the infection-free equilibrium point (E_0) is locally asymptotically stable. Otherwise, it is unstable.*

Proof. The Jacobian matrix of equation (3.1.1)-(3.1.6) at E_0 is

$$J(E_0) = \begin{bmatrix} -\sigma & 0 & 0 & -(1-u_1)\beta x_0 & 0 & 0 \\ 0 & -\sigma & 0 & (1-u_1)\beta e^{-(m+\lambda)\tau_1}x_0 & 0 & 0 \\ 0 & (1-u_2)a & -(\alpha+\delta) & 0 & 0 & 0 \\ 0 & 0 & \alpha & -\mu & 0 & 0 \\ 0 & 0 & 0 & 0 & -h & 0 \\ 0 & 0 & 0 & 0 & 0 & -\epsilon \end{bmatrix}.$$

From Jacobian matrix above, we have the characteristic equation as

$$(\lambda+\epsilon)(\lambda+h)(\lambda+\sigma)\Big((\lambda+\sigma)(\lambda+\alpha+\delta)(\lambda+\mu)-(1-u_1)(1-u_2)a\alpha\beta e^{-(m+\lambda)\tau_1}x_0\Big)=0. \tag{3.5.1}$$

Thus, $\lambda_1 = -\epsilon < 0,\ \lambda_2 = -h < 0,\ \lambda_3 = -\sigma < 0.$
Since, $x_0 = \dfrac{\Lambda}{\sigma}$ and $R_0 = \dfrac{(1-u_1)(1-u_2)\beta e^{-m\tau_1}\Lambda a\alpha}{\sigma^2\mu(\alpha+\delta)}$, we write the rest of the term as

$$\begin{aligned}(\lambda+\sigma)(\lambda+\alpha+\delta)(\lambda+\mu)-(1-u_1)(1-u_2)a\alpha\beta e^{-(m+\lambda)\tau_1}\frac{\Lambda}{\sigma}&=0,\\ (\lambda+\sigma)(\lambda+\alpha+\delta)(\lambda+\mu)&=(1-u_1)(1-u_2)a\alpha\beta e^{-(m+\lambda)\tau_1}\frac{\Lambda}{\sigma},\\ (\lambda+\sigma)(\lambda+\alpha+\delta)(\lambda+\mu)&=\mu\sigma(\alpha+\delta)R_0e^{-\lambda\tau_1}.\end{aligned} \tag{3.5.2}$$

For $R_0 < 1$, if λ has a non-negative real part then the modulus of the left-hand side of equation (3.5.2) satisfies

$$|(\lambda+\sigma)(\lambda+\alpha+\delta)(\lambda+\mu)| \geq \sigma(\alpha+\delta)\mu. \tag{3.5.3}$$

Consider the modulus of the right-hand side of equation (3.5.2),

$$|\mu\sigma(\alpha+\delta)R_0e^{-\lambda\tau_1}| \leq \mu\sigma(\alpha+\delta)R_0 < \mu\sigma(\alpha+\delta), \tag{3.5.4}$$

which is contradiction. Hence, when $R_0 < 1$, the real part of λ has no non-negative real part and the infection-free state E_0 is locally asymptotically stable.
For $R_0 > 1$, we let

$$h(\lambda) = (\lambda+\sigma)(\lambda+\alpha+\delta)(\lambda+\mu) - \mu\sigma(\alpha+\delta)R_0e^{-\lambda\tau_1}. \tag{3.5.5}$$

Then

$$h(0) = \mu\sigma(\alpha+\delta) - \mu\sigma(\alpha+\delta)R_0 < 0, \tag{3.5.6}$$

and $\lim_{\lambda\to\infty} h(\lambda) = +\infty$.
By the continuity of $h(\lambda)$, there exists at least one positive root of $h(\lambda) = 0$. Thus, the infection-free equilibrium point, E_0 is unstable when $R_0 > 1$. This completes the proof. □

3.5.2 Global stability of infection-free equilibrium point

Theorem 3.5.2. *The infection-free equilibrium point (E_0) is globally asymptotically stable when $R_0 < 1$.*

Proof. Let the Lyapunov functions be

$$L(t) = x_0\left(\frac{x}{x_0} - \ln\left(\frac{x}{x_0}\right) - 1\right) + e^{m\tau_1}y(t) + \frac{(1-u_1)\beta\Lambda\alpha c(t)}{\mu\sigma(\alpha+\delta)} + \frac{(1-u_1)\beta\Lambda v(t)}{\mu\sigma} + \frac{(1-u_1)\beta\Lambda\gamma w(t)}{g\mu\sigma} + (1-u_1)\beta\int_{t-\tau_1}^{t} x(s)v(s)ds, \tag{3.5.7}$$

where L is positive definite. The derivative of L along the solutions of the system (3.1.1)-(3.1.6) is

$$\begin{aligned}\frac{dL}{dt} = {} & \left(1-\frac{x_0}{x}\right)\left(\Lambda - \sigma x - (1-u_1)\beta xv\right) + e^{m\tau_1}\Big((1-u_1)\beta e^{-m\tau_1}x(t-\tau_1)v(t-\tau_1) \\ & - \sigma y - qyz\Big) + \frac{(1-u_1)\beta\Lambda\alpha}{\mu\sigma(\alpha+\delta)}\Big((1-u_2)ay - (\alpha+\delta)c\Big) + \frac{(1-u_1)\beta\Lambda}{\mu\sigma}\Big(\alpha c - \gamma vw \\ & - \mu v\Big) + \frac{(1-u_1)\beta\Lambda\gamma}{g\mu\sigma}\Big(gvw - hw\Big) + (1-u_1)\beta\Big(xv - x(t-\tau_1)v(t-\tau_1)\Big).\end{aligned}$$

Since $\frac{dx_0}{dt} = \Lambda - \sigma x_0 - (1-u_1)\beta x_0 v_0 = 0$, we have $\Lambda = \sigma x_0$. Then

$$\begin{aligned}\frac{dL}{dt} = {} & \left(1-\frac{x_0}{x}\right)\left(\sigma x_0 - \sigma x - (1-u_1)\beta xv\right) \\ & + (1-u_1)\beta x(t-\tau_1)v(t-\tau_1) - \sigma y e^{m\tau_1} - qyze^{m\tau_1} \\ & + \frac{(1-u_1)(1-u_2)\beta\Lambda\alpha ay}{\mu\sigma(\alpha+\delta)} - \frac{(1-u_1)\beta\Lambda\alpha c}{\mu\sigma} + \frac{(1-u_1)\beta\Lambda\alpha c}{\mu\sigma} \\ & - \frac{(1-u_1)\beta\Lambda\gamma vw}{\mu\sigma} - \frac{(1-u_1)\beta\Lambda v}{\sigma} + \frac{(1-u_1)\beta\Lambda\gamma vw}{\mu\sigma} \\ & - \frac{(1-u_1)\beta\Lambda\gamma hw}{g\mu\sigma} + (1-u_1)\beta xv - (1-u_1)\beta x(t-\tau_1)v(t-\tau_1) \\ = {} & \frac{-\sigma(x-x_0)^2}{x} - qyze^{m\tau_1} + \sigma ye^{m\tau_1}\left(\frac{(1-u_1)(1-u_2)\beta\Lambda\alpha ae^{-m\tau_1}}{\sigma^2\mu(\alpha+\delta)} - 1\right) \\ & - \frac{(1-u_1)\beta\Lambda\gamma hw}{g\mu\sigma} \\ = {} & -\frac{\sigma^2}{x\sigma}(x-x_0)^2 - qyze^{m\tau_1} + \sigma ye^{m\tau_1}\Big(R_0 - 1\Big) - \frac{(1-u_1)\beta\Lambda\gamma hw}{g\mu\sigma}.\end{aligned} \tag{3.5.8}$$

We obtain that $\dfrac{dL}{dt} < 0$ when $R_0 < 1$ and $\dfrac{dL}{dt} = 0$ at E_0. Therefore, E_0 is globally asymptotically stable when $R_0 < 1$. □

3.5.3 Local stability of immune-free equilibrium point

Theorem 3.5.3. *If* $1 < R_0 < 1 + \inf\{A_1, A_2\}$, *where* $A_1 = \dfrac{(1-u_1)(1-u_2)\epsilon a\beta\alpha}{k\sigma\mu(\alpha+\delta)}$ *and* $A_2 = \dfrac{(1-u_1)h\beta}{g\sigma}$, *then the immune-free equilibrium point* (E_1) *is locally asymptotically stable. If* $R_0 > 1 + \inf\{A_1, A_2\}$, *then* E_1 *is unstable.*

Proof. We first set $det(J(E_1) - \lambda I) = 0$ to find eigenvalues, then we obtain

$$0 = \begin{vmatrix} -\sigma-(1-u_1)\beta v_1-\lambda & 0 & 0 & -(1-u_1)\beta x_1 & 0 & 0 \\ (1-u_1)\beta v_1 e^{-(m+\lambda)\tau_1} & -\sigma-\lambda & 0 & (1-u_1)\beta e^{-(m+\lambda)\tau_1}x_1 & 0 & -qy_1 \\ 0 & (1-u_2)a & -(\alpha+\delta)-\lambda & 0 & 0 & 0 \\ 0 & 0 & \alpha & -\mu-\lambda & -\gamma v_1 & 0 \\ 0 & 0 & 0 & 0 & gv_1-h-\lambda & 0 \\ 0 & 0 & 0 & 0 & 0 & ky_1e^{-\lambda\tau_2}-\epsilon-\lambda \end{vmatrix}.$$

$$= (ky_1e^{-\lambda\tau_2}-\epsilon-\lambda)(gv_1-h-\lambda)\begin{vmatrix} -\sigma-(1-u_1)\beta v_1-\lambda & 0 & 0 & -(1-u_1)\beta x_1 \\ (1-u_1)\beta v_1 e^{-(m+\lambda)\tau_1} & -\sigma-\lambda & 0 & (1-u_1)\beta x_1 e^{-(m+\lambda)\tau_1} \\ 0 & (1-u_2)a & -(\alpha+\delta)-\lambda & 0 \\ 0 & 0 & \alpha & -\mu-\lambda \end{vmatrix}$$

$$= (ky_1e^{-\lambda\tau_2}-\epsilon-\lambda)(gv_1-h-\lambda)(-\sigma-(1-u_1)\beta v_1-\lambda)\begin{vmatrix} -\sigma-\lambda & 0 & (1-u_1)\beta x_1 e^{-(m+\lambda)\tau_1} \\ (1-u_2)a & -(\alpha+\delta)-\lambda & 0 \\ 0 & \alpha & -\mu-\lambda \end{vmatrix}$$

$$-(ky_1e^{-\lambda\tau_2}-\epsilon-\lambda)(gv_1-h-\lambda)(1-u_1)\beta v_1 e^{-(m+\lambda)\tau_1}\begin{vmatrix} 0 & 0 & -(1-u_1)\beta x_1 \\ (1-u_2)a & -(\alpha+\delta)-\lambda & 0 \\ 0 & \alpha & -\mu-\lambda \end{vmatrix}$$

$$= (ky_1e^{-\lambda\tau_2}-\epsilon-\lambda)(gv_1-h-\lambda)(\sigma+(1-u_1)\beta v_1+\lambda)(\sigma+\lambda)\begin{vmatrix} -(\alpha+\delta)-\lambda & 0 \\ \alpha & -\mu-\lambda \end{vmatrix}$$

$$+(ky_1e^{-\lambda\tau_2}-\epsilon-\lambda)(gv_1-h-\lambda)(\sigma+(1-u_1)\beta v_1+\lambda)(1-u_2)a\begin{vmatrix} 0 & (1-u_1)\beta x_1 e^{-(m+\lambda)\tau_1} \\ \alpha & -\mu-\lambda \end{vmatrix}$$

$$+(ky_1e^{-\lambda\tau_2}-\epsilon-\lambda)(gv_1-h-\lambda)(1-u_1)(1-u_2)\beta v_1 a e^{-(m+\lambda)\tau_1}\begin{vmatrix} 0 & -(1-u_1)\beta x_1 \\ \alpha & -\mu-\lambda \end{vmatrix}$$

By calculating above expression, we have characteristic equation as

$$(ky_1e^{-(m+\lambda)\tau_2}-\epsilon-\lambda)(gv_1-h-\lambda)\Big[\lambda^4+a_1\lambda^3+a_2\lambda^2+a_3\lambda+a_4+(a_5\lambda+a_6)e^{-\lambda\tau_1}\Big]=0$$

where

$$\begin{aligned} a_1 &= \alpha+\delta+\mu+2\sigma+(1-u_1)\beta v_1, \\ a_2 &= (2\sigma+(1-u_1)\beta v_1)(\alpha+\delta+\mu)+(\sigma+(1-u_1)\beta v_1)\sigma+\mu(\alpha+\delta), \\ a_3 &= (2\sigma+(1-u_1)\beta v_1)(\alpha+\delta)\mu+(\sigma+(1-u_1)\beta v_1)\sigma(\alpha+\delta+\mu), \\ a_4 &= (\sigma+(1-u_1)\beta v_1)\sigma(\alpha+\delta)\mu, \\ a_5 &= -(1-u_1)(1-u_2)\beta a\alpha x_1 e^{-m\tau_1}, \\ a_6 &= -(1-u_1)(1-u_2)\beta a\alpha x_1(\sigma+(1-u_1)\beta v_1)e^{-m\tau_1} \\ &\quad +(1-u_1)^2(1-u_2)\beta^2 x_1 v_1 \alpha a e^{-m\tau_1}. \end{aligned} \tag{3.5.9}$$

Therefore, it gives $\lambda_1 = ky_1e^{-\lambda\tau_2}-\epsilon$ and $\lambda_2 = gv_1-h$.

First, we consider

$$\lambda_1 = ky_1e^{-\lambda\tau_2}-\epsilon. \tag{3.5.10}$$

For $\tau_2 = 0$, then $\lambda_1 = ky_1 - \epsilon$. Since $y_1 = \frac{\sigma\mu(\alpha+\delta)(R_0-1)}{(1-u_1)(1-u_2)\beta\alpha a}$, thus,

$$\begin{aligned}\lambda_1 &= k\left(\frac{\sigma\mu(\alpha+\delta)(R_0-1)}{(1-u_1)(1-u_2)\beta\alpha a}\right) - \epsilon \\ &= \frac{k\sigma\mu(\alpha+\delta)(R_0-1) - \epsilon(1-u_1)(1-u_2)\beta\alpha a}{(1-u_1)(1-u_2)\beta\alpha a}.\end{aligned}$$

So, we have

$$\lambda_1 < \frac{k\sigma\mu(\alpha+\delta)(1+\frac{(1-u_1)(1-u_2)\epsilon a\beta\alpha}{k\sigma\mu(\alpha+\delta)} - 1) - \epsilon(1-u_1)(1-u_2)\beta\alpha a}{(1-u_1)(1-u_2)\beta\alpha a} = 0,$$
$$\text{when } 1 \le R_0 \le 1 + \frac{(1-u_1)(1-u_2)\epsilon a\beta\alpha}{k\sigma\mu(\alpha+\delta)}.$$

Thus, $\lambda_1 < 0$, when $1 \le R_0 \le 1 + \frac{(1-u_1)(1-u_2)\epsilon a\beta\alpha}{k\sigma\mu(\alpha+\delta)}$.

This shows that $\lambda_1 < 0$ for $\tau_2 = 0$. Next, we consider the case when $\tau_2 > 0$. By letting $\lambda_1 = \omega i$ $(\omega > 0)$ be a purely imaginary root for some $\omega > 0$, we have

$$\begin{aligned}(i\omega) - ky_1 e^{-i\omega\tau_2} + \epsilon &= 0 \\ i\omega - ky_1(\cos(\omega\tau_2) - i\sin(\omega\tau_2)) + \epsilon &= 0 \\ (i\omega) + \epsilon &= ky_1(\cos(\omega\tau_2) - i\sin(\omega\tau_2)).\end{aligned}$$

Thus, this implies that $\epsilon = ky_1\cos(\omega\tau_2)$ and $\omega = -ky_1\sin(\omega\tau_2)$.
Then,

$$\begin{aligned}\omega^2 + \epsilon^2 &= (ky_1)^2(\cos^2(\omega\tau_2) + \sin^2(\omega\tau_2)) \\ \omega^2 &= (ky_1)^2 - \epsilon^2 \\ \omega^2 &= \left(\frac{k\sigma\mu(\alpha+\delta)(R_0-1)}{(1-u_1)(1-u_2)\beta\alpha a}\right)^2 - \epsilon^2.\end{aligned}$$

Since $1 < R_0 < 1 + \frac{(1-u_1)(1-u_2)\epsilon a\beta\alpha}{k\sigma\mu(\alpha+\delta)}$, then

$$\omega^2 < \left(\frac{k\sigma\mu(\alpha+\delta)\left(1+\frac{(1-u_1)(1-u_2)\epsilon a\beta\alpha}{k\sigma\mu(\alpha+\delta)} - 1\right)}{(1-u_1)(1-u_2)\beta\alpha a}\right)^2 - \epsilon^2 = 0$$

Thus, $\omega^2 < 0$ which is contradiction.

Next, suppose that $\lambda_1 = b + \omega i$ where b is positive real number and $\omega > 0$, we can write

$$\lambda_1 = h - \epsilon, \text{ where } h = ky_1 e^{-\lambda\tau_2}. \tag{3.5.11}$$

Then, b is positive real number, the magnitude of h is as follows

$$|h| = |ky_1 e^{-(b+\omega i)\tau_2}| = ky_1 e^{-b\tau_2}|e^{-i\omega\tau_2}|.$$

Since $e^{-\omega i\tau_2} = \cos(\omega\tau_2) - i\sin(\omega\tau_2)$, and $|e^{-i\omega\tau_2}| = 1$, then $|h| = ky_1 e^{-b\tau_2} \leq ky_1$.

(3.5.12)

Substituting y_1 into (3.5.12), we have

$$\begin{aligned} |h| &\leq \frac{k\sigma\mu(\alpha+\delta)(R_0-1)}{(1-u_1)(1-u_2)a\beta\alpha} \\ &< \frac{k\sigma\mu(\alpha+\delta)(1+\frac{(1-u_1)(1-u_2)\epsilon a\beta\alpha}{k\sigma\mu(\alpha+\delta)}-1)}{(1-u_1)(1-u_2)a\beta\alpha} = \epsilon. \end{aligned} \tag{3.5.13}$$

Thus, $|h| < \epsilon$ implies that $h \in B(0,\epsilon)$. If $h = D + Ci$ where $D > 0$, then h is complex number in the right-half of complex plane. However, if $h - \epsilon = D + Ci - \epsilon$, then $D - \epsilon$ is negative real part. Therefore, we have $h - \epsilon$ is a complex number in the left-half of complex plane, then consider the left hand side of the equation (3.5.11) as

$$\lambda_1 = b + \omega i. \tag{3.5.14}$$

Since we suppose that $b > 0$ and $\lambda_1 = h - \epsilon$, then λ_1 will be a complex number on the right-half of complex plane. We have

$$b + \omega i = D - \epsilon + Ci. \tag{3.5.15}$$

By assumption that $b > 0$, then $D - \epsilon < 0$. This is contradiction, because b can not be a positive real part.

Therefore, λ_1 has a negative real part, when $1 < R_0 < 1 + \dfrac{(1-u_1)(1-u_2)\epsilon a\beta\alpha}{k\sigma\mu(\alpha+\delta)}$.

Next, we consider $\lambda_2 = gv_1 - h$. If $1 < R_0 < 1 + \dfrac{h(1-u_1)\beta}{g\sigma}$, then

$$\lambda_2 = g\left(\frac{\sigma(R_0-1)}{(1-u_1)\beta}\right) - h$$

$$< \frac{g\sigma(1+\frac{h(1-u_1)\beta}{g\sigma}-1)}{(1-u_1)\beta} - h = 0.$$

Hence, $\lambda_2 < 0$. Thus, λ_2 is negative when $1 < R_0 < 1 + \dfrac{h(1-u_1)\beta}{g\sigma}$.
Next, we consider the characteristic equation where $\tau_1 > 0$,

$$\lambda^4 + a_1\lambda^3 + a_2\lambda^2 + a_3\lambda + a_4 + (a_5\lambda + a_6)e^{-\lambda\tau_1} = 0 \tag{3.5.16}$$

where $a_1 - a_6$ are defined in (3.5.9).
Thus, we have

$$|\lambda^4 + a_1\lambda^3 + a_2\lambda^2 + a_3\lambda + a_4|^2 = |a_5\lambda + a_6|^2|e^{-\lambda\tau_1}|^2. \tag{3.5.17}$$

Suppose (3.5.16) has a purely imaginary root $\lambda = i\omega$ $(\omega > 0)$, by substituting $\lambda = i\omega$ into (3.5.17) and separating the real and imaginary parts, we have

$$|(i\omega)^4 + a_1(i\omega)^3 + a_2(i\omega)^2 + a_3(i\omega) + a_4|^2 = |a_5(i\omega) + a_6|^2|e^{-i\omega\tau_1}|^2.$$

Since $|e^{-i\omega\tau_1}| = |\cos(-\omega\tau_1) + i\sin(-\omega\tau_1)| = \sqrt{\cos^2(\omega\tau_1) + \sin^2(\omega\tau_1)} = 1$, then we have

$$|\omega^4 - a_1\omega^3 i - a_2\omega^2 + a_3\omega i + a_4|^2 = |a_5\omega i + a_6|.^2 \tag{3.5.18}$$

Thus, we have

$$\begin{aligned}|\omega^4 - a_1\omega^3 i - a_2\omega^2 + a_3\omega i + a_4|^2 &= (\omega^4 - a_1\omega^3 i - a_2\omega^2 + a_3\omega i + a_4)(\omega^4 + a_1\omega^3 i \\ &\quad - a_2\omega^2 - a_3\omega i + a_4) \\ &= \omega^8 - a_2\omega^6 + a_4\omega^4 + a_1^2\omega^6 - a_1a_3\omega^4 - a_2\omega^6 \\ &\quad + a_2^2\omega^4 - a_2a_4\omega^2 - a_1a_3\omega^4 + a_3^2\omega^2 + a_4\omega^4 \\ &\quad - a_2a_4\omega^2 + a_4^2,\end{aligned} \tag{3.5.19}$$

and

$$|a_5\omega i + a_6|^2 = (a_5\omega i + a_6)(-a_5\omega i + a_6) = a_5^2\omega^2 + a_6^2. \tag{3.5.20}$$

Thus, equation (3.5.18) becomes

$$\omega^8 + D_1\omega^6 + D_2\omega^4 + D_3\omega^2 + D_4 = 0 \tag{3.5.21}$$

where

$$D_1 = -2a_2 + a_1^2,\ D_2 = 2a_4 - 2a_1a_3 + a_2^2,\ D_3 = a_3^2 - 2a_2a_4 - a_5^2,\ D_4 = a_4^2 - a_6^2. \tag{3.5.22}$$

We let $X = \omega^2$ and define a function $G(X)$ as the left-hand side of (3.5.21), the above equation can be simplified to

$$G(X) = X^4 + D_1X^3 + D_2X^2 + D_3X + D_4. \tag{3.5.23}$$

Therefore, if the characteristic equation (3.5.16) has a purely imaginary root ($\lambda = i\omega$), it is equivalent to the fact that $G(X) = 0$ has a positive real root ($X = \omega^2$)

Theorem 3.5.4. *If $G(X) = 0$ has no positive real roots, then the positive equilibrium point E_1 is locally asymptotically stable for any $\tau_1 > 0$.*

Proof. If $G(X) = 0$ has no positive real roots, we obtain that X can be zero or negative root. Since $X = \omega^2$, so ω can be either zero or bi for $b > 0$. But from the hypothesis that $\omega > 0$, we then have $\omega = bi$, implying that (3.5.16) have negative roots i.e. $\lambda = \omega i = (bi)i = -b$. Therefore, the equilibrium E_1 is locally asymptotically stable for any $\tau_1 > 0$ when $G(X) = 0$ has no positive real roots. □

Next, we consider E_1 being locally asymptotically stable for $[0, \tau_1^0)$ such that $\tau_1^0 = \min\{\tau_{1_n}^j | 1 \leq n \leq \tilde{n}\}$ where $\tilde{n}$ is the number of roots of $G(X)$.
Substituting $\lambda = i\omega$ into (3.5.16), we obtain the real part as

$$\omega^4 - a_2\omega^2 + a_4 + a_6\cos(\omega\tau_1) + a_5\omega\sin(\omega\tau_1) = 0 \tag{3.5.24}$$

and the imaginary part as

$$a_1\omega^3 - a_3\omega + a_6\sin(\omega\tau_1) - a_5\omega\cos(\omega\tau_1) = 0. \tag{3.5.25}$$

Next, we solve for $\cos(\omega\tau_1)$ and $\sin(\omega\tau_1)$ from equation (3.5.24) and (3.5.25). Assuming that $G(X) = 0$ has $(1 \leq \tilde{n} \leq 4)$ positive real roots, denoted by $X_n (1 \leq n \leq \tilde{n})$. As $\sqrt{X_n} = \omega$, (3.5.25) then becomes

$$a_1(\sqrt{X_n})^3 - a_3\sqrt{X_n} - a_5\cos(\sqrt{X_n}\tau_1) = -a_6\sin\sqrt{X_n}\tau_1.$$

Thus,

$$\sin(\sqrt{X_n}\tau_1) = \frac{a_3\sqrt{X_n} + a_5\cos(\sqrt{X_n}\tau_1) - a_1(\sqrt{X_n})^3}{a_6}. \tag{3.5.26}$$

Substituting (3.5.26) into (3.5.24), we have

$$\cos(\sqrt{X_n}\tau_1) = \frac{\left[(a_1a_5 - a_6)X_n^2 + (a_2a_6 - a_3a_5)X_n - a_4a_6\right]}{a_6^2 + a_5^2\sqrt{X_n}}. \tag{3.5.27}$$

Then, substitute (3.5.27) into (3.5.26), gives

$$\sin(\sqrt{X_n}\tau_1) = \frac{a_2a_5X_n + a_3a_6\sqrt{X_n} - a_5a_6X_n^2 - a_1a_6(\sqrt{X_n})^3 - a_4a_5}{a_6^2 + a_5^2\sqrt{X_n}}. \tag{3.5.28}$$

Let

$$\begin{aligned}
\cos(\sqrt{X_n}\tau_1) = Q_n &= \frac{\left[(a_1a_5 - a_6)X_n^2 + (a_2a_6 - a_3a_5)X_n - a_4a_6\right]}{a_6^2 + a_5^2\sqrt{X_n}} \\
\sin(\sqrt{X_n}\tau_1) = P_n &= \frac{a_2a_5X_n + a_3a_6\sqrt{X_n} - a_5a_6X_n^2 - a_1a_6(\sqrt{X_n})^3 - a_4a_5}{a_6^2 + a_5^2\sqrt{X_n}}.
\end{aligned} \tag{3.5.29}$$

Therefore, for the imaginary root $\lambda = i\omega$ of (3.5.16), we have two sequences as follows:

$$\tau_{1_n}^j = \begin{cases} \frac{1}{\sqrt{X_n}}(\arccos(Q_n) + 2j\pi), & \text{if } P_n \geq 0 \\ \frac{1}{\sqrt{X_n}}(2\pi - \arccos(Q_n) + 2j\pi), & \text{if } P_n < 0 \end{cases}$$

where $j = 0, 1, 2, 3, ...$ and $1 \leq n \leq \tilde{n}$.

Assuming $\tau_{1_n}^{(0)} = \min\{\tau_{1_n}^{(j)} | 1 \leq n \leq \tilde{n}, j = 0, 1, 2\}$, i.e., $\tau_{1_n}^{(0)}$ is the minimum value associated with the imaginary solution $i\omega_0$ of the characteristic equation (3.5.16).

Therefore, the characteristic equation (3.5.16) has a pair of purely imaginary roots $\pm i\sqrt{X_n}$. For every integer j and $1 \leq n \leq \tilde{n}$, define $\lambda_n^{(j)}(\tau_1) = \alpha_n^{(j)}(\tau_1) + i\omega_n^{(j)}(\tau_1)$ as the root of (3.5.16) near $\tau_{1_n}^{(j)}$, satisfying $\alpha_{1_n}^{(j)}(\tau_{1_n}^{(j)}) = 0$ and $\omega_n^{(j)}(\tau_{1_n}^{(j)}) = \sqrt{X_n}$. Then the following theorem is obtained.

Theorem 3.5.5. *If $G(X) = 0$ has some positive real roots, then E_1 is locally asymptotically stable for $\tau_1 \in [0, \tau_{1_n}^{(0)})$, when $\tau_{1_n}^{(0)} = min\{\tau_{1_n}^{(j)} | 1 \leq n \leq \tilde{n},\ j = 0, 1, 2, ...\}$.*

Proof. For $\tau_{1_n}^{(0)} = \min\{\tau_{1_n}^{(j)} \leq n \leq \tilde{n},\ j = 0, 1, 2, ...\}$, $G(X) = 0$ has no positive real roots when $\tau_1 \in [0, \tau_{1_n}^{(0)})$, which means that all the root of (3.5.16) have strictly negative real part when $\tau_1 \in [0, \tau_{1_n}^{(0)})$.
Therefore, E_1 is locally asymptotically stable for $\tau_1 \in [0, \tau_{1_n}^{(0)})$. □

Theorem 3.5.6. *If X_{n_0} is a simple root of $G(X) = 0$, then there is a Hopf bifurcation for the system as τ_1 increases past $\tau_{1_{n_0}}^{(0)}$.*

Proof. The characteristic equation (3.5.16) can be written into the following form:

$$f_0(\lambda) + f_1(\lambda)e^{-\lambda\tau_1} = 0, \tag{3.5.30}$$

where $f_0(\lambda) = \lambda^4 + a_1\lambda^3 + a_2\lambda^2 + a_3\lambda + a_4$, and $f_1(\lambda) = a_5\lambda + a_6$, and $f_0(\lambda)$ and $f_1(\lambda)$ are continuously differentiable to λ.

Next, we determine $\text{sign}\left\{\frac{dRe(\lambda)}{d\tau_1}\Big|_{\tau_1=\tau_{1_n}^{(0)}}\right\}$, where sign is the sign function and $Re(\lambda)$ is the real part of λ. We assume that $\lambda(\tau_1) = v(\tau_1) + i\omega(\tau_1)$ is the solution of (3.5.16) with respect to τ_1. Suppose that one of the roots of (3.5.30) is $\lambda(\tau_1) = \alpha(\tau_1) + i\omega(\tau_1)$, satisfying $\alpha(\tau_{1_0}) = 0$ and $\omega(\tau_{1_0}) = \omega_0$ for a positive real number τ_{1_0}.
Let

$$\phi(\omega) = |f_0(i\omega)|^2 - |f_1(i\omega)|^2. \tag{3.5.31}$$

Since

$$\begin{aligned}
|f_0(i\omega)|^2 &= (\overline{f_0(i\omega)})(f_0(i\omega)) \\
&= \omega^8 + a_1\omega^7 i - a_2\omega^6 - a_3\omega^5 i + a_4\omega^4 - a_1\omega^7 i + a_1^2\omega^6 + a_1a_2\omega^5 i \\
&\quad - a_1a_3\omega^4 - a_1a_4\omega^3 i - a_2\omega^6 - a_1a_2\omega^5 i + a_2^2\omega^4 + a_2a_3\omega^3 i \\
&\quad - a_2a_4\omega^2 + a_3\omega^5 i - a_1a_3\omega^4 - a_2a_3\omega^3 i + a_3^2\omega^2 + a_3a_4\omega i + a_4\omega^4 \\
&\quad + a_1a_4\omega^3 i - a_2a_4\omega^2 - a_3a_4\omega i + a_4^2.
\end{aligned} \tag{3.5.32}$$

Then,

$$\frac{d(|f_0(i\omega)|^2)}{d\omega} = 8\omega^7 + (6a_1^2 - 12a_2)\omega^5 + (4a_2^2 + 8a_4 - 8a_1a_3)\omega^3 + (2a_3^2 - 4a_2a_4)\omega. \tag{3.5.33}$$

And since $f_1(i\omega) = a_5(i\omega) + a_6 = a_5 i\omega + a_6$, then

$$\begin{aligned} |f_1(i\omega)|^2 &= (f_1(i\omega))(\overline{f_1(i\omega)}) \\ &= (a_5 i\omega + a_6)(-a_5 i\omega + a_6) \\ &= a_5^2\omega^2 + a_6. \end{aligned} \tag{3.5.34}$$

And, $\frac{d|f_1(i\omega)|^2}{d\omega} = 2a_5^2\omega$. □

Thus, we have

$$\begin{aligned} \frac{1}{2\omega}\frac{d\phi}{d\omega} &= \frac{1}{2\omega}\frac{d(|f_0(i\omega)|^2 - |f_1(i\omega)|^2)}{d\omega} \\ &= \frac{1}{2\omega}\left(\frac{d|f_0(i\omega)|^2}{d\omega} - \frac{d|f_1(i\omega)|^2}{d\omega}\right) \\ &= \frac{1}{2\omega}\left(-2Im(\overline{f_0(i\omega)}\dot{f}_0(i\omega)) + 2Im(\overline{f_1(i\omega)}\dot{f}_1(i\omega))\right) \\ &= Im\left[\frac{\dot{f}_1(i\omega)\overline{f_1(i\omega)}f_1(i\omega)}{\omega f_1(i\omega)} - \frac{\dot{f}_0(i\omega)\overline{f_0(i\omega)}f_0(i\omega)}{\omega f_0(i\omega)}\right] \\ &= Im\left[|f_1(i\omega)|^2\frac{\dot{f}_1(i\omega)}{\omega f_1(i\omega)} - |f_0(i\omega)|^2\frac{\dot{f}_0(i\omega)}{\omega f_0(i\omega)}\right]. \end{aligned} \tag{3.5.35}$$

Because $|f_0(i\omega_0)|^2 = |f_1(i\omega_0)|^2$, we have

$$\left(\frac{1}{2\omega}\frac{d\phi}{d\omega}\right)\Big|_{\omega=\omega_0} = |f_0(i\omega)|^2 Im\left[\frac{\dot{f}_1(i\omega_0)}{\omega_0 f_1(i\omega_0)} - \frac{\dot{f}_0(i\omega_0)}{\omega_0 f_0(i\omega_0)}\right]. \tag{3.5.36}$$

Next, differentiate both sides of (3.5.30) with respect to τ_1, we have

$$\dot{f}_0(\lambda)\frac{d\lambda}{d\tau_1} + \dot{f}_1(\lambda)\frac{d\lambda}{d\tau_1}e^{-\lambda\tau_1} - \left(\lambda + \tau_1\frac{d\lambda}{d\tau_1}\right)f_1(\lambda)e^{-\lambda\tau_1} = 0. \tag{3.5.37}$$

We can write (3.5.37) as

$$\begin{aligned} \left(\frac{d\lambda}{d\tau_1}\right)^{-1} &= \frac{\dot{f}_0(\lambda) + \dot{f}_1(\lambda)e^{-\lambda\tau_1} - f_1(\lambda)\tau_1 e^{-\lambda\tau_1}}{\lambda f_1(\lambda)e^{-\lambda\tau_1}} \\ &= \frac{\dot{f}_0(\lambda)e^{\lambda\tau_1} + \dot{f}_1(\lambda)}{\lambda f_1(\lambda)} - \frac{\tau_1}{\lambda}. \end{aligned} \tag{3.5.38}$$

Since $f_0(i\omega_0) + f_1(i\omega_0)e^{-i\omega_0\tau_1} = 0$, we obtain that

$$\begin{aligned} Re\left[\left(\frac{d\lambda}{d\tau_1}\right)^{-1}\Big|_{\tau_1=\tau_0}\right] &= Re\left[\frac{\dot{f}_0(i\omega_0)e^{i\omega_0\tau_1} + \dot{f}_1(i\omega_0)}{i\omega_0 f_1(i\omega_0)}\right] \\ &= Re\left[\frac{\dot{f}_0(i\omega_0)e^{i\omega_0\tau_1}}{i\omega_0 f_1(i\omega_0)} + \frac{\dot{f}_1(i\omega_0)}{i\omega_0 f_1(i\omega_0)}\right] \end{aligned}$$

$$= Re\left[-\frac{\dot{f}_0(i\omega_0)e^{i\omega_0\tau_1}}{i\omega_0 f_0(i\omega_0)e^{i\omega_0\tau_1}} + \frac{\dot{f}_1(i\omega_0)}{i\omega_0 f_1(i\omega_0)}\right]$$
$$= Re\left[\frac{\dot{f}_0(i\omega_0)e^{i\omega_0\tau_1}}{\omega_0 f_0(i\omega_0)e^{i\omega_0\tau_1}}(i) - \frac{\dot{f}_1(i\omega_0)}{\omega_0 f_1(i\omega_0)}(i)\right]$$
$$= Im\left[\frac{\dot{f}_1(i\omega_0)}{\omega_0 f_1(i\omega_0)} - \frac{\dot{f}_0(i\omega_0)}{\omega_0 f_0(i\omega_0)}\right]. \tag{3.5.39}$$

From (3.5.36) and (3.5.39), we have

$$sign\left[\frac{dRe(\lambda)}{d\tau_1}\bigg|_{\tau_1=\tau_0}\right] = \text{sign } Re\left[\left(\frac{d\lambda}{d\tau_1}\bigg|_{\tau_1=\tau_0}\right)\right]$$
$$= \text{sign } Re\left[\frac{d\lambda}{d\tau_1}\bigg|_{\tau_1=\tau_0}\right]^{-1}$$
$$= \text{sign } Re\left[Im\left[\frac{\dot{f}_1(i\omega_0)}{\omega_0 f_1(i\omega_0)} - \frac{\dot{f}_0(i\omega_0)}{\omega_0 f_0(i\omega_0)}\right]\right]$$
$$= \text{sign } Re\left[|f_0(i\omega)|^2 Im\left[\frac{\dot{f}_1(i\omega_0)}{\omega_0 f_1(i\omega_0)} - \frac{\dot{f}_0(i\omega_0)}{\omega_0 f_0(i\omega_0)}\right]\right]$$
$$= \text{sign}\left[\left(\frac{1}{2\omega}\times\frac{d\phi}{d\omega}\right)\bigg|_{\omega=\omega_0}\right]. \tag{3.5.40}$$

When $Re(\lambda) = \alpha_n^{(j)}(\tau_1)$, we have

$$\text{sign}\left[\frac{d\alpha_n^j(\tau_1)}{d\tau_1}\bigg|_{\tau_1=\tau_{1n}^j}\right] = \text{sign}\left[\left(\frac{dG}{dx}\right)\bigg|_{X=X_n}\right]. \tag{3.5.41}$$

As X_{n_0} is a simple root of $G(X)=0$, we know $\dot{G}(X_{n_0}) \neq 0$. From (3.5.41), we know $\left(\frac{d\alpha_{n_0}^{(0)}}{d\tau_1}\Big|_{\tau_1=\tau_{1n}^{(0)}} \neq 0\right)$. If $\frac{d\alpha_{n_0}^{(0)}}{d\tau_1}\Big|_{\tau_1=\tau_{1n}^{(0)}} < 0$, then we obtain that the root of (3.5.16) has positive real part when $\tau_1 \in [0, \tau_{1_{n_0}}^{(0)})$ which contrasts to Theorem 3.5.5. Hence, we can see that $\frac{d\alpha_{n_0}^{(0)}}{d\tau_1}\Big|_{\tau_1=\tau_{1n}^{(0)}} > 0$. When $\tau_1 = \tau_{1_{n_0}}^{(0)}$, except for the pair of purely imaginary root, the remaining roots of (3.5.16) have strictly negative real parts, so the system has Hopf bifurcation. This completes the proof. □

3.5.4 Global stability of immune-free equilibrium point

Theorem 3.5.7. *The immune-free equilibrium point E_1 is globally asymptotically stable when $1 < R_0 < 1 + \inf\{A_1, A_2\}$, where $A_1 = \frac{(1-u_1)(1-u_2)\epsilon a\beta\alpha}{k\sigma\mu(\alpha+\delta)}$ and $A_2 = \frac{(1-u_1)h\beta}{g\sigma}$.*

Proof. We consider the function $F(x) = x-1-\ln x$ $(x > 0)$. Note that $F(x) \geq 0, \forall x$ and that $F(x) = 0$ if and only if $x = 1$. We define a Lyapunov function L_1 as follows:

$$\begin{aligned}
L_1 = {} & x_1\left(\frac{x}{x_1} - 1 - \ln\frac{x}{x_1}\right) + e^{m\tau_1}y_1\left(\frac{y}{y_1} - 1 - \ln\frac{y}{y_1}\right) + \frac{(1-u_1)\beta x_1 v_1 c_1}{(\alpha+\delta)c_1}\left(\frac{c}{c_1} - 1 - \ln\frac{c}{c_1}\right) \\
& + \frac{(1-u_1)\beta x_1 v_1 v_1}{\alpha c_1}\left(\frac{v}{v_1} - 1 - \ln\frac{v}{v_1}\right) + \frac{(1-u_1)\beta x_1 v_1 \gamma w}{g\alpha c_1} + \frac{qe^{m\tau_1}z}{k} \\
& + (1-u_1)\beta x_1 v_1 \int_{t-\tau_1}^{t} G\left(\frac{x(s)v(s)}{x_1 v_1}\right)ds + qe^{m\tau_1}\int_{t-\tau_2}^{t} y(s)z(s)ds. \qquad (3.5.42)
\end{aligned}$$

$$\begin{aligned}
\frac{dL_1}{dt} = {} & \left(1 - \frac{x_1}{x}\right)\left(\Lambda - \sigma x - (1-u_1)\beta x v\right) + e^{m\tau_1}\left(1 - \frac{y_1}{y}\right)\Big((1-u_1)\beta e^{-m\tau_1}x(t-\tau_1)v(t-\tau_1) \\
& - \sigma y - qyz\Big) + \frac{(1-u_1)\beta x_1 v_1 c_1}{(\alpha+\delta)}\left(1 - \frac{c_1}{c}\right)\Big((1-u_2)ay - (\alpha+\delta)c\Big) \\
& + \frac{(1-u_1)\beta x_1 v_1 c_1}{(\alpha+\delta)}\left(1 - \frac{v_1}{v}\right)\Big(\alpha c - \gamma v w - \mu v\Big) + \frac{(1-u_1)\beta x_1 v_1 \gamma}{g\alpha c_1}\Big(gvw - hw\Big) \\
& + \frac{qe^{m\tau_1}}{k}\Big(ky(t-\tau_2)z(t-\tau_2) - \epsilon z\Big) \\
& + (1-u_1)\beta x_1 v_1\left(\frac{xv}{x_1 v_1} - \frac{x(t-\tau_1)v(t-\tau_1)}{x_1 v_1} + \ln\frac{x(t-\tau_1)v(t-\tau_1)}{xv}\right) \\
& + qe^{m\tau_1}\Big(yz - y(t-\tau_2)z(t-\tau_2)\Big).
\end{aligned}$$

Since $\dfrac{dx_1}{dt} = 0$, then $\Lambda = \sigma x_1 + (1-u_1)\beta x_1 v_1$. Therefore,

$$\begin{aligned}
\frac{dL_1}{dt} = {} & \left(1 - \frac{x_1}{x}\right)\Big(\sigma x_1 + (1-u_1)\beta x_1 v_1 - \sigma - (1-u_1)\beta x v\Big) \\
& + (1-u_1)\beta x(t-\tau_1)v(t-\tau_1) - \sigma e^{m\tau_1}y - qe^{m\tau_1}yz - \frac{y_1}{y}(1-u_1)\beta x(t-\tau_1)v(t-\tau_1) \\
& + \sigma e^{m\tau_1}y_1 + qe^{m\tau_1}y_1 z + \frac{(1-u_1)(1-u_2)\beta x_1 v_1 ay}{(\alpha+\delta)c_1} - (1-u_1)\beta x_1 v_1\frac{c}{c_1} \\
& - \frac{(1-u_1)(1-u_2)\beta x_1 v_1 a y c_1}{(\alpha+\delta)c_1 c} + (1-u_1)\beta x_1 v_1 + (1-u_1)\beta x_1 v_1\frac{c}{c_1} \\
& - \frac{(1-u_1)\beta x_1 v_1 \gamma v w}{\alpha c_1} - \frac{(1-u_1)\beta x_1 v_1 \mu v}{\alpha c_1} - \frac{(1-u_1)\beta x_1 v_1^2 \alpha c}{\alpha c_1 v} \\
& + \frac{(1-u_1)\beta x_1 v_1^2 \gamma v w}{\alpha c_1 v} + \frac{(1-u_1)\beta x_1 v_1^2 \mu}{\alpha c_1} + \frac{(1-u_1)\beta x_1 v_1 v w}{\alpha c_1} \\
& - \frac{(1-u_1)\beta x_1 v_1 \gamma h w}{g\alpha c_1} + \frac{qe^{m\tau_1}ky(t-\tau_2)z(t-\tau_2)}{k} - \frac{qe^{m\tau_1}\epsilon z}{k} \\
& + (1-u_1)\beta x_1 v_1\left(\frac{xv}{x_1 v_1} - \frac{x(t-\tau_1)v(t-\tau_1)}{x_1 v_1} + \ln\frac{x(t-\tau_1)v(t-\tau_1)}{xv}\right) \\
& + qe^{m\tau_1}yz - qe^{m\tau_1}y(t-\tau_2)z(t-\tau_2).
\end{aligned}$$

$$\frac{dL_1}{dt} = -\sigma\frac{(x-x_1)^2}{x} + 2(1-u_1)\beta x_1 v_1 - (1-u_1)\beta x_1 v_1\frac{x_1}{x} + (1-u_1)\beta x_1 v$$

$$+(1-u_1)\beta x(t-\tau_1)v(t-\tau_1)-\sigma e^{m\tau_1}y-\frac{y_1}{y}(1-u_1)\beta x(t-\tau_1)v(t-\tau_1)$$
$$+\sigma e^{m\tau_1}y_1+qe^{m\tau_1}y_1z+\frac{(1-u_1)(1-u_2)\beta x_1v_1ay}{(\alpha+\delta)c_1}$$
$$-\frac{(1-u_1)(1-u_2)\beta x_1v_1ayc_1}{(\alpha+\delta)c_1c}-\frac{(1-u_1)\beta x_1v_1\mu v}{\alpha c_1}-\frac{(1-u_1)\beta x_1v_1^2c}{c_1v}$$
$$+\frac{(1-u_1)\beta x_1v_1^2\gamma w}{\alpha c_1}+\frac{(1-u_1)\beta x_1v_1^2\mu}{\alpha c_1}-\frac{(1-u_1)\beta x_1v_1\gamma hw}{g\alpha c_1}-\frac{qe^{m\tau_1}\epsilon z}{k}$$
$$+(1-u_1)\beta x_1v_1\bigg(-\frac{x(t-\tau_1)v(t-\tau_1)}{x_1v_1}+\ln\frac{x(t-\tau_1)v(t-\tau_1)}{xv}\bigg). \tag{3.5.43}$$

Since $c_1=\dfrac{(1-u_2)ay_1}{\alpha+\delta}$, we have $\dfrac{(1-u_1)(1-u_2)\beta x_1v_1ayc_1}{(\alpha+\delta)c_1c}=\dfrac{(1-u_1)\beta x_1v_1yc_1}{y_1c}$.
Since $v_1=\dfrac{\alpha c_1}{\mu}$, then $\dfrac{(1-u_1)\beta x_1v_1\mu v_1}{\alpha c_1}=(1-u_1)\beta x_1v_1$ and since $\dfrac{dy_1}{dt}=0$, we have $(1-u_1)\beta x_1v_1=\sigma y_1e^{m\tau_1}$. Then,

$$\frac{dL_1}{dt}=-\sigma\frac{(x-x_1)^2}{x}+(1-u_1)\beta x_1v_1\bigg(4-\frac{x_1}{x}-\frac{y_1x(t-\tau_1)v(t-\tau_1)}{yx_1v_1}-\frac{yc_1}{y_1c}-\frac{v_1c}{vc_1}$$
$$+\ln\frac{x(t-\tau_1)v(t-\tau_1)}{xv}\bigg)-\sigma e^{m\tau_1}y+qe^{m\tau_1}y_1z+\frac{(1-u_1)(1-u_2)\beta x_1v_1ay}{(\alpha+\delta)c_1}$$
$$+\frac{(1-u_1)\beta x_1v_1\gamma wv_1}{\alpha c_1}-\frac{(1-u_1)\beta x_1v_1\gamma hw}{g\alpha c_1}-\frac{qe^{m\tau_1}\epsilon z}{k}. \tag{3.5.44}$$

Substituting $x_1=\dfrac{\sigma\mu(\alpha+\delta)}{(1-u_1)(1-u_2)\beta e^{-m\tau_1}a\alpha}$, $c_1=\dfrac{(1-u_2)ay_1}{\alpha+\delta}$ and $v_1=\dfrac{\alpha c_1}{\mu}$ into $\dfrac{(1-u_1)(1-u_2)\beta x_1v_1ay}{(\alpha+\delta)c_1}=\sigma e^{m\tau_1}y$.

We have $v_1=\frac{\sigma(R_0-1)}{(1-u_1)\beta}$ from $1<R_0<1+\dfrac{(1-u_1)g\beta}{g\sigma}$ then $v_1<\dfrac{h}{g}$ and $y_1=\dfrac{(\alpha+\delta)\sigma\mu(R_0-1)}{(1-u_1)(1-u_2)\beta a\alpha}$ from $1<R_0<\dfrac{(1-u_1)(1-u_2)\epsilon a\beta\alpha}{k\sigma\mu(\alpha+\delta)}$, we have $y_1<\dfrac{\epsilon}{k}$.
Then,

$$\frac{dL_1}{dt}=-\sigma\frac{(x-x_1)^2}{x}+(1-u_1)\beta x_1v_1\bigg(4-\frac{x_1}{x}-\frac{y_1x(t-\tau_1)v(t-\tau_1)}{yx_1v_1}-\frac{yc_1}{y_1c}-\frac{v_1c}{vc_1}$$
$$+\ln\frac{x(t-\tau_1)v(t-\tau_1)}{xv}\bigg)+qe^{m\tau_1}z(y_1-\frac{\epsilon}{k})+\frac{(1-u_1)\beta x_1v_1\gamma w}{\alpha c_1}(v_1-\frac{h}{g}). \tag{3.5.45}$$

We obtain that $\dfrac{dL}{dt}<0$ when $1<R_0<1+\inf\{A_1,A_2\}$, where $A_1=\dfrac{(1-u_1)(1-u_2)\epsilon a\beta\alpha}{k\sigma\mu(\alpha+\delta)}$ and $A_2=\dfrac{(1-u_1)h\beta}{g\sigma}$ and $\dfrac{dL}{dt}=0$ at E_1. Therefore, E_1 is globally asymptotically stable when $1<R_0<1+\inf\{A_1,A_2\}$, where $A_1=\dfrac{(1-u_1)(1-u_2)\epsilon a\beta\alpha}{k\sigma\mu(\alpha+\delta)}$ and $A_2=\dfrac{(1-u_1)h\beta}{g\sigma}$. □

3.5.5 Global stability of immune-activated equilibrium point

Theorem 3.5.8. *The immune-activated equilibrium point E_2 is globally asymptotically stable when $R_0 > 1$ and $A > B$ (where A and B are defined in the proof).*

Proof. We consider the function $F(x) = x-1-\ln x$ $(x > 0)$. Note that $F(x) \geq 0, \forall x$ and that $F(x) = 0$ if and only if $x = 1$. We define a Lyapunov function L_2 as follows:

$$\begin{aligned}
L_2 = {} & x_2\left(\frac{x}{x_2} - 1 - \ln\frac{x}{x_2}\right) + e^{m\tau_1}y_2\left(\frac{y}{y_2} - 1 - \ln\frac{y}{y_2}\right) + \left(\frac{(1-u_1)\beta x_2 v_2}{(\alpha+\delta)c_2}\right)c_2\left(\frac{c}{c_2} - 1 - \ln\frac{c}{c_2}\right) \\
& + \left(\frac{(1-u_1)\beta x_2 v_2}{\alpha c_2}\right)v_2\left(\frac{v}{v_2} - 1 - \ln\frac{v}{v_2}\right) + \left(\frac{(1-u_1)\beta\gamma x_2 v_2}{\alpha g c_2}\right)w_2\left(\frac{w}{w_2} - 1 - \ln\frac{w}{w_2}\right) \\
& + \left(\frac{qe^{m\tau_1}}{k}\right)z_2\left(\frac{z}{z_2} - 1 - \ln\frac{z}{z_2}\right) + (1-u_1)\beta x_2 v_2\int_{t-\tau_1}^{t} G\left(\frac{x(\theta)v(\theta)}{x_2 v_2}\right)d\theta \\
& + qe^{m\tau_1}y_2 z_2\int_{t-\tau_2}^{t} G\left(\frac{y(\theta)z(\theta)}{y_2 z_2}\right)d\theta. \qquad (3.5.46)
\end{aligned}$$

Then,

$$\begin{aligned}
\frac{dL_2}{dt} = {} & \left(1 - \frac{x_2}{x}\right)\Big(\Lambda - \sigma x(t) - (1-u_1)\beta x(t)v(t)\Big) \\
& + e^{m\tau_1}\left(1 - \frac{y_2}{y}\right)\Big((1-u_1)\beta e^{-m\tau_1}x(t-\tau_1)v(t-\tau_1) - \sigma y(t) - qy(t)z(t)\Big) \\
& + \left(\frac{(1-u_1)\beta x_2 v_2}{(\alpha+\delta)c_2}\right)\left(1 - \frac{c_2}{c}\right)\Big((1-u_2)ay(t) - \alpha c(t) - \delta c(t)\Big) \\
& + \left(\frac{(1-u_1)\beta x_2 v_2}{\alpha c_2}\right)\left(1 - \frac{v_2}{v}\right)\Big(\alpha c(t) - \gamma v(t)w(t) - \mu v(t)\Big) \\
& + \left(\frac{(1-u_1)\beta\gamma x_2 v_2}{\alpha g c_2}\right)\left(1 - \frac{w_2}{w}\right)\Big(gv(t)w(t) - hw(t)\Big) \\
& + \left(\frac{qe^{m\tau_1}}{k}\right)\left(1 - \frac{z_2}{z}\right)\Big(ky(t-\tau_2)z(t-\tau_2) - \epsilon z(t)\Big) \\
& + (1-u_1)\beta x_2 v_2\left(\frac{x(t)v(t)}{x_2 v_2} - \frac{x(t-\tau_1)v(t-\tau_1)}{x_2 v_2} + \ln\frac{x(t-\tau_1)v(t-\tau_1)}{x(t)v(t)}\right) \\
& + qe^{m\tau_1}y_2 z_2\left(\frac{y(t)z(t)}{y_2 z_2} - \frac{y(t-\tau_2)z(t-\tau_2)}{y_2 z_2} + \ln\frac{y(t-\tau_2)z(t-\tau_2)}{y(t)z(t)}\right). \qquad (3.5.47)
\end{aligned}$$

Since $\dfrac{dx_2}{dt} = 0$ then $\Lambda = \sigma x_2 + (1-u_1)\beta x_2 v_2$ and $y_2 = \dfrac{\epsilon}{k}$, we have

$$\begin{aligned}
\frac{dL_2}{dt} = {} & -\sigma\frac{(x-x_2)^2}{x} - \frac{x_2}{x}(1-u_1)\beta x_2 v_2 + (1-u_1)\beta x_2 v + (1-u_1)\beta x_2 v_2 - \sigma e^{m\tau_1}y \\
& - \frac{y_2}{y}(1-u_1)\beta x(t-\tau_1)v(t-\tau_1) + \sigma^{m\tau_1}y_2 + \frac{(1-u_1)(1-u_2)\beta x_2 v_2 ay}{(\alpha+\delta)c_2} \\
& - (1-u_1)\beta x_2 v_2\frac{c}{c_2} - \frac{(1-u_1)(1-u_2)\beta x_2 v_2 ay}{(\alpha+\delta)c} + (1-u_1)\beta x_2 v_2
\end{aligned}$$

$$+\left(\frac{(1-u_1)\beta x_2 v_2}{\alpha c_2}\right)\left(1-\frac{v_2}{v}\right)\left(\alpha c(t)-\gamma v(t)w(t)-\mu v(t)\right)$$
$$+\left(\frac{(1-u_1)\beta\gamma x_2 v_2}{\alpha g c_2}\right)\left(1-\frac{w_2}{w}\right)\left(gv(t)w(t)-hw(t)\right)$$
$$-\frac{z_2}{z}qe^{m\tau_1}y(t-\tau_2)z(t-\tau_2)+qe^{m\tau_1}y_2z_2+(1-u_1)\beta x_2v_2\ln\frac{x(t-\tau_1)v(t-\tau_1)}{xv}$$
$$+qe^{m\tau_1}y_2z_2\ln\frac{y(t-\tau_2)z(t-\tau_2)}{y(t)z(t)}. \tag{3.5.48}$$

$$\frac{dL_2}{dt}=-\sigma\frac{(x-x_2)^2}{x}+(1-u_1)\beta x_2v_2\left(2-\frac{x_2}{x}-\frac{y_2}{y}\frac{x(t-\tau_1)v(t-\tau_1)}{x_2v_2}-\frac{c}{c_2}+\ln\frac{x(t-\tau_1)v(t-\tau_1)}{xv}\right)$$
$$+qe^{m\tau_1}y_2z_2\left(1-\frac{z_2}{z}\frac{y(t-\tau_2)z(t-\tau_2)}{y_2z_2}+\ln\frac{y(t-\tau_2)z(t-\tau_2)}{yz}\right)+(1-u_1)\beta x_2v$$
$$-\sigma e^{m\tau_1}y+\sigma e^{m\tau_1}y_2+\frac{(1-u_1)(1-u_2)\beta x_2v_2ay}{(\alpha+\delta)c_2}-\frac{(1-u_1)(1-u_2)\beta x_2v_2ay}{(\alpha+\delta)c}$$
$$+\left(\frac{(1-u_1)\beta x_2v_2}{\alpha c_2}\right)\left(1-\frac{v_2}{v}\right)\left(\alpha c(t)-\gamma v(t)w(t)-\mu v(t)\right)$$
$$+\left(\frac{(1-u_1)\beta r x_2v_2}{\alpha g c_2}\right)\left(1-\frac{w_2}{w}\right)\left(gv(t)w(t)-hw(t)\right). \tag{3.5.49}$$

From $\frac{dy_2}{dt}=0$ and $\frac{dc_2}{dt}=0$, we have $(1-u_1)\beta x_2v_2-qy_2z_2e^{m\tau_1}=\sigma e^{m\tau_1}y_2$ and $(1-u_2)ay_2=(\alpha+\delta)c_2$. Then,

$$\frac{dL_2}{dt}=-\sigma\frac{(x-x_2)^2}{x}+(1-u_1)\beta x_2v_2\left(3-\frac{x_2}{x}-\frac{y_2}{y}\frac{x(t-\tau_1)v(t-\tau_1)}{x_2v_2}-\frac{c}{c_2}\right.$$
$$\left.+\ln\frac{x(t-\tau_1)v(t-\tau_1)}{xv}-\frac{c_2y}{cy_2}\right)+qe^{m\tau_1}y_2z_2\left(2-\frac{y_2}{y}-\frac{y(t-\tau_2)z(t-\tau_2)}{y_2z}\right.$$
$$\left.+\ln\frac{y(t-\tau_2)z(t-\tau_2)}{yz}\right)+\frac{qe^{m\tau_1}y_2^2z_2}{y}+(1-u_1)\beta x_2v+qz_2e^{m\tau_1}y-2qe^{m\tau_1}y_2z_2$$
$$+(1-u_1)\beta x_2v_2\frac{c}{c_2}-\frac{(1-u_1)\beta x_2v_2}{\alpha c_2}\gamma vw-(1-u_1)\beta x_2v_2\frac{cv_2}{c_2v}$$
$$+\frac{(1-u_1)\beta x_2v_2^2\gamma w}{\alpha c_2}+\frac{(1-u_1)\beta x_2v_2^2\mu}{\alpha c_2}-\frac{(1-u_1)\beta x_2v_2\mu v}{\alpha c_2}$$
$$+\frac{(1-u_1)\beta x_2v_2\gamma vw}{\alpha c_2}-\frac{(1-u_1)\beta x_2v_2\gamma hw}{\alpha g c_2}-\frac{(1-u_1)\beta x_2v_2\gamma w_2v}{\alpha c_2}$$
$$+\frac{(1-u_1)\beta x_2v_2\gamma hw_2}{\alpha g c_2}. \tag{3.5.50}$$

And since, $\dfrac{dv_2}{dt}=0$, then $\gamma w_2=\dfrac{\alpha c_2-\mu v_2}{v_2}$ and $v_2=\dfrac{h}{g}$, then

$$\frac{dL_2}{dt}=-\sigma\frac{(x-x_2)^2}{x}+(1-u_1)\beta x_2v_2\left(4-\frac{x_2}{x}-\frac{y_2}{y}\frac{x(t-\tau_1)v(t-\tau_1)}{x_2v_2}-\frac{cv_2}{c_2v}\right.$$
$$\left.-\frac{c_2y}{cy_2}+\ln\frac{x(t-\tau_1)v(t-\tau_1)}{xv}\right)+qe^{m\tau_1}y_2z_2\left(2-\frac{y_2}{y}-\frac{y(t-\tau_2)z(t-\tau_2)}{y_2z}\right.$$
$$\left.+\ln\frac{y(t-\tau_2)z(t-\tau_2)}{yz}\right)+\frac{qe^{m\tau_1}y_2^2z_2}{y}+qe^{m\tau_1}yz_2-2qe^{m\tau_1}y_2z_2. \tag{3.5.51}$$

Let $A=\sigma\frac{(x-x_2)^2}{x}-(1-u_1)\beta x_2v_2\left(4-\frac{x_2}{x}-\frac{y_2}{y}\frac{x(t-\tau_1)v(t-\tau_1)}{x_2v_2}-\frac{cv_2}{c_2v}-\frac{c_2y}{cy_2}+\ln\frac{x(t-\tau_1)v(t-\tau_1)}{xv}\right)-$

$qe^{m\tau_1}y_2z_2\left(2-\frac{y_2}{y}-\frac{y(t-\tau_2)z(t-\tau_2)}{y_2z}+\ln\frac{y(t-\tau_2)z(t-\tau_2)}{yz}\right)+2qe^{m\tau_1}y_2z_2$ and $B=qe^{m\tau_1}yz_2+\frac{qe^{m\tau_1}y_2^2z_2}{y}$. Thus, the global stability of immune activate steady state equilibrium point is globally asymptotically stable when $R_0>1$ and $A>B$. □

3.6 Numerical simulations

In this section, the numerical simulations of system (3.1.1)-(3.1.6) are performed with the use of parameters values from Table 1. We divide the results into 4 cases as below to investigate the impact of controls (u_1 and u_2) and to explore the dynamics of model in the different values of time delays.

(i) when u_1 varies, $u_2=0.5$ and $\tau_1=\tau_2=0$

(ii) when u_2 varies, $u_1=0.5$ and $\tau_1=\tau_2=0$

(iii) when τ_1 varies and $\tau_2=5$

(iv) when τ_2 varies and $\tau_1=5$.

3.6.1 Case I : when u_1 varies, $u_2=0.5$ and $\tau_1=\tau_2=0$

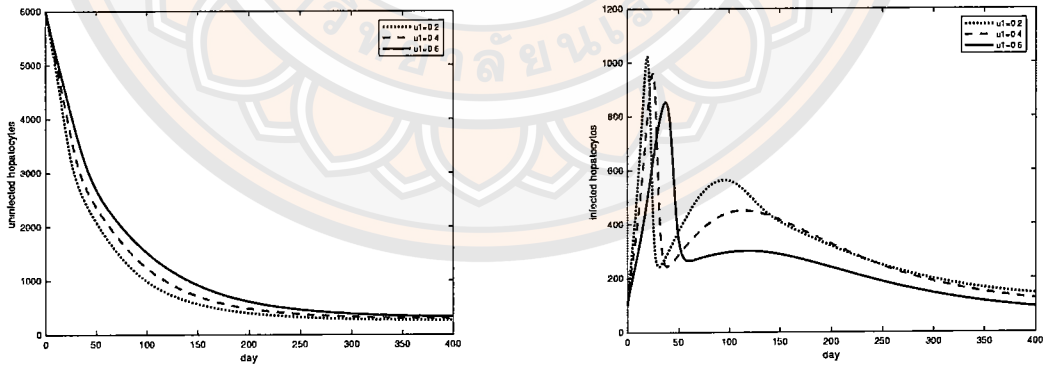

(a) (b)

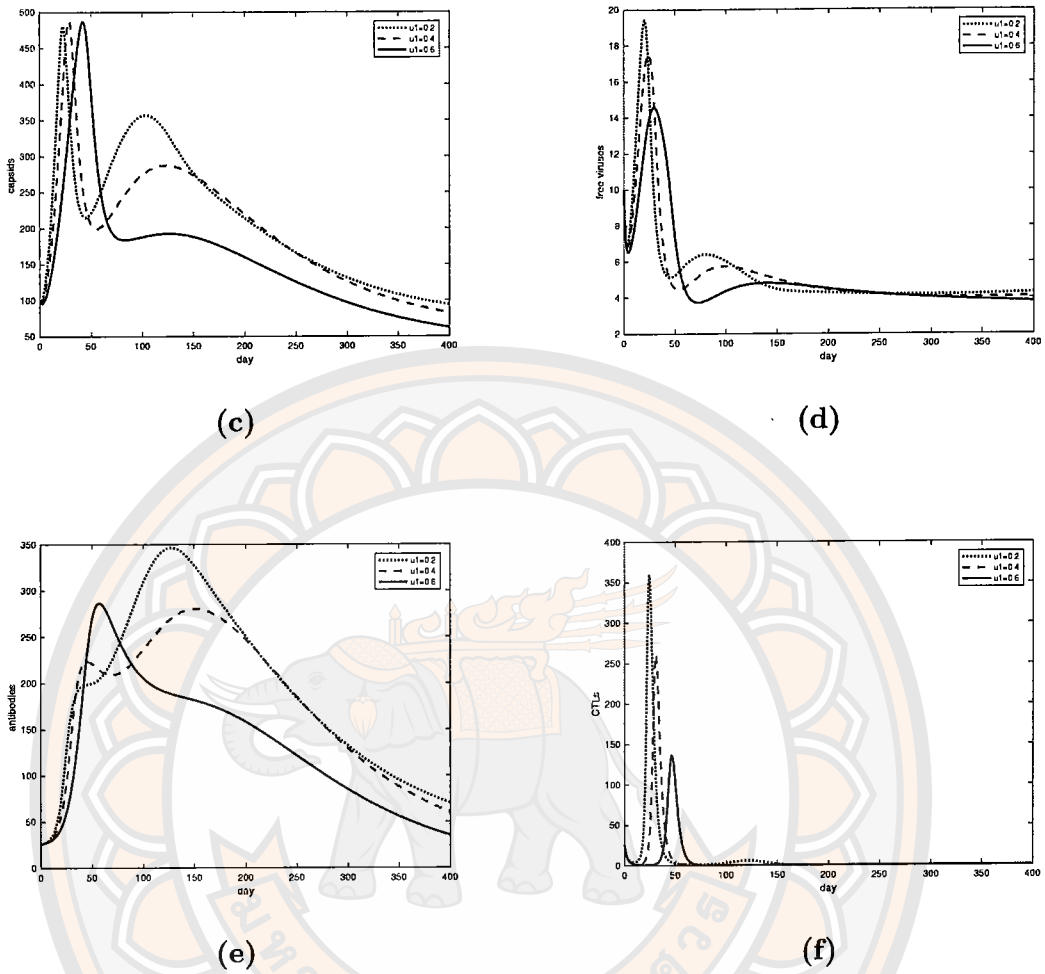

Figure 15 Simulation results of the HBV model (3.1.1)-(3.1.6) with both controls ($u_1 = 0.2, 0.4, 0.6$ and $u_2 = 0.5$)when $\tau_1 = \tau_2 = 0$. (a) the concentration of uninfected hepatocytes, (b) the concentration of infected hepatocytes, (c) the concentration of intracellular HBV DNA-containing capsids, (d) the concentration of free viruses, (e) the concentration of antibodies and (f) the concentration of CTLs. u_1 is the efficiency of drug therapy in blocking new infection and u_2 is the efficiency of drug therapy in inhibiting viral production.

Figure 15a - 15f shows the dynamics of the concentration of the uninfected hepatocytes, infected hepatocytes, intracellular HBV DNA-containing capsid, free viruses, antibodies, and CTLs, respectively where they are treated by u_1 and u_2 representing the efficiency of drug therapy in blocking new infection and the

efficiency of drug therapy in inhibiting viral production, respectively. We choose $u_1 = 0.2,\ 0.4,\ 0.6$ and $u_2 = 0.5$. From 15a, we can see that a larger value of u_1 can slow down the decline of the concentration of uninfected hepatocytes when compare with the smaller u_1. At the end, they tend to reach the same equilibrium value. Figures 15b and 15c give a similar pattern, the concentration of infected hepatocytes and intracellular HBV DNA-containing capsids rises since the beginning for all values of u_1. Figure 15b shows that the greater value of u_1, the smaller the peak of the concentration of infected hepatocytes with a slight slower time for the peak to occur. In the case when $u_1 = 0.2$ and 0.4, it tends to give the second peak in the period of 80th to 150th day, whereas when $u_1 = 0.6$ there is no second peak. Further, it reaches lower equilibrium value when compare with smaller u_1. The different of Figure 15c to Figure 15b is that the first peak of all three cases are at the same level. At the start in Figure 15d, the concentration of free viruses decreases for a few days and goes up sharply to reach a peak. When u_1 increases, the peak height is smaller, respectively with slower time for the peak to occur and reaches the smaller equilibrium value. Further, for the case $u_1 = 0.2$ and 0.4, the second peak is observed between 50th-150th day. Figure 15e shows interesting results i.e. there are two peaks of the concentration of antibodies when $u_1 = 0.2$ and 0.4, where their second peak is larger than their first peak. Only one peak of the concentration of antibodies is obtained for $u_1 = 0.6$. Time for the peak to occur is slightly slower when u_1 increases. The dynamics tends to reach lower equilibrium value with the larger value of u_1. Interestingly, Figure 15f shows a significant reduction of the concentration of CTLs and a slower time for the peak to occur when u_1 increases. Further, in the case of $u_1 = 0.2$, on the 100th day, the concentration of CTLs rise again to reach a small peak ranging the period of 50 days then goes down to zero. Overall, from the results above u_1 has shown to play a main role in significantly reducing the concentration of infected hepatocytes, free viruses and CTLs.

3.6.2 Case II : when u_2 varies, $u_1 = 0.5$ and $\tau_1 = \tau_2 = 0$

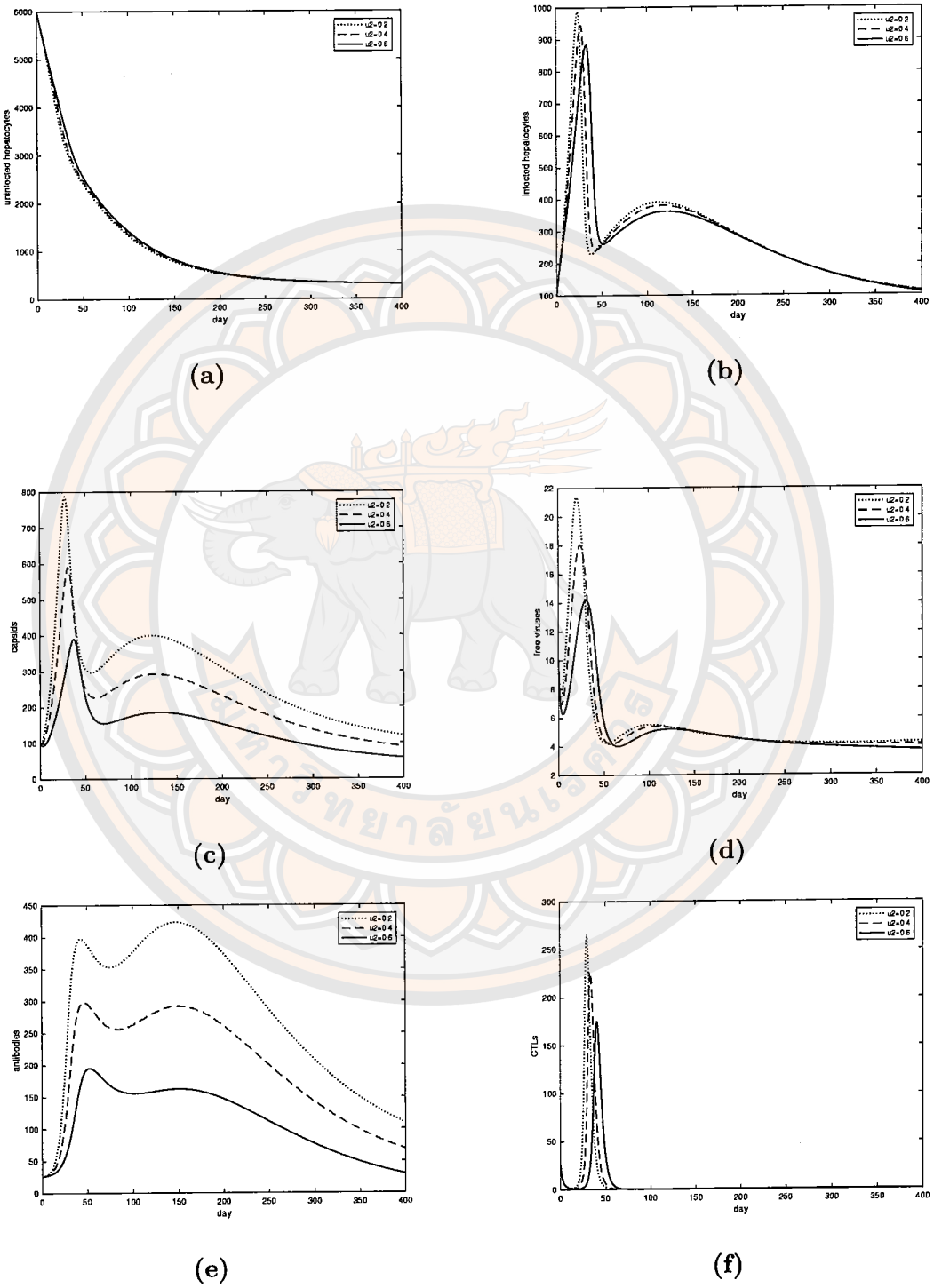

Figure 16 Simulation results of the HBV model (3.1.1)-(3.1.6) with both controls ($u_2 = 0.2, 0.4, 0.6$ and $u_1 = 0.5$) when $\tau_1 = \tau_2 = 0$. (a) the concentration of uninfected hepatocytes, (b) the concentration of infected hepatocytes, (c) the concentration of intracellular HBV DNA-containing capsids, (d) the concentration of free viruses, (e) the concentration of antibodies and (f) the concentration of CTLs. u_1 is the efficiency of drug therapy in blocking new infection and u_2 is the efficiency of drug therapy in inhibiting viral production.

In Figure 16a - 16f, the value of u_2 is varied by choosing $u_2 = 0.2, 0.4, 0.6$ and $u_1 = 0.5$. In Figure 16a, our results show that with an increase of u_2, the concentration of uninfected hepatocytes decreases slightly slower than the concentration of the smaller u_2 and it tends towards the same equilibrium value at the end. Figure 16b demonstrates double peaks of the concentration of infected hepatocytes where the higher value of u_2, the lower peak height for both peaks. It reaches a peak at 1000 cells/ml in the case $u_2 = 0.2$, whereas it reaches a peak at less than 900 cells/ml for $u_2 = 0.6$. After the first peak, they drop down to between 200-300 cells/ml and gradually rise up again as the second peak on approximately 100th day. Figure 16c gives a very interesting result i.e. with $u_2 = 0.2, 0.4$ and 0.6, the concentration of intracellular HBV DNA-containing capsids go up to reach the peak at 800 cells/ml, 600 cells/ml and 400cells/ml, respectively. Although when $u_2 = 0.2$ and $u_2 = 0.4$, it tends to give the second peak in the period of 100th to 150th day, with $u_2 = 0.6$ there is no second peak. Further, with the larger value of u_2, it tends to reach a lower equilibrium value. Figure 16d shows a significant decrease of the concentration of free viruses when u_2 increases, and time for the peak to occur is slightly slower. Figure 16e shows the concentration of antibodies increases from the beginning for all u_2 values, there is a double peak for $u_2 = 0.2$, it reaches the first peak at 400 cells/ml on 45th day and slightly declines to 350 cells/ml then it rises up again to the higher second peak. At $u_2 = 0.4$, the double peak is smaller than the case of u_2 and than its first peak. With higher value of u_2, the concentration of antibodies decreases largely, respectively and tends to reach lower equilibrium value. Figure 16f shows that when u_2 increases, the

concentration of CTLs decreases significantly, and the time for the peak to occur is slightly slower, respectively. On the whole, from the results above u_2 has shown to play a main role in greatly reducing the concentration of intracellular HBV DNA-containing capsids, free viruses, antibodies and CTLs.

3.6.3 Case III : when τ_1 varies and $\tau_2 = 5$

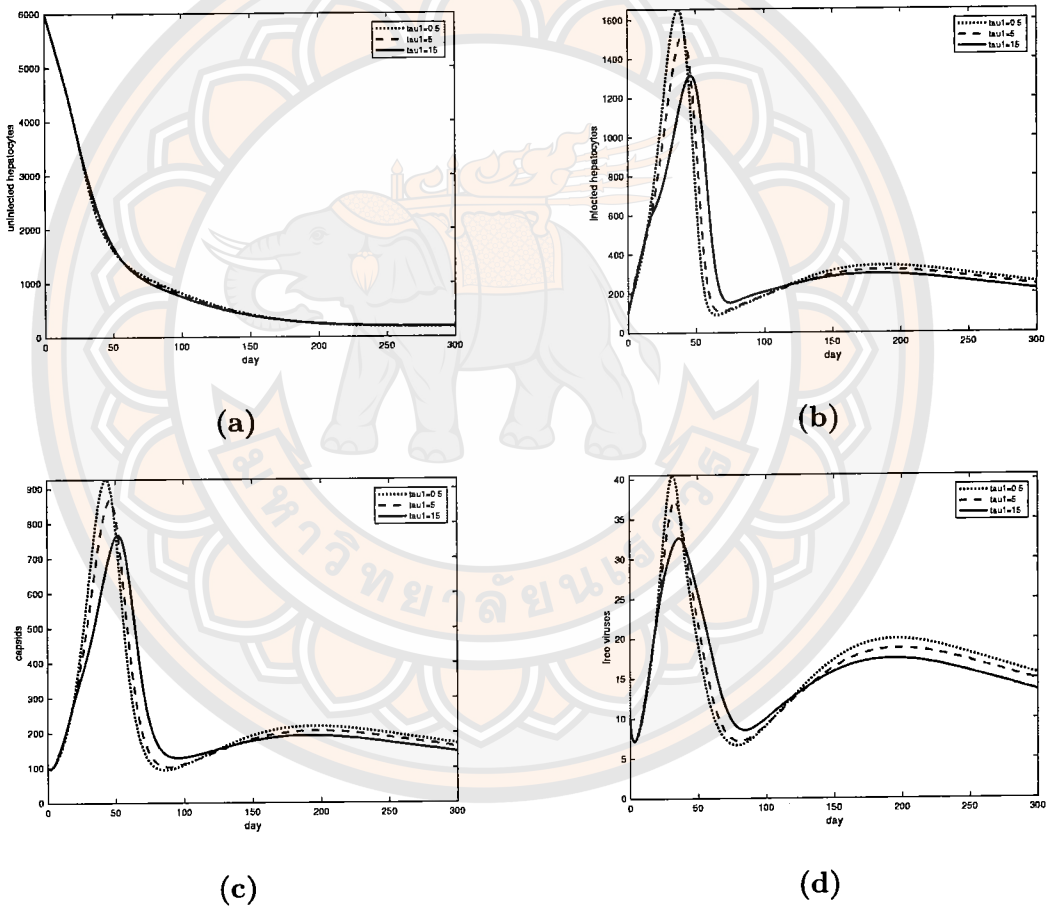

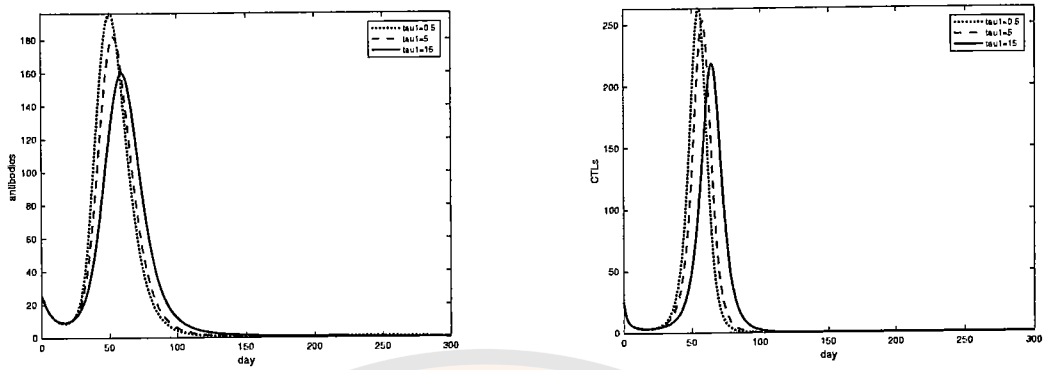

(e) (f)

Figure 17 Simulation results of the HBV model (3.1.1)-(3.1.6) with τ_1 and τ_2 represent the delay in the productively infected hepatocytes and the delay in an antigenic stimulation generating CTLs, respectively. We vary the value of τ_1 to be $\tau_1 = 0.5, 5, 15$ where $\tau_2 = 5$. (a) the concentration of uninfected hepatocytes, (b) the concentration of infected hepatocytes, (c) the concentration of intracellular HBV DNA-containing capsids, (d) the concentration of free viruses, (e) the concentration of antibodies and (f) the concentration of CTLs.

In Figure 17a - 17f, we vary the value of τ_1 where τ_2 is 5. From Figure 17a, we can see that the dynamics of concentration of uninfected hepatocytes is hardly changed when τ_1 varies. Figures 17b and 17c show a similar pattern, the concentration of infected hepatocyte and intracellular HBV DNA-containing capsids goes up since the beginning for all values of τ_1. They show that the higher the value of τ_1, the smaller the peak and the longer it takes for the peak to appear. Further, it reaches lower equilibrium value when τ_1 is larger. Figure 17d shows double peaks in the concentration of free viruses, the lower peak height for both peaks obtained with the larger value of τ_1. The dynamics drop down after the first peak, then gradually rise to the second peak, which occur between the 150th and 250th day. Finally, it tends to reach lower equilibrium value when τ_1 increases. Figures 17e and 17f show that in the case when τ_1 increases, the concentration of antibodies and CTLs decrease with slower time for the peak to occur, respectively. In summary, from the result above τ_1 has shown to have an impact to a reduction in the concentration

of infected hepatocytes, intracellular HBV DNA-containing capsids, free viruses, antibodies and CTLs. Also, the epidemic peak occurs slower when τ_1 increases.

3.6.4 Case IV : when τ_2 varies and $\tau_1 = 5$

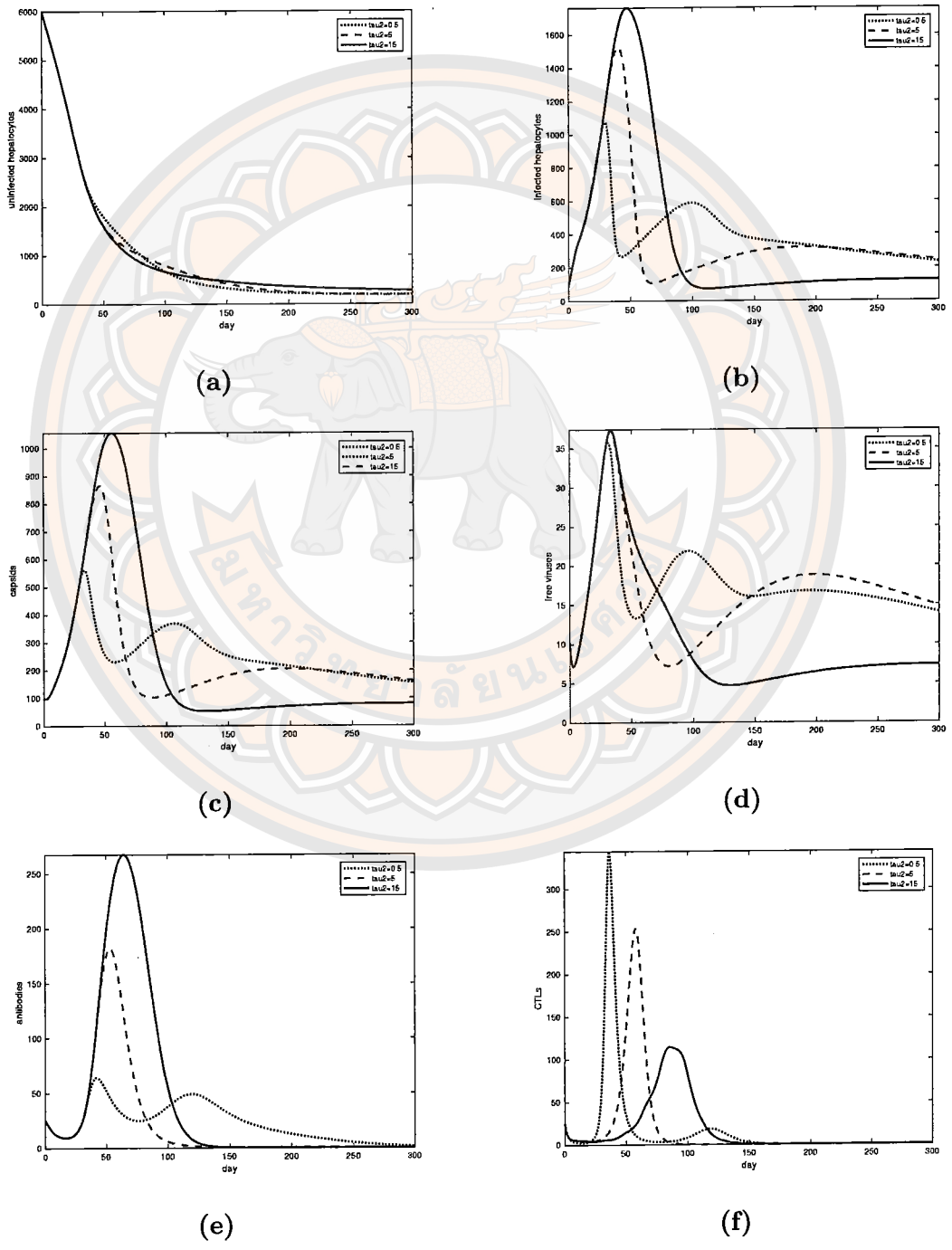

Figure 18 Simulation results of the HBV model (3.1.1)-(3.1.6) with τ_1 and τ_2 represent the delay in the productively infected hepatocytes and the delay in an antigenic stimulation generating CTLs, respectively. We vary the value of τ_2 to be $\tau_2 = 0.5, 5, 15$, where $\tau_1 = 5$ (a) the concentration of uninfected hepatocytes, (b) the concentration of infected hepatocytes, (c) the concentration of intracellular HBV DNA-containing capsids, (d) the concentration of free viruses, (e) the concentration of antibodies and (f) the concentration of CTLs.

When τ_2 increases, the concentration of uninfected hepatocytes drops faster on the first 100th day, as shown in Figure 18a. After that, however, the concentration of uninfected hepatocytes tends to decrease slower than the case of smaller τ_2. Figure 18b and 18c give a similar pattern when τ_2 increases, the concentration of infected hepatocytes and intracellular HBV DNA-containing capsids largely increase, with slower time for the peak to occur. Interestingly, with $\tau_2 = 0.5$ and 5, there are two peaks occured, whereas only one peak observed in the case $\tau_2 = 15$. Further, with $\tau_2 = 15$ it reaches lower equilibrium value when compare to $\tau_2 = 0.5$, and 5. When τ_2 increases, the concentration of free viruses increases to almost the same level of peak as shown in Figure 18d. However, it tends to give the second peak for the case $\tau_2 = 0.5$ and 5, while in the case $\tau_2 = 15$ there is only one peak. At the start in Figure 18e, when τ_2 increases, the concentration of antibodies significantly increases with a slower time for the peak to occur. With $\tau_2 = 0.5$, after the 70th day, it goes up again to the small second peak at a smaller level. On the other hand, Figure 18f shows a large reduction of the concentration of CTLs with a slower time for the peak to occur, when τ_2 increases. Further, in the case $\tau_2 = 0.5$, on the 80th day, it tends to rise to give the second peak ranging the period of 70 days then goes down to zero. On the whole, from the results above, τ_2 has shown to give an impact in boosting up the concentration of infected hepatocytes, intracellular HBV DNA-containing capsids, free viruses, and antibodies with longer period of an epidemic time. However, it shows to play a main role in greatly reducing the concentration of

CTLs. This means that the delay of antigenic stimulation generating CTLs causing longer duration with a large quantity of the hepatitis B virus infection.

3.7 Conclusion

In this chapter, we demonstrate multiple delays within-host model for HBV infection model with 6 variables consisting of the uninfected hepatocytes, infected hepatocytes, intracellular HBV-DNA containing capsids, free viruses, antibodies, and cytotoxic T-lymphocyte (CTLs). We incorporate the two delays which are the delay in the productively infected since viruses attack and an additional delay in an antigenic stimulation generating CTLs. The model also involves two drug therapies. We have proved that all solutions are non-negative and bounded. Three equilibrium states are determined in this model i.e. infection-free, the immune-free and the immune-activated. The basic reproduction number is determined and becomes threshold in determining the stability of the infection-free equilibrium point. Further, the global stability of immune-free and immune-activated equilibrium points is analyzed and presented in Theorem 3.5.7 and 3.5.5, respectively. Our numerical simulations have shown that both drug therapies play a key role in reducing an HBV infection overall. From Figure 17a - 17f, we obtain that τ_1 affects the time for the peak to occur i.e. it is slower when τ_1 increases. Also, a smaller epidemic is observed in larger value of τ_1. In addition, with the results of Figure 18a - 18f obtained, they show that the greater the delay in an antigenic stimulation generating CTLs τ_2, the more severe HBV infection occur. Hence, by including both adaptive immune response which are CTLs and antibodies with time delays would make this model more realistic and this could bring to the better understanding of HBV infection. As a future work, it might be reasonable to include spatial component and diffusion for virus into the model.

CHAPTER IV

OPTIMAL CONTROL OF TIME DELAY MODEL OF HEPATITIS B VIRUS INFECTION

4.1 Model description and formulation

The model consists of six variables, namely the concentrations (units: mm^{-3}) of uninfected hepatocytes $x(t)$, infected hepatocytes $y(t)$, intracellular HBV DNA-containing capsids $c(t)$, free viruses $v(t)$, antibodies $w(t)$, and cytotoxic T-lymphocytes $z(t)$. The model also includes two-time delays representing τ_1 as a virus production delay and τ_2 as an antigenic stimulation generating CTLs delay. In addition, two controls are considered: a control $u_1(t)$ on the effectiveness of drug therapy in reducing new infections of hepatocytes, and a control $u_2(t)$ on the effectiveness of drug therapy in inhibiting viral production. The other parameters used in the model include Λ, representing the production rate of uninfected hepatocytes, whereas the natural death rate of hepatocytes is denoted by σ. Additionally, β denotes the infection rate of uninfected hepatocytes by free viruses, further, we consider where infected hepatocytes are restored to uninfected status by a non-cytolytic cure process at a rate of p. The infected hepatocytes $y(t)$ are eliminated by the CTLs, $z(t)$, with a rate q. The term $(1-u_2)ay(t)$ describes how effectively drug therapy inhibits viral production (u_2 with a production rate a), which is incorporated into the production of intracellular HBV DNA-containing capsids $c(t)$. The internal HBV DNA-containing capsids decay at a rate of δ and are released into the bloodstream at a rate of α. The neutralization rate of antibodies γ reduces the free viruses, which then die at a rate of μ. The antibodies are enhanced in response to the free viruses at a rate g and decay at a rate h. Moreover, the immunological response in this model cannot be ignored due to the second time delay, indicating that τ_2 may be needed for the activation of CTLs that produce antigens. Consequently, we incorporate the term $ky(t-\tau_2)z(t-\tau_2)$, and the CTLs decay at a rate of ϵ. The flow chart of the model is presented in Figure ??.

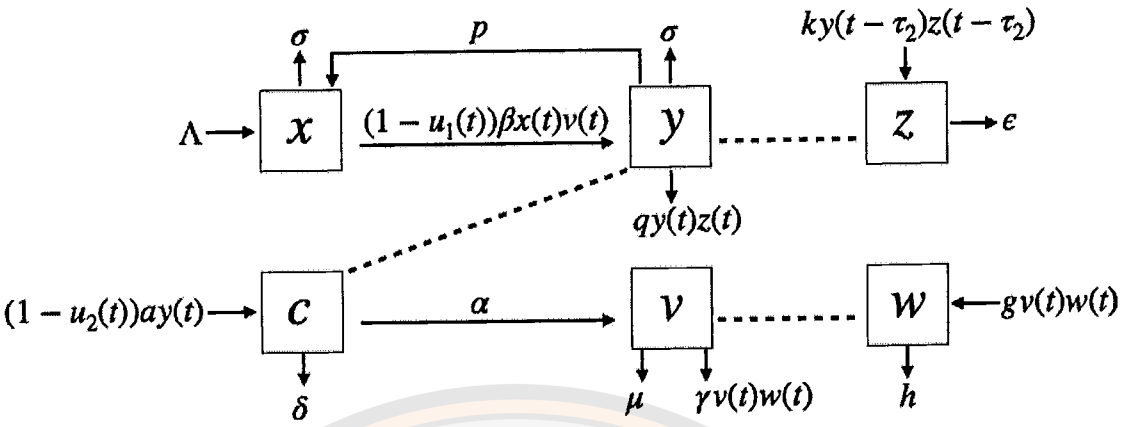

Figure 19 The flow chart of the optimal control model of HBV infection including immune response and multiple delays. The solid lines represent the transferring from one class to another class, whereas the dotted lines represent an involvement or influence of one class on another class.

The equations for the model are shown in Eq. (4.1.1) - (4.1.6), the initial conditions are given in Eq. (4.1.7), and the definitions and assumed values for all parameters are shown in Table 2.

$$\frac{dx}{dt} = \Lambda - \sigma x(t) - (1-u_1(t))\beta x(t)v(t) + py(t), \tag{4.1.1}$$

$$\frac{dy}{dt} = (1-u_1(t))\beta e^{-m\tau_1}x(t-\tau_1)v(t-\tau_1) - (\sigma+p)y(t) - qy(t)z(t), \tag{4.1.2}$$

$$\frac{dc}{dt} = (1-u_2(t))ay(t) - \alpha c(t) - \delta c(t), \tag{4.1.3}$$

$$\frac{dv}{dt} = \alpha c(t) - \gamma v(t)w(t) - \mu v(t), \tag{4.1.4}$$

$$\frac{dw}{dt} = gv(t)w(t) - hw(t), \tag{4.1.5}$$

$$\frac{dz}{dt} = ky(t-\tau_2)z(t-\tau_2) - \varepsilon z(t), \tag{4.1.6}$$

where $\{x(t), y(t), c(t), v(t), w(t), z(t)\} \in \Re^6$ are state variables, $\tau_1 > 0$ and $\tau_2 > 0$ are time delays, and $u_1(t) \in [0,1]$, $u_2(t) \in [0,1]$ are control variables. Then, for the maximum time delay $\tau = \max\{\tau_1, \tau_2\}$ and for nonnegative constants $x_0, y_0, c_0, v_0, w_0, z_0$, we define the initial conditions for the system of state equations (4.1.1) - (4.1.6) as follows. For $t \in [-\tau, 0]$, let

$$x(t) = x_0 \geq 0,\ y(t) = y_0 \geq 0,\ c(t) = c_0 \geq 0,\ v(0) = v_0 \geq 0,\ w(t) = w_0 \geq 0,\ z(t) = z_0 \geq 0. \tag{4.1.7}$$

Table 2 Parameters used in the model of equations (4.1.1)-(4.1.6)

Parameter	Description	Value	Units	Source
$u_1(t)$	Efficiency of drug therapy in blocking new infection.	0–1	fraction	-
$u_2(t)$	Efficiency of drug therapy in inhibiting viral production.	0–1	fraction	-
Λ	Production rate of uninfected hepatocytes.	1	$day^{-1}mm^{-3}$	[33]
σ	Natural death rate of hepatocytes.	0.011	day^{-1}	[41]
β	Rate of infection of hepatocytes by the free virus.	0.0014	mm^3day^{-1}	[33]
$e^{-m\tau_1}$	Probability of surviving of hepatocytes in the time period from $t-\tau_1$ to t.			
m	Death rate of infected hepatocytes in the time period from $t-\tau_1$ to t.	0.011	day^{-1}	[18]
τ_1	Delay in the production of infected hepatocytes.	2	day	assumed
τ_2	Delay in antigenic stimulation generating CTLs.	4	day	assumed
p	Cure rate of infected hepatocytes by non-cytolytic cure process.	0.01, 0.012	day^{-1}	[110]
q	Death rate of infected hepatocytes due to the CTLs response.	0.001	mm^3day^{-1}	[18]
a	Production rate of intracellular HBV DNA-containing capsids.	0.15	day^{-1}	assumed
α	Growth rate of virions in blood.	0.87	day^{-1}	[111]
δ	Clearance rate of intracellular HBV DNA-containing capsids.	0.053	day^{-1}	[19]

Table 2 Parameters used in the model of equations (4.1.1)-(4.1.6)

Parameter	Description	Value	Units	Source
γ	Rate that viruses are neutralized by antibodies.	0.01	mm^3day^{-1}	[18]
μ	Death rate of free viruses.	0.0693	day^{-1}	[33]
g	Expansion rate of antibodies in response to free viruses.	0.008	mm^3day^{-1}	[111]
h	Decay rate of antibodies.	0.15	day^{-1}	[18]
k	Expansion rate of CTLs in response to viral antigen derived from infected hepatocytes.	0.001	mm^3day^{-1}	assumed
ε	Decay rate of CTLs in the absence of antigenic stimulation.	0.5	day^{-1}	[112]

Note that, in Table 2, we assumed values for parameters τ_1, τ_2, a and k. Our motivation for the value for τ_1 comes from the works by Meskaf et al. [18], Danane et al. [53] and Manna [68], who used values for τ_1 ranging from 0.5 to 5; therefore we assumed the value 2. Zhuang [79] and Sun and Liu [45] used values ranging from 0.03 to 10 for τ_2; we assumed a value equal to 2. Next, in Manna and Hattaf [80] a production rate of intracellular HBV DNA-containing capsids (a in our model) was taken to be 1.5, while the production rate of uninfected cells (Λ in our model) was 10. In our study Λ equals 1, and we set a equal to 0.15. Finally, the expansion rate of CTLs in response to viral antigen derived from infected hepatocytes (k in our model) equals 0.0012 in the work of Harroudi et al. [81]; we assumed this value to be 0.001.

4.2 Nonnegativity and boundedness of solutions

In this section, we are interested in finding optimal conditions on the control variables $u_1(t)$ and $u_2(t)$ that drive the infected hepacyte population $y(t)$ or the free virus population $v(t)$ to zero. Therefore, starting with the nonnegative initial conditions (4.1.7), we will integrate the system up to a finite time T defined as in Theorem 4.2.1. We now prove the following theorem.

Theorem 4.2.1. *Solutions of equations* (4.1.1) - (4.1.6) *with initial conditions* (4.1.7) *are nonnegative for* $-\tau \leq t \leq T$, $T = \min\{T_f, T_y, T_v\}$ *where* T_f *is a specified finite time,* T_y *is the time at which* $y(t)$ *first becomes zero and* T_v *is the time at which* $v(t)$ *first becomes zero.*

Proof. As stated in (4.1.7), the initial values of the variables of equations (4.1.1) - (4.1.6) are assumed to be nonnegative for $t \in [-\tau, 0]$. We now prove that all variables are nonnegative for $0 \leq t \leq T$.

We first note that the variables $y(t)$ and $v(t)$ cannot become negative for $0 < t \leq T$ since, by definition of T, $y(t) \geq 0$ for $0 \leq t = T_y \geq T$ and $v(t) \geq 0$ for $0 \leq t = T_v \geq T$.

We now look at possible solutions of the equations in (4.1.1) - (4.1.6).

We begin with Eq. (4.1.1).

$$\frac{dx}{dt} = \Lambda - (\sigma - (1 - u_1(t))\beta v(t))x(t) + py(t).$$

In this case, if $y(t) = 0$, the equation becomes

$$\frac{dx_1}{dt} = \Lambda - (\sigma - (1 - u_1(t))\beta v(t))x_1(t), \tag{4.2.1}$$

and the solution is $x_1(t) = \Lambda t + x_1(0)e^{-\int_0^t (1-u_1(s))\beta v(s)ds} > 0$, since $\Lambda > 0$ and $x_1(0) \geq 0$. Next, since $y(t) > 0$ for $t < T$ and $y(T) \geq 0$, we have $\frac{dx}{dt} > \frac{dx_1}{dt}$ for $t < T$ and $\frac{dx}{dt} \geq \frac{dx_1}{dt}$ for $t = T$, and therefore $x(t) \geq x_1(t) > 0$ for $t \leq T$.

Next, consider the equation (4.1.3),

$$\frac{dc}{dt} = (1 - u_2(t))ay(t) - (\alpha + \delta)c(t).$$

If $y(t) = 0$, then the equation becomes $\frac{dc_1}{dt} = -(\alpha + \delta)c_1(t)$ and the solution is $c_1(0)e^{-(\alpha+\delta)t} > 0$ since $c_1(0) \geq 0$. Next, since $y(t) > 0$ for $t < T$ and $y(T) \geq 0$, we have $\frac{dc}{dt} > \frac{dc_1}{dt}$ for $t < T$ and $\frac{dc}{dt} \geq \frac{dc_1}{dt}$ for $t = T$, and therefore $c(t) \geq c_1(t) > 0$ for $t \leq T$.

The equation (4.1.5),

$$\frac{dw}{dt} = (gv(t) - h)w(t),$$

which has the exponential solution $w(t) = w(0)e^{\int_0^t (gv(s)-h)ds}$. Since, by assumption, $w(0) \geq 0$, we have $w(t) \geq 0$ for all $t > 0$.

The equation (4.1.6),

$$\frac{dz}{dt} = ky(t-\tau_2)z(t-\tau_2) - \varepsilon z(t).$$

We first note that the equation $\frac{dz_1(t)}{dt} = -\varepsilon z_1(t)$ has the solution $z_1(t) = z_1(0)e^{-\varepsilon t} \geq 0$ for all $t \geq 0$ if $z_1(0) \geq 0$.
Also, we have $y(t-\tau_2) > 0$ for $0 \leq t \leq T + \tau_2$. Hence, if $z(t-\tau_2) \geq 0$ for $0 \leq t \leq T + \tau_2$, we have $\frac{dz(t)}{dt} \geq \frac{dz_1(t)}{dt}$ and $z(t) \geq z_1(t) > 0$. Note that, in this case, since $z(t) \geq 0$ for $-\tau_2 \leq t \leq 0$, we have that $z(t)$ cannot become zero, unless $z(t-\tau_2)$ is already negative.
The proof is complete. □

We will next prove that the solutions are bounded above.

Theorem 4.2.2. *For each solution $X(t)$ of an equation in system* (4.1.1) - (4.1.6) *there exists an upper bound (supremum $\bar{X}$) such that if $0 \leq X(t) \leq \bar{X}$ for $t \in [-\tau, 0]$, then $X(t) \leq \bar{X}$ for all $0 < t \leq T$.*

Proof. We have already proved in Theorem 4.2.1 that all variables are nonnegative for all $0 \leq t \leq T$, and therefore they are bounded below. In the proof, we will use the following Condition 1.

Condition 1: If a variable $X(t)$ and derivative $\frac{dX}{dt}$ are continuous, a necessary and sufficient condition for the solution $X(t)$ of a differential equation variable to be bounded above (i.e., for a supremum $\bar{X}$ to exist) is that $X(0) \leq \bar{X}$ and that $\frac{dX}{dt} \leq 0$ for $X(t) \geq \bar{X}$ for all $0 \leq t \leq T$.

Note: In this definition, we are assuming that it is possible to substitute initial conditions in the differential equation that give a solution greater than or equal to the supremum, but the derivative must then be negative or zero for all such initial conditions.

We will use Condition 1 to prove that all variables in the system (4.1.1) - (4.1.6) are bounded above for $0 \leq t \leq T$.

Without loss of generality, we will assume that $x(t)+y(t) \leq \frac{\Lambda}{\sigma}$ for $t \in [-\tau, 0]$. We will first consider the variables x and y in system (4.1.1) - (4.1.2). From the x and y equations in system (4.1.1) - (4.1.2), we have

$$\begin{aligned}\frac{d(x+y)}{dt} &= \Lambda - \sigma(x(t)+y(t)) - qy(t)z(t) \\ &\quad -(1-u_1(t))\beta\left(x(t)v(t) - e^{-m\tau_1}x(t-\tau_1)v(t-\tau_1)\right). \quad (4.2.2)\end{aligned}$$

Clearly, from (4.2.2), if

$$x(t)v(t) - e^{-m\tau_1}x(t-\tau_1)v(t-\tau_1) \geq 0, \quad (4.2.3)$$

then, since $y \geq 0$ and $z \geq 0$, we have $\frac{d(x+y)}{dt} \leq 0$ for $x+y \geq \frac{\Lambda}{\sigma}$, and therefore $x+y \leq \frac{\Lambda}{\sigma}$ is bounded above. Also, since x and y are nonnegative, both x and y must be bounded above. However, in this case, it is possible that $v(t)$ is unbounded.

On the other hand, if condition (4.2.3) is not satisfied, then it is possible that $\frac{d(x+y)}{dt} > 0$ for all $x+y$ and that $x+y$ is not bounded. However, this case can only occur if $x(t)v(t)$ is a decreasing function of t in which case $x(t)v(t)$ must be bounded. In this case, it is possible that $y(t)$ could be unbounded.

The possibilities from (4.2.2) are therefore as follows:

Case 1. x and v are bounded and y is unbounded.

Case 2. x and y are bounded and v is unbounded.

Case 3. x, v and y are all bounded.

We next prove that Case 1 is impossible, i.e., we prove that if x and v are bounded, then y is also bounded. Let $\bar{x}$ and $\bar{v}$ be the upper bounds on x and v respectively. Then, from the y equation in (4.1.2), we have

$$\begin{aligned}\frac{dy}{dt} &= (1-u_1(t))\beta e^{-m\tau_1}x(t-\tau_1)v(t-\tau_1) - (\sigma+p)y(t) - qy(t)z(t), \\ &\leq (1-u_1(t))\beta e^{-m\tau_1}\bar{x}\bar{v} - (\sigma+p)y(t) - qy(t)z(t), \\ &\leq 0 \text{ for } y(t) \geq \frac{(1-u_1(t))\beta e^{-m\tau_1}\bar{x}\bar{v}}{\sigma+p}. \quad (4.2.4)\end{aligned}$$

Therefore, using Condition 1, we have $y(t)$ is bounded above by $\bar{y} = \frac{(1-u_1(t))\beta e^{-m\tau_1}\bar{x}\bar{v}}{(\sigma+p)}$.

Hence, the only two possibilities are Cases 2 and 3, i.e., that x and y are bounded above and v is either bounded or unbounded. We now consider the equations for $\frac{dc}{dt}$, $\frac{dv}{dt}$, $\frac{dw}{dt}$ and $\frac{dz}{dt}$ in (4.1.3) - (4.1.6). We assume that $\bar{x}$ and $\bar{y}$ are the upper bounds on x and y, respectively. In the proofs, we use Condition 1 to prove that each variable is bounded above.

1. For $c(t)$, we have from (4.1.3) that

$$\begin{aligned} \frac{dc}{dt} &= (1-u_2(t))ay(t) - \alpha c(t) - \delta c(t), \\ &\leq (1-u_2(t))a\bar{y} - (\alpha+\delta)c(t), \\ &\leq 0 \quad \text{for } c(t) \geq \frac{(1-u_2(t))a\bar{y}}{\alpha+\delta}. \end{aligned} \tag{4.2.5}$$

   Therefore, $c(t)$ is bounded above by $\bar{c} = \frac{(1-u_2(t))a\bar{y}}{\alpha+\delta}$.

2. For $v(t)$, we have

$$\begin{aligned} \frac{dv}{dt} &= \alpha c(t) - \gamma v(t)w(t) - \mu v(t), \\ &\leq \alpha\bar{c} - (\gamma w(t) + \mu)v(t), \\ &\leq 0 \quad \text{for } v(t) \geq \frac{\alpha\bar{c}}{\gamma w(t)+\mu}. \end{aligned} \tag{4.2.6}$$

   Therefore, since $w \geq 0$, $v(t)$ is bounded above by $\bar{v} = \frac{\alpha\bar{c}}{\mu}$.

   We have therefore proved that Case 3 above is the only possibility.

3. For $w(t)$, we have

$$\begin{aligned} \frac{dw}{dt} &= gv(t)w(t) - hw(t), \\ &\leq (g\bar{v} - h)w(t). \end{aligned} \tag{4.2.7}$$

   For the model that we are considering it is clear that the extra condition $h > g\bar{v}$ is required to prove boundedness of the antibody concentration w.

4. For $z(t)$, we have

$$\begin{aligned} \frac{dz}{dt} &= ky(t-\tau_2)z(t-\tau_2) - \varepsilon z(t), \\ &\leq (k\bar{y} - \varepsilon)z(t). \end{aligned} \tag{4.2.8}$$

   For the model that we are considering it is clear that the extra condition $\varepsilon > k\bar{y}$ is required to prove boundedness of the concentration of cytotoxic T-lymphocytes $z(t)$.

The proof is complete. □

4.3 Existence of unique solution

Theorem 4.3.1. *System of Eq.* (4.1.1) - (4.1.6) *with specified initial conditions* (4.1.7) *and specified values of the controls* $(u_1(t), u_2(t))$ *has a unique solution.*

Proof. We will prove that the system of Eq. (4.1.1) - (4.1.6) satisfies Lipschitz conditions (see, e.g., [82, 83]) and therefore that the solution exists and is unique. Note: In the proof, we are assuming that the control functions $(u_1(t), u_2(t))$ are fixed functions and that $u_1(t) \in [0, 1]$ and $u_2(t) \in [0, 1]$. Changing the values of these functions will, of course, change the solution.

$$\frac{dX}{dt} = F(t, \xi_t), \quad X(t) \text{ given}, \ t \in [-\tau, 0], \tag{4.3.1}$$

where, as above, $\tau = \max\{\tau_1, \tau_2\}$, and where we define

$$X(t) = \begin{bmatrix} x(t) \\ y(t) \\ c(t) \\ v(t) \\ w(t) \\ z(t) \end{bmatrix}, \quad \xi_t = \left[\xi_{1,t}, \xi_{2,t}\right] = \begin{bmatrix} x(t) & x(t-\tau_1) \\ y(t) & y(t-\tau_2) \\ c(t) & 0 \\ v(t) & v(t-\tau_1) \\ w(t) & 0 \\ z(t) & z(t-\tau_2) \end{bmatrix} \tag{4.3.2}$$

and

$$\begin{aligned}
F_1(t, \xi_t) &= \Lambda - \sigma x(t) - (1 - u_1(t))\beta x(t) v(t) + p y(t), \\
F_2(t, \xi_t) &= (1 - u_1(t))\beta e^{-m\tau_1} x(t-\tau_1) v(t-\tau_1) - (\sigma + p) y(t) - q y(t) z(t), \\
F_3(t, \xi_t) &= (1 - u_2(t)) a y(t) - \alpha c(t) - \delta c(t), \\
F_4(t, \xi_t) &= \alpha c(t) - \gamma v(t) w(t) - \mu v(t), \\
F_5(t, \xi_t) &= g v(t) w(t) - h w(t), \\
F_6(t, \xi_t) &= k y(t-\tau_2) z(t-\tau_2) - \varepsilon z(t).
\end{aligned} \tag{4.3.3}$$

We now prove that the system (4.3.1)–(4.3.3) satisfies the Lipschitz condition of [83] (Definition Eq. (4), p.258), i.e.,

$$\|F(t, \xi_t) - F(t, \hat{\xi}_t)\|_1 \leq L \|\xi_t - \hat{\xi}_t\|_1, \tag{4.3.4}$$

for some $L > 0$ and where the one-norm $\|\xi_t - \hat{\xi}_t\|_1$ is the maximum absolute column sum of $\xi_t - \hat{\xi}_t$ (see, e.g., [84]). We begin by writing system (4.3.1) in the following matrix form:

$$F(t, \xi_t) = A(t)\xi_{1,t} + B(\xi_{1,t}) + C(\xi_{2,t}), \tag{4.3.5}$$

where

$$A(t) = \begin{bmatrix} -\sigma & p & 0 & 0 & 0 & 0 \\ 0 & -(\sigma + p) & 0 & 0 & 0 & 0 \\ 0 & (1 - u_2(t))a & -(\alpha + \delta) & 0 & 0 & 0 \\ 0 & 0 & \alpha & -\mu & 0 & 0 \\ 0 & 0 & 0 & 0 & -h & 0 \\ 0 & 0 & 0 & 0 & 0 & -\varepsilon \end{bmatrix}, \tag{4.3.6}$$

$$B(\xi_{1,t}) = \begin{bmatrix} \Lambda - (1 - u_1(t))\beta x(t)v(t) \\ -qy(t)z(t) \\ 0 \\ -\gamma v(t)w(t) \\ gv(t)w(t) \\ 0 \end{bmatrix}, \tag{4.3.7}$$

$$C(\xi_{2,t}) = \begin{bmatrix} 0 \\ (1 - u_1(t))\beta e^{-m\tau_1} x(t - \tau_1)v(t - \tau_1) \\ 0 \\ 0 \\ 0 \\ ky(t - \tau_2)z(t - \tau_2) \end{bmatrix}. \tag{4.3.8}$$

The next step is to prove that the function $F(t, \xi_t)$ satisfies the Lipschitz conditions in (4.3.4). We first note that, from the properties of norms,

$$\begin{aligned} \|F(t, \xi_t) - F(t, \hat{\xi}_t)\|_1 &= \|A(t)(\xi_1(t) - \hat{\xi}_{1,t}) + B(\xi_{1,t}) - B(\hat{\xi}_{1,t}) + C(\xi_{2,t}) - C(\hat{\xi}_{2,t})\|_1 \\ &\leq \|A(t)(\xi_{1,t} - \hat{\xi}_{1,t})\|_1 + \|B(\xi_{1,t}) - B(\hat{\xi}_{1,t})\|_1 \end{aligned}$$

$$+\|C(\xi_{2,t}) - C(\hat{\xi}_{2,t})\|_1. \tag{4.3.9}$$

We consider each term in (4.3.9) separately.

For the $A(t)$ term, we have

$$\|A(t)(\xi_{1,t} - \hat{\xi}_{1,t})\|_1 \leq \|A(t)\|_1 \|\xi_{1,t} - \hat{\xi}_{1,t}\|_1 = L_1(t)\|\xi_{1,t} - \hat{\xi}_{1,t}\|_1, \tag{4.3.10}$$

where $L_1(t) = \|A(t)\|_1 = \max\{\sigma,\ \sigma + 2p + (1 - u_2(t)a,\ 2\alpha + \delta,\ \mu,\ h,\ \varepsilon\}$ is the maximum absolute column sum of $A(t)$.

For the one-norm of $B(\xi_{1,t}) - B(\hat{\xi}_{1,t})$, we have

$$\|B(\xi_{1,t}) - B(\hat{\xi}_{1,t})\|_1 = \left\| \begin{array}{c} (-(1-u_1(t))\beta[x_1(t)v_1(t) - \hat{x}_1(t)\hat{v}_1(t)] \\ -q[y_1(t)z_1(t) - \hat{y}_1(t)\hat{z}_1(t)] \\ 0 \\ -\gamma[v_1(t)w_1(t) - \hat{v}_1(t)\hat{w}_1(t)] \\ g[v_1(t)w_1(t) - \hat{v}_1(t)\hat{w}_1(t))] \\ 0 \end{array} \right\|_1. \tag{4.3.11}$$

Then, since the one-norm of a vector is the sum of absolute values of components, and since the absolute value of a product of the form $x_1y_1 - \hat{x}_1\hat{y}_1$ can be rewritten as

$$\begin{aligned} |x_1(t)y_1(t) - \hat{x}_1(t)\hat{y}_1(t)| &= |[x_1(t) - \hat{x}_1(t)]y_1(t) + \hat{x}_1(t)[y_1(t) - \hat{y}_1(t)]| \\ &\leq |(x_1(t) - \hat{x}_1(t))||y_1(t)| + |\hat{x}_1(t)||(y_1(t) - \hat{y}_1(t)|, \end{aligned} \tag{4.3.12}$$

we obtain the following:

$$\begin{aligned} |B(\xi_{1,t}) - B(\hat{\xi}_{1,t})|_1 &= |(1-u_1(t))\beta[x_1(t)v_1(t) - \hat{x}_1(t)\hat{v}_1(t)]| \\ &\quad + |q([y_1(t)z_1(t) - \hat{y}_1(t)\hat{z}_1(t)]| \\ &\quad + |\gamma[v_1(t)w_1(t) - \hat{v}_1(t)\hat{w}_1(t)]| \\ &\quad + |g[v_1(t)w_1(t) - \hat{v}_1(t)\hat{w}_1(t)]| \\ &\leq (1-u_1(t))\beta|x_1(t) - \hat{x}_1(t)||v_1(t)| \\ &\quad + (1-u_1(t))\beta|\hat{x}_1(t)||v_1(t) - \hat{v}_1(t)| \\ &\quad + q|y_1(t) - \hat{y}_1(t)||z_1(t)| + q|\hat{y}_1(t)||z_1(t) - \hat{z}_1(t)| \end{aligned}$$

$$
\begin{aligned}
&+(\gamma+g)|v_1(t)-\hat{v}_1(t)||w_1(t)| \\
&+(\gamma+g)|\hat{v}_1(t)||w_1(t)-\hat{w}_1(t)| \\
= \;& (1-u_1(t))\beta|v_1(t)||x_1(t)-\hat{x}_1(t)|+q|z_1(t)||y_1(t)-\hat{y}_1(t)| \\
&+\left((1-u_1(t))\beta|\hat{x}_1(t)|+(\gamma+g)|w_1(t)|\right)|v_1(t)-\hat{v}_1(t)| \\
&+(\gamma+g)|\hat{v}_1(t)|||w_1(t)-\hat{w}_1(t)|+q|\hat{y}_1(t)||z_1(t)-\hat{z}_1(t)|.
\end{aligned} \tag{4.3.13}
$$

Then, defining $L_2(t)$ as

$$
\begin{aligned}
L_2(t) \;=\; & \max\{(1-u_1(t))\beta|v_1(t)|,\, q|z_1(t)|, \\
& \left((1-u_1(t))\beta|\hat{x}_1(t)|+(\gamma+g)|w_1(t)|\right),\, (\gamma+g)|\hat{v}_1(t)|,\, q|\hat{y}_1(t)|\},
\end{aligned}
$$

we obtain

$$
\begin{aligned}
|B(\xi_{1,t})-B(\hat{\xi}_{1,t})|_1 \;\le\; & L_2(t)\left(|x_1(t)-\hat{x}_1(t)|+|y_1(t)-\hat{y}_1(t)|+|v_1(t)-\hat{v}_1(t)|\right. \\
& \left.+|w_1(t)-\hat{w}_1(t)|+|z_1(t)-\hat{z}_1(t)|\right) \\
\le\; & L_2(t)\left(|x_1(t)-\hat{x}_1(t)|+|y_1(t)-\hat{y}_1(t)|+|c_1(t)-\hat{c}_1(t)|\right. \\
& \left.+|v_1(t)-\hat{v}_1(t)|+|w_1(t)-\hat{w}_1(t)|+|z_1(t)-\hat{z}_1(t)|\right) \\
=\; & L_2(t)\|\xi_{1,t})-\hat{\xi}_{1,t}\|_1.
\end{aligned} \tag{4.3.14}
$$

For the one-norm $\|C(\xi_{2,t})-C(\hat{\xi}_{2,t})\|_1$, we have from (4.3.8) and use (4.3.12)

$$
\begin{aligned}
\|C(\xi_{2,t})-C(\hat{\xi}_{2,t})\|_1 \;=\; & (1-u_1(t))\beta e^{-m\tau_1}|x_1(t-\tau_1)v_1(t-\tau_1)-\hat{x}_1(t-\tau_1)\hat{v}_1(t-\tau_1)| \\
& +k|y_1(t-\tau_2)z_1(t-\tau_2)-\hat{y}_1(t-\tau_2)\hat{z}_1(t-\tau_2)| \\
\le\; & (1-u_1(t))\beta e^{-m\tau_1}|v_1(t-\tau_1)||x_1(t-\tau_1)-\hat{x}_1(t-\tau_1)| \\
& +(1-u_1(t))\beta e^{-m\tau_1}|\hat{x}_1(t-\tau_1)||v_1(t-\tau_1)-\hat{v}_1(t-\tau_1)| \\
& +k|z_1(t-\tau_2)||y_1(t-\tau_2)-\hat{y}_1(t-\tau_2)| \\
& +k|\hat{y}_1(t-\tau_2)||z_1(t-\tau_2)-\hat{z}_1(t-\tau_2)| \\
\le\; & L_3(t)\|\xi_{2,t}-\hat{\xi}_{2,t}\|_1,
\end{aligned} \tag{4.3.15}
$$

where

$$
\begin{aligned}
L_3(t) \;=\; & \max\{(1-u_1(t))\beta e^{-m\tau_1}|v_1(t-\tau_1)|,(1-u_1(t))\beta e^{-m\tau_1}|v_1(t-\tau_1)|, \\
& k|z_1(t-\tau_2)|,k|\hat{y}_1(t-\tau_2)|\}\|\xi_{2,t}-\hat{\xi}_{2,t}\|_1.
\end{aligned} \tag{4.3.16}
$$

Combining the results in (4.3.10), (4.3.14) and (4.3.15), we obtain

$$\|F(t,\xi_t) - F(t,\hat{\xi}_t)\|_1 \leq (L_1(t) + L_2(t))\|\xi_{1,t} - \hat{\xi}_{1,t}\|_1 + L_3(t)\|\xi_{2,t} - \hat{\xi}_{2,t}\|_1. \quad (4.3.17)$$

Finally, from Theorems 4.2.1 and 4.2.2 all variables are nonegative and bounded, we can replace $L_1(t), L_2(t), L_3(t)$ by upper bounds defined by

$$\begin{aligned} L_1 &= \max\{\sigma,\ \sigma + 2p + (1-u_{2,\min})a,\ 2\alpha + \delta,\ \mu,\ h,\ \varepsilon\}, \\ L_2 &= \max\left\{(1-u_{1,\min})\beta\bar{v},\ q\bar{z},\ ((1-u_{1,\min})\beta\bar{x} + (\gamma+g)\bar{w}),\ (\gamma+g)\bar{v},\ q\bar{y}\right\}, \\ L_3 &= \max\{(1-u_{1,\min})\beta e^{-m\tau_1}\bar{v},\ (1-u_{1,\min})\beta e^{-m\tau_1}\bar{x}\}, k\bar{z}, k\bar{y}\}, \end{aligned} \quad (4.3.18)$$

where, e.g., $\bar{x}$ means the upper bound on $x(t)$ and $u_{1,\min} \in [0,1]$, and $u_{2,\min} \in [0,1]$ are the minimum values of $u_1(t)$ and $u_2(t)$ for $t \geq -\tau$, respectively.

Then, using (4.3.18), we can rewrite (4.3.9) as the Lipschitz condition

$$\|F(t,\xi_t)) - F(\hat{\xi}_t)\|_1 \leq (L_1 + L_2 + L_3)\|\xi_t - \hat{\xi}_t\|_1 = L\|\xi_t - \hat{\xi}_t\|_1. \quad (4.3.19)$$

The proof is complete. □

4.4 Equilibrium points

The system of equations (4.1.1) - (4.1.6) has three equilibrium states:

1. Infection-free equilibrium point :

$$E_0 = (x_0, y_0, c_0, v_0, w_0, z_0) = \left(\frac{\Lambda}{\sigma}, 0, 0, 0, 0, 0\right). \quad (4.4.1)$$

2. Immune-free equilibrium point: $E_1 = (x_1, y_1, c_1, v_1, 0, 0)$, where

$$\begin{aligned} x_1 &= \frac{(\sigma+p)(\alpha+\delta)\mu}{(1-u_1)(1-u_2)\beta e^{-m\tau_1}a\alpha}, \quad y_1 = \frac{(\alpha+\delta)c_1}{(1-u_2)a} \\ c_1 &= \frac{\sigma\mu(\sigma+p)(\alpha+\delta)(R_0-1)}{(1-u_1)\beta\alpha\left((\sigma+p)(\alpha+\delta) - p(\alpha+\delta)e^{-m\tau_1}\right)}, \quad v_1 = \frac{\alpha c_1}{\mu}, \end{aligned} \quad (4.4.2)$$

where

$$R_0 = \frac{(1-u_1)(1-u_2)\beta e^{-m\tau_1}\Lambda a\alpha}{\mu\sigma(\sigma+p)(\alpha+\delta)} \quad (4.4.3)$$

can be identified as the basic reproduction number (see subsection 4.5). Note that the infected populations y_1 and c_1 and free virus population v_1 are positive if and only if $R_0 > 1$.

3. Immune-activated equilibrium point: $(E_2) = (x_2, y_2, c_2, v_2, w_2, z_2)$, where

$$x_2 = \frac{(\Lambda k + p\varepsilon)g}{(\sigma g + (1-u_1)\beta h)k}, \quad y_2 = \frac{\varepsilon}{k}, \quad c_2 = \frac{(1-u_2)a\varepsilon}{k(\alpha+\delta)}, \quad v_2 = \frac{h}{g},$$
$$w_2 = \frac{(1-u_2)a\varepsilon\alpha g}{(\alpha+\delta)\gamma hk} - \frac{\mu}{\gamma}, \quad z_2 = \frac{(1-u_1)\beta e^{-m\tau_1} khx_2}{qg\varepsilon} - \frac{\sigma+p}{q}. \tag{4.4.4}$$

Note that the immune-activated equilibrium exists if and only if the antibody population w_2 and cytotoxic T-lymphocytes population z_2 are positive.

4.5 The basic reproduction number (R_0)

The basic reproduction number (R_0) is the expected concentration of secondary cases produced when a typical infected hepatocyte (y) enters an infection-free population. To calculate R_0, we use the next-generation method of [73]. We obtain

$$\mathcal{F} = \begin{bmatrix} (1-u_1)\beta e^{-m\tau_1} xv \\ 0 \\ 0 \end{bmatrix} \text{ and } \mathcal{V} = \begin{bmatrix} (\sigma+p)y + qzy \\ \alpha c + \delta c - (1-u_2)ay \\ \gamma vw + \mu v - \alpha c \end{bmatrix}.$$

Then we have

$$F = \begin{bmatrix} 0 & 0 & (1-u_1)\beta e^{-m\tau_1} x \\ 0 & 0 & 0 \\ 0 & 0 & 0 \end{bmatrix} \text{ and } V = \begin{bmatrix} (\sigma+p)+qz & 0 & 0 \\ -(1-u_2)a & \alpha+\delta & 0 \\ 0 & -\alpha & \gamma w + \mu \end{bmatrix}.$$

By substituting the infection-free equilibrium point $E_0 = \left(\frac{\Lambda}{\sigma}, 0, 0, 0, 0, 0\right)$ into the Jacobian matrices F and V and computing the inverse V^{-1}, we obtain the next-generation matrix

$$FV^{-1} = \begin{bmatrix} \frac{(1-u_1)(1-u_2)\beta e^{-m\tau_1}\Lambda a\alpha}{\mu\sigma(\sigma+p)(\alpha+\delta)} & \frac{(1-u_1)\beta e^{-m\tau_1}\Lambda\alpha}{\mu\sigma(\sigma+p)(\alpha+\delta)} & \frac{(1-u_1)\beta e^{-m\tau_1}\Lambda}{\sigma\mu} \\ 0 & 0 & 0 \\ 0 & 0 & 0 \end{bmatrix}.$$

The basic reproduction number R_0 is then the maximum eigenvalue $\rho(FV^{-1})$, which is given by equation (4.4.3). From the next-generation method, $R_0 < 1$ is the condition for local asymptotic stability of the infection-free equilibrium E_0 and, as shown above, $R_0 > 1$ is also the condition for the existence of the immune-free equilibrium E_1.

4.6 Sensitivity analysis

These indices demonstrate the sensitivity of the parameter associated with the basic reproduction number (R_0). It determines whether it increases or decreases the values of the basic reproduction number (R_0) and provides crucial details on the comparative changes in significant parameters. As a result, they support the development of effective strategies for controlling the transmission of HBV.

With sensitivity analysis, we can investigate how each parameter used in the model affects the value of the basic reproduction number. We use the method of normalized forward sensitivity index (see, e.g., Samsuzzoha et al. [74] and Ngoteya et al. [75]), where the normalized forward sensitivity index of the basic reproduction number R_0 with respect to a parameter value h is given by :

$$S_h^{R_0} = \frac{h}{R_0}\frac{\partial R_0}{\partial h} = h\frac{\partial \log(R_0)}{\partial h}. \tag{4.6.1}$$

Using equations (4.6.1) and (4.4.3), we obtain the values of the sensitivity indices shown in Table 3 for the parameters in Table 2. From these calculations,

Table 3 Numerical values of sensitivity indices of (R_0).

Parameter	Index at Parameter Value	Sign
Λ	+1	+ve
β	+1	+ve
m	-0.0220	-ve
τ_1	-0.0220	-ve
a	+1	+ve
u_1	-0.1111	-ve
u_2	-0.1111	-ve
α	0.0574	+ve
σ	-1.0840	-ve
μ	-1	-ve
p	-0.9160	-ve
δ	-0.0574	-ve

we can rank the indices in order of effectiveness in reducing HBV infection. Table 3 shows that increasing the values of parameters $\Lambda, \beta, a, \alpha$ by 10% will increase the values of R_0 by 10%, 10%, 10% and 0.57%, respectively. On the other hand, Table 3 shows that increasing the values of $m, \tau_1, u_1, u_2, \sigma, \mu, p, \delta$ by 10% will decrease the values of R_0 by 0.22%, 0.22%, 1.11%, 1.11%, 10.84%, 10%, 9.16%, and 0.57%, respectively. Therefore, if we want to reduce R_0, we should focus on increasing the values of σ, μ and p and reducing the values of Λ, β and a because these are the factors that are most effective in reducing the infection. It can also be seen that increasing the values of the controls u_1 and u_2 have the same effect as reducing the values of the parameters Λ, β, a and α, the first three of which are the most effective in reducing the values of R_0.

4.7 Optimal control

We consider the optimal control of the time delay model for HBV infections defined in Section 4.1. The optimal control problem is as follows:

$$\begin{aligned}
&\max_{u_1,u_2} J(u_1,u_2) = \int_0^T f_0(x(t),w(t),z(t),u_1(t),u_2(t))dt,\\
&\text{where } f_0(x(t),w(t),z(t),u_1(t),u_2(t))\\
&\qquad = x(t)+w(t)+z(t)-\frac{1}{2}A_1u_1^2(t)-\frac{1}{2}A_2u_2^2(t),\\
&\qquad 0\le u_1(t)\le 1, \quad 0\le u_2(t)\le 1,
\end{aligned} \tag{4.7.1}$$

subject to the HBV equations in system (4.1.1) - (4.1.6):

$$\begin{aligned}
\frac{dx}{dt} &= f_1(x(t),v(t),y(t),u_1(t))\\
&= \Lambda-\sigma x(t)-(1-u_1(t))\beta x(t)v(t)+py(t),\\
\frac{dy}{dt} &= f_2(y(t),z(t),x(t-\tau_1),v(t-\tau_1),u_1(t))\\
&= (1-u_1(t))\beta e^{-m\tau_1}x(t-\tau_1)v(t-\tau_1)-(\sigma+p)y(t)-qy(t)z(t),\\
\frac{dc}{dt} &= f_3(y(t),c(t),u_2(t)) = (1-u_2(t))ay(t)-(\alpha+\delta)c(t),\\
\frac{dv}{dt} &= f_4(c(t),v(t),w(t)) = \alpha c(t)-\gamma v(t)w(t)-\mu v(t),\\
\frac{dw}{dt} &= f_5(v(t),w(t)) = gv(t)w(t)-hw(t),\\
\frac{dz}{dt} &= f_6(z(t),y(t-\tau_2),z(t-\tau_2)) = ky(t-\tau_2)z(t-\tau_2)-\varepsilon z(t),
\end{aligned} \tag{4.7.2}$$

with initial conditions

$$\begin{aligned} &x(t) \geq 0, \quad \text{given } -\tau_1 \leq t \leq 0, \quad && y(t) \geq 0, \text{ given } -\tau_2 \leq t \leq 0, \\ &c(0) \geq 0, && v(t) \geq 0, \text{ given } -\tau_1 \leq t \leq 0, \\ &w(0) \geq 0, && z(t) \geq 0, \text{ given } -\tau_2 \leq t \leq 0, \end{aligned} \tag{4.7.3}$$

where T is the period of therapy, and A_1 and A_2 are measures of the relative costs of the interventions associated with the controls u_1 and u_2, respectively. The expression $\frac{A_1 u_1^2}{2}$ represents cost associated with $u_1(t)$ and $\frac{A_2 u_2^2}{2}$ represents cost associated with $u_2(t)$. The two control functions, $u_1(t)$ and $u_2(t)$ are assumed to be bounded and Lebesgue integrable. We have assumed a quadratic cost for administering the controls u_1 and u_2 for two reasons. Firstly, there are typically increasing costs with reaching higher fractions of a population. The quadratic is the simplest nonlinear function and therefore we have used it in our model. Secondly, assuming a linear cost for the control leads to a "bang-bang" solution, where the solution is always to maximize or minimize the drug cost at each point in time. Our target is to maximize the objective functional defined in equation (4.7.1) by increasing the number of the uninfected hepatocytes $x(t)$, the antibodies $w(t)$ and the CTLs immune responses $z(t)$ and decreasing the viral load for minimum therapy cost, i.e., we are finding the optimal control pair (u_1^*, u_2^*) such that

$$J(u_1^*, u_2^*) = \max_{(u_1,u_2)\in U} J(u_1, u_2), \tag{4.7.4}$$

where the control set U is defined by

$$U = \{(u_1(t), u_2(t)) : u_i(t) \text{ measurable } 0 \leq u_i(t) \leq 1, t \in [0, T], i = 1, 2\}. \tag{4.7.5}$$

4.7.1 Existence of an optimal control pair

The following theorem proves the existence of an optimal control pair. The proof is based on a result of [85] which is based on a theorem of [86].

Theorem 4.7.1. *There exists an optimal control pair $(u_1^*, u_2^*) \in U$ such that*

$$J(u_1^*, u_2^*) = \max_{(u_1,u_2)\in U} J(u_1, u_2). \tag{4.7.6}$$

Proof. To use the result of [85], we need to check the following properties:

(P_1) The set of state variables and controls is nonempty.

(P_2) The set of controls (U) is closed and convex.

(P_3) The right hand side of the state system is bounded by a linear function in the state and control variables.

(P_4) The integrand of the objective functional is concave on U.

(P_5) There exists a constant $\zeta > 1$ and positive numbers η_1, $\eta_2 > 0$, such that the integrand $I(x, w, z, u_1, u_2)$ of the objective functional satisfies

$$I(x, w, z, u_1, u_2) \leq \eta_1 - \eta_2(|u_1|^2 + |u_2|^2)^{\frac{\zeta}{2}}, \tag{4.7.7}$$

where $I(x, w, z, u_1, u_2) = x(t) + w(t) + z(t) - \left(\frac{A_1}{2}u_1^2(t) + \frac{A_2}{2}u_2^2(t)\right)$.

The proofs that our model satisfies the conditions are as follows.

(P_1) From Theorem 4.3.1, the solution of the system of equation (4.1.1) - (4.1.6) exists and is unique for given initial conditions and given controls in the set U. Therefore, the set of state variables and controls is nonempty and condition P_1 is satisfied.

(P_2) The control set U defined in (4.7.5) is clearly convex and closed.

(P_3) From Theorem 4.3.1, the right-hand-side of equation (4.1.1) - (4.1.6) is bounded by a linear function in the state and control variables.

(P_4) The integrand of the objective functional in (4.7.1) is clearly concave on U.

(P_5) Since, from Theorem 4.2.2, $x(t) \leq \bar{x}$, $w(t) \leq \bar{w}$, $z(t) \leq \bar{z}$ are bounded above, and A_1, $A_2 > 0$, we have

$$\begin{aligned} I(x, w, z, u_1, u_2) &= x(t) + w(t) + z(t) - \left(\frac{A_1}{2}u_1^2(t) + \frac{A_2}{2}u_2^2(t)\right) \\ &\leq \bar{x} + \bar{w} + \bar{z} - \frac{1}{2}\min\{A_1, A_2\}(u_1^2(t) + u_2^2(t)) \\ &= \eta_1 - \eta_2(|u_1|^2 + |u_2|^2)^{\frac{\zeta}{2}}, \end{aligned} \tag{4.7.8}$$

where $\eta_1 = \bar{x} + \bar{w} + \bar{z}$, $\eta_2 = \frac{1}{2}\min\{A_1, A_2\}$ and $\zeta = 2$.

This completes the proof. □

4.7.2 Pontryagin maximum principle

Derivations of the Pontryagin maximum principle can be found in many books and papers for both no-delay problems (see, e.g., [76–78]) and for time delay problems (see, e.g. [52, 87, 88]). In this section, we will summarize the necessary conditions that the Pontryagin maximum principle gives for the solution of the time delay optimal control problem of equations (4.7.1), (4.7.2) and (4.7.3).

The Hamiltonian for the system (4.7.1) and (4.7.2) is given by

$$\begin{aligned}
&H(\mathbf{x}(t), x(t-\tau_1), y(t-\tau_2), v(t-\tau_1), z(t-\tau_2), u_1(t), u_2(t), \lambda(t)) \\
&= f_0(x(t), w(t), z(t), u_1(t), u_2(t)) + \lambda_1(t) f_1(x(t), v(t), y(t), u_1(t)) \\
&\quad + \lambda_2(t) f_2(y(t), z(t), x(t-\tau_1), v(t-\tau_1), u_1(t)) \\
&\quad + \lambda_3(t) f_3(y(t), c(t), u_2(t)) + \lambda_4(t) f_4(c(t), v(t), w(t)) \\
&\quad + \lambda_5(t) f_5(v(t), w(t)) + \lambda_6(t) f_6(z(t), y(t-\tau_2), z(t-\tau_2)),
\end{aligned} \tag{4.7.9}$$

where, for ease of writing, we define

$$\mathbf{x}(t) = (x_1(t), x_2(t), x_3(t), x_4(t), x_5(t), x_6(t))^T \tag{4.7.10}$$

with $x_1(t) = x(t)$, $x_2(t) = y(t)$, $x_3(t) = c(t)$, $x_4(t) = v(t)$, $x_5(t) = w(t)$, $x_6(t) = z(t)$, and $\lambda(t) = (\lambda_1(t), \lambda_2(t), \lambda_3(t), \lambda_4(t), \lambda_5(t), \lambda_6(t))^T$.

Following the definitions of the costate equations in [52], we separate the costate equations into 3 types: 1) no time delay, 2) time delay τ_1, and 3) time delay τ_2.

1. No time delay. Since the state variables $x_3(t) = c(t)$ and $x_5(t) = w(t)$ have no time delay, the costate equations for $\lambda_3(t)$ and $\lambda_5(t)$ are as follows:

$$\begin{aligned}
\dot{\lambda}_3(t) &= -\frac{\partial H(\mathbf{x}(t), x(t-\tau_1), y(t-\tau_2), v(t-\tau_1), z(t-\tau_2), u_1(t), u_2(t), \lambda(t))}{\partial c(t)} \\
&= -\lambda_3(t)\frac{\partial f_3(y(t), c(t), u_2(t))}{\partial c(t)} - \lambda_4(t)\frac{\partial f_4(c(t), v(t), w(t))}{\partial c(t)} \\
&= (\alpha + \delta)\lambda_3(t) - \alpha\lambda_4(t). \qquad (4.7.11) \\
\dot{\lambda}_5(t) &= -\frac{\partial H(\mathbf{x}(t), x(t-\tau_1), y(t-\tau_2), v(t-\tau_1), z(t-\tau_2), u_1(t), u_2(t), \lambda(t))(t))}{\partial w(t)}
\end{aligned}$$

$$= -\frac{\partial f_0(x(t), w(t), z(t), u_1(t), u_2(t))}{\partial w(t)} - \lambda_4(t)\frac{\partial f_4(c(t), v(t), w(t))}{\partial w(t)}$$
$$- \lambda_5(t)\frac{\partial f_5(v(t), w(t))}{\partial w(t)}$$
$$= -1 + \lambda_4(t)\gamma v(t) - \lambda_5(t)(gv(t) - h). \tag{4.7.12}$$

The time interval for the two costate equations is $0 \leq t \leq T$ with the boundary conditions $\lambda_3(T) = \lambda_5(T) = 0$.

2. Time delay τ_1. The state variable $x_1(t) = x(t)$ also has a time delay term $x(t - \tau_1)$ and the variable $x_4(t) = v(t)$ also has a time delay term $v(t - \tau_1)$. Therefore, the costate equations for $\lambda_1(t)$ and $\lambda_4(t)$ are defined separately for the time intervals $0 \leq t \leq T - \tau_1$ and $T - \tau_1 \leq t \leq T$.

The time delay equations for $\lambda_1(t)$ are given by

$$\dot{\lambda}_1(t) = -\frac{\partial H(\mathbf{x}(t), x(t-\tau_1), y(t-\tau_2), v(t-\tau_1), z(t-\tau_2), u_1(t), u_2(t), \lambda(t))}{\partial x(t)}$$
$$- \frac{\partial H(\mathbf{x}(t+\tau_1), x(t), y(t+\tau_1-\tau_2), v(t), z(t+\tau_1-\tau_2), u_1(t+\tau_1), u_2(t+\tau_1), \lambda(t+\tau_1))}{\partial x(t)},$$
$$= -\frac{\partial f_0(x(t), w(t), z(t), u_1(t), u_2(t))}{\partial x(t)} - \lambda_1(t)\frac{\partial f_1(x(t), v(t), y(t), u_1(t))}{\partial x(t)}$$
$$- \lambda_2(t+\tau_1)\frac{\partial f_2(y(t+\tau_1), z(t+\tau_1), x(t), v(t), u_1(t+\tau_1))}{\partial x(t)},$$
$$= -1 + \lambda_1(t)(\sigma + (1 - u_1(t))\beta v(t)) - \lambda_2(t+\tau_1)(1 - u_1(t+\tau_1))\beta e^{-m\tau_1} v(t),$$
for $0 \leq t \leq T - \tau_1$.

And,

$$\dot{\lambda}_1(t) = -\frac{\partial H(\mathbf{x}(t), x(t-\tau_1), y(t-\tau_2), v(t-\tau_1), z(t-\tau_2), u_1(t), u_2(t), \lambda(t))}{\partial x(t)}$$
$$= -1 + \lambda_1(t)(\sigma + (1 - u_1(t))\beta v(t)),$$
for $T - \tau_1 \leq t \leq T$. (4.7.13)

The time delay equations for $\lambda_4(t)$ are given by

$$\dot{\lambda}_4(t) = -\frac{\partial H(\mathbf{x}(t), x(t-\tau_1), y(t-\tau_2), v(t-\tau_1), z(t-\tau_2), u_1(t), u_2(t), \lambda(t))}{\partial v(t)}$$
$$- \frac{\partial H(\mathbf{x}(t+\tau_1), x(t), y(t+\tau_1-\tau_2), v(t), z(t+\tau_1-\tau_2), u_1(t+\tau_1), u_2(t+\tau_1), \lambda(t+\tau_1))}{\partial v(t)},$$
$$= -\lambda_1(t)\frac{\partial f_1(x(t), v(t), y(t), u_1(t))}{\partial v(t)} - \lambda_4(t)\frac{\partial f_4(c(t), v(t), w(t))}{\partial v(t)} - \lambda_5(t)\frac{\partial f_5(v(t), w(t))}{\partial v(t)}$$
$$- \lambda_2(t+\tau_1)\frac{\partial f_2(y(t+\tau_1), z(t+\tau_1), x(t), v(t), u_1(t+\tau_1))}{\partial v(t)},$$

$$= \lambda_1(t)(1-u_1(t))\beta x(t) + \lambda_4(t)(\gamma w(t)+\mu) - \lambda_5(t)gw(t)$$
$$- \lambda_2(t+\tau_1)(1-u_1(t+\tau_1))\beta e^{-m\tau_1}x(t),$$
for $0 \le t \le T-\tau_1$.

And,

$$\dot{\lambda}_4(t) = -\frac{\partial H(\mathbf{x}(t), x(t-\tau_1), y(t-\tau_2), v(t-\tau_1), z(t-\tau_2), u_1(t), u_2(t), \lambda(t))}{\partial v(t)}$$
$$= \lambda_1(t)(1-u_1(t))\beta x(t) + \lambda_4(t)(\gamma w(t)+\mu) - \lambda_5(t)gw(t),$$
for $T-\tau_1 \le t \le T$. (4.7.14)

The conditions on the costate equations are continuity of $x(t)$ and $v(t)$ at $t = T-\tau_1$ and $\lambda_1(T) = \lambda_4(T) = 0$.

3. Time delay τ_2. The state variable $x_2(t) = y(t)$ also has a time delay term $y(t-\tau_2)$ and the variable $x_6(t) = z(t)$ also has a time delay term $z(t-\tau_2)$. Therefore, the costate equations for $\lambda_2(t)$ and $\lambda_6(t)$ are defined separately for the time intervals $0 \le t \le T-\tau_2$ and $T-\tau_2 \le t \le T$.
The time delay equations for $\lambda_2(t)$ are given by

$$\dot{\lambda}_2(t) = -\frac{\partial H(\mathbf{x}(t), x(t-\tau_1), y(t-\tau_2), v(t-\tau_1), z(t-\tau_2), u_1(t), u_2(t), \lambda(t))}{\partial y(t)}$$
$$- \frac{\partial H(\mathbf{x}(t+\tau_2), x(t-\tau_1+\tau_2), y(t), v(t-\tau_1+\tau_2), z(t), u_1(t+\tau_2), u_2(t+\tau_2), \lambda(t+\tau_2))}{\partial y(t)},$$
$$- \lambda_1(t)\frac{\partial f_1(x(t), v(t), y(t), u_1(t))}{\partial y(t)} - \lambda_2(t)\frac{\partial f_2(y(t), z(t), x(t-\tau_1), v(t-\tau_1), u_1(t))}{\partial y(t)}$$
$$- \lambda_3(t)\frac{\partial f_3(y(t), c(t), u_2(t))}{\partial y(t)} - \lambda_6(t+\tau_2)\frac{\partial f_6(z(t+\tau_2), y(t), z(t))}{\partial y(t)},$$
$$= -\lambda_1(t)p + \lambda_2(t)(\sigma + p + qz(t)) - \lambda_3(t)a(1-u_2(t)) - \lambda_6(t+\tau_2)kz(t),$$
for $0 \le t \le T-\tau_2$.

And,

$$\dot{\lambda}_2(t) = -\frac{\partial H(\mathbf{x}(t), x(t-\tau_1), y(t-\tau_2), v(t-\tau_1), z(t-\tau_2), u_1(t), u_2(t), \lambda(t))}{\partial y(t)}$$
$$- \lambda_1(t)p + \lambda_2(t)(\sigma + p + qz(t)) - \lambda_3(t)a(1-u_2(t)),$$
for $T-\tau_2 \le t \le T$. (4.7.15)

The time delay equations for $\lambda_6(t)$ are given by

$$\dot{\lambda}_6(t) = -\frac{\partial H(\mathbf{x}(t), x(t-\tau_1), y(t-\tau_2), v(t-\tau_1), z(t-\tau_2), u_1(t), u_2(t), \lambda(t))}{\partial z(t)}$$
$$- \frac{\partial H(\mathbf{x}(t+\tau_2), x(t-\tau_1+\tau_2), y(t), v(t-\tau_1+\tau_2), z(t), u_1(t+\tau_2), u_2(t+\tau_2), \lambda(t+\tau_2))}{\partial z(t)},$$

$$= -\frac{\partial f_0(x(t), w(t), z(t), u_1(t), u_2(t))}{\partial z(t)} - \lambda_2(t)\frac{\partial f_2(y(t), z(t), x(t-\tau_1), v(t-\tau_1), u_1(t))}{\partial z(t)}$$
$$- \lambda_6(t)\frac{\partial f_6(z(t), y(t-\tau_2), z(t-\tau_2))}{\partial z(t)} - \lambda_6(t+\tau_2)\frac{\partial f_6(z(t+\tau_2), y(t), z(t))}{\partial z(t)},$$
$$= -1 + \lambda_2(t)qy(t) + \varepsilon\lambda_6(t) - \lambda_6(t+\tau_2)ky(t),$$
for $0 \le t \le T - \tau_2$.

And,

$$\dot{\lambda}_6(t) = -\frac{\partial H(\mathbf{x}(t), x(t-\tau_1), y(t-\tau_2), v(t-\tau_1), z(t-\tau_2), u_1(t), u_2(t), \lambda(t))}{\partial z(t)}$$
$$= -1 + \lambda_2(t)qy(t) + \varepsilon\lambda_6(t), \text{for } T - \tau_2 \le t \le T. \tag{4.7.16}$$

The conditions on the costate equations are continuity of $y(t)$ and $z(t)$ at $t = T - \tau_2$ and $\lambda_2(T) = \lambda_6(T) = 0$.

4.7.3 Maximum control values

In the Pontryagin maximum principle, the optimal values of the state and costate variables $\mathbf{x}^*(t)$ and $\lambda^*(t)$ values occur for values of $u_1^*(t)$ and $u_2^*(t)$ which give local maximum values of the Hamiltonian. For the case of bounded controls with a concave Hamiltonian, there are 3 differerent possibilities:

1. An internal point of $0 \le u_1(t) \le 1$ or $0 \le u_2(t) \le 1$. For $u_1(t)$, the condition is:

$$0 = \frac{\partial H(\mathbf{x}^*(t), x^*(t-\tau_1), y^*(t-\tau_2), v^*(t-\tau_1), z^*(t-\tau_2), u_1(t), u_2(t), \lambda^*(t))}{\partial u_1(t)},$$
$$= \frac{\partial f_0(x^*(t), w^*(t), z^*(t), u_1(t), u_2(t))}{\partial u_1(t)} + \lambda_1(t)\frac{\partial f_1(x^*(t), v^*(t), y^*(t), u_1(t))}{\partial u_1(t)}$$
$$+\lambda_2^*(t)\frac{\partial f_2(y^*(t), z^*(t), x^*(t-\tau_1), v^*(t-\tau_1), u_1(t))}{\partial u_1(t)},$$
$$= -A_1u_1(t) + \lambda_1^*(t)\beta x^*(t)v^*(t) - \lambda_2^*(t)\beta e^{-m\tau_1}x^*(t-\tau_1)v^*(t-\tau_1). \tag{4.7.17}$$

Therefore, a possible internal point for the first control is:

$$\bar{u}_1(t) = \frac{\beta}{A_1}\big(\lambda_1^*(t)x^*(t)v^*(t) - \lambda_2^*(t)e^{-m\tau_1}x^*(t-\tau_1)v^*(t-\tau_1)\big). \tag{4.7.18}$$

This is a maximum point of H since $\dfrac{\partial^2 H}{\partial u_1^2} = -A_1 < 0$ and H is a concave function of u_1.

For $u_2(t)$, the condition is:

$$0 = \frac{\partial H(\mathbf{x}(t), x(t-\tau_1), y(t-\tau_2), v(t-\tau_1), z(t-\tau_2), u_1(t), u_2(t), \lambda(t))}{\partial u_2(t)},$$

$$= \frac{\partial f_0(x(t), w(t), z(t), u_1(t), u_2(t))}{\partial u_2(t)} + \lambda_3(t)\frac{\partial f_3(y(t), c(t), u_2(t))}{\partial u_2(t)},$$
$$= -A_2 u_2(t) - \lambda_3(t) a y(t). \tag{4.7.19}$$

Therefore, a possible internal point for the second control is:

$$\bar{u}_2(t) = -\frac{1}{A_2}\lambda_3^*(t) a y^*(t). \tag{4.7.20}$$

This is a maximum point of H since $\frac{\partial^2 H}{\partial u_2^2} = -A_2 < 0$ and H is a concave function of u_2.

2. At lower bounds $u_1(t) = 0$ or $u_2(t) = 0$.

3. At upper bounds $u_1(t) = 1$ or $u_2(t) = 1$.

There are therefore 9 possible choices for the optimal control pair $(u_1^*(t), u_2^*(t))$.

In summary.

1. If the internal point $\bar{u}_1(t) \in [0, 1]$, then $u_1^*(t) = \bar{u}_1(t)$ is the maximum point. If $\bar{u}_1(t) < 0$, then $u_1^*(t) = 0$ is the maximum point. If $\bar{u}_1(t) > 1$, then $u_1^*(t) = 1$ is the maximum point.
   This is written in the literature as $u_1^*(t) = \max(0, \min(1, \bar{u}_1(t))$.

2. If the internal point $\bar{u}_2(t) \in [0, 1]$, then $u_2^*(t) = \bar{u}_2(t)$ is the maximum point. If $\bar{u}_2(t) < 0$, then $u_2^*(t) = 0$ is the maximum point. If $\bar{u}_2(t) > 1$, then $u_2^*(t) = 1$ is the maximum point.
   This is written in the literature as $u_2^*(t) = \max(0, \min(1, \bar{u}_2(t))$.

4.7.4 Algorithm for solution of the optimal control problem

The algorithm that we use to compute the optimal controls with Matlab is as follows:

1. Select an initial feasible control pair $(u_1^{(0)}(t), u_2^{(0)}(t))$.
   For $k = 0, 1, \ldots, k_{max}$

(a) For the given initial conditions and the given control pair, integrate the system of state equations (4.1.1) - (4.1.6) using an ODE delay solver such as *dde23* in Matlab.

(b) Since the costate equations (4.7.11)–(4.7.16) defined in the Pontryagin Maximum Principle section 4.7.2 must be integrated in the backwards direction in time for numerical stability, time-reverse the system of costate equations, and then integrate the time-reversed system of costate equations in the forward direction using the same ODE solver *dde23* as for the state equations.

(c) Use the methods described in section 4.7.3 to find the values of the new control pair
$(u_1^{(k+1)}(t), u_2^{(k+1)}(t))$ that maximize the Hamiltonian for the given values of $\mathbf{x}(t)$ and $\lambda(t)$ obtained from the state and costate integrations in (a) and (b).

(d) Compare the new control pair $(u_1^{(k+1)}(t), u_2^{(k+1)}(t))$ with the previous control pair $(u_1^{(k)}(t), u_2^{(k)}(t))$.

2. If the two control pairs are the same to a specified tolerance stop.
Otherwise replace $(u_1^{(k)}(t), u_2^{(k)}(t))$ by $(u_1^{(k+1)}(t), u_2^{(k+1)}(t))$ and repeat steps (a), (b), (c), and (d) for the new control pair.

4.8 Numerical simulations

We begin by looking at the solutions of system of equation (4.1.1) - (4.1.6) for zero controls $u_1 = u_2 = 0$ for the zero delay case and for the nonzero delay cases : $\tau_1 = 2$ days for the delay in the production of infected hepatocytes by free virus and $\tau_2 = 4$ days for the delay in the antigenic stimulation generating CTLs. We then look at the optimal control problem (4.7.1) for system of equation (4.1.1) - (4.1.6) for the nonzero delay cases.

In the numerical simulations, we have used the values of the parameters given in Table 2, i.e., $\Lambda = 1$, $\sigma = 0.011$, $\beta = 0.0014$, $p = 0.012$, $m = 0.011$, $q = 0.001$, $a = 0.15$, $\alpha = 0.87$, $\mu = 0.693$, $g = 0.008$, $h = 0.15$, $k = 0.001$,$\varepsilon = 0.5$. As noted

in Table 2, the values have been selected from published sources, if available, or reasonable values have been assumed for parameters if no published values could be found.

4.8.1 Case I : zero control

The numerical results for the zero delay and nonzero delay cases for zero control are shown in Figures 20(a)–(f). In all figures, the zero delay results are plotted as blue dashed lines and the nonzero delay results as red solid lines.

Figure 20(a) shows that the concentration of uninfected hepatocytes (x) with nonzero delay declines faster than the concentration with zero delay during the first 30 days, whereas the concentration with zero delay decreases faster than the nonzero delay from the 30th to the 80th day when both cases reach the same value. The reason for this behavior can be seen in the different infection rates of hepatocytes shown in Figure 20(b) for the zero and nonzero delay cases.

Figure 20(b) shows that for zero delay the concentration of infected hepatocytes (y) has an initial peak of 1950 cells/ml at 3 days, a second peak of 900 cells/ml at 40 days, a third peak of 330 cells/ml at 100 days and then decreases to a small equilibrium value. For the nonzero delay case, the concentration has a higher initial peak of approximately 3100 cells/ml at 13 days and then a much smaller second peak of 520 cells/ml at 88 days before decreasing to an equilibrium level similar to that of the zero delay case. A possible reason for the much slower initial infection rate in the nonzero delay case is that the delay $\tau_1 = 2$ days slows down the initial growth rate of the infection. In both cases, the second peak is lower than the first peak. A possible explanation is that the high number of infections in the first peak causes rapid increases in the concentrations of antibodies and CTLs (see Figures 20(e) and (f)) which then help to reduce the concentrations of infected hepatocytes in the later peaks.

Figure 20(c) for the intracellular HBV DNA-containing capsids (c) shows a similar dynamical pattern to the pattern of the infected hepatocytes for both zero and nonzero delay cases. For zero delay, the concentration of capsids rises to an intial peak of 280 cells/ml at 10 days, a second peak of 150 cells/ml at 45 days and a third peak of 50 cells/ml at 100 days. For nonzero delay, the concentration rises

to a high initial peak of 500 cells/ml at 13 days and a second peak of 85 cells/ml at 88 days. Finally, in both cases the concentrations decay at similar rates to equilibrium values.

Figure 20(d) for the free viruses (v) again shows a similar dynamical pattern to the patterns for the infected hepatocytes and the capsids for both zero and nonzero delay cases. For zero delay the concentration of free viruses rises to an intial peak of 105 cells/ml at 5 days and a second peak of 37 cells/ml at 35 days. For nonzero delay, the concentration initially rises to an initial peak of 90 cells/ml at 7 day and a second peak of 47 cells/ml at 78 days. Finally, in both cases the concentrations decay at similar rates to equilibrium values.

Figure 20(e) for the antibodies (w) again shows a similar dynamical pattern to the patterns for the infected hepatocytes, capsids and free viruses for both zero and nonzero delay cases. For zero delay, the concentration rises to an intial peak of 422 cells/ml at 8 days, a second peak of 500 cells/ml at 50 days and a third peak of 190 cells/ml at 100 days. For nonzero delay, the concentration rises to an initial peak of 1650 cells/ml at 18 days and a second peak of 300 cells/ml at 100 days. Finally, in both cases the concentrations decay at similar rates to equilibrium values. As noted above, it can be seen that the pattern of the concentration of antibodies are in the same pattern as the concentration of the infected hepatocytes, capsids and free viruses. However, the peaks in the antibodies occur after the peaks in the infections as the antibodies occur as a response to the infections.

Finally, Figure 20(f) for the CTLs (z) again shows a similar dynamical pattern to the patterns for the infected hepatocytes, capsids, free viruses and antibodies for both zero and nonzero delay cases. For zero delay, the concentration of CTLs has an initial peak of 1390 cells/ml at 8 days and a second peak of 135 cells/ml at 50 days. For nonzero delay, the concentration of CTLs has only one peak of 790 cells at 25 days. In both cases the concentrations reduce to zero equilibrium value. As for the antibodies, the peaks in the CTLs occur after the peaks in the infections.

In summary, it can be seen that the presence of the delay causes the initial peaks to occur later than in the zero delay case and that the initial peaks of the concentrations are much higher than the later peaks in both cases. The reduction

in peak size of the concentrations of infected hepatocytes, capsids and free viruses is almost certainly due to the increased concentrations of antibodies and CTLs resulting from the initial infections.

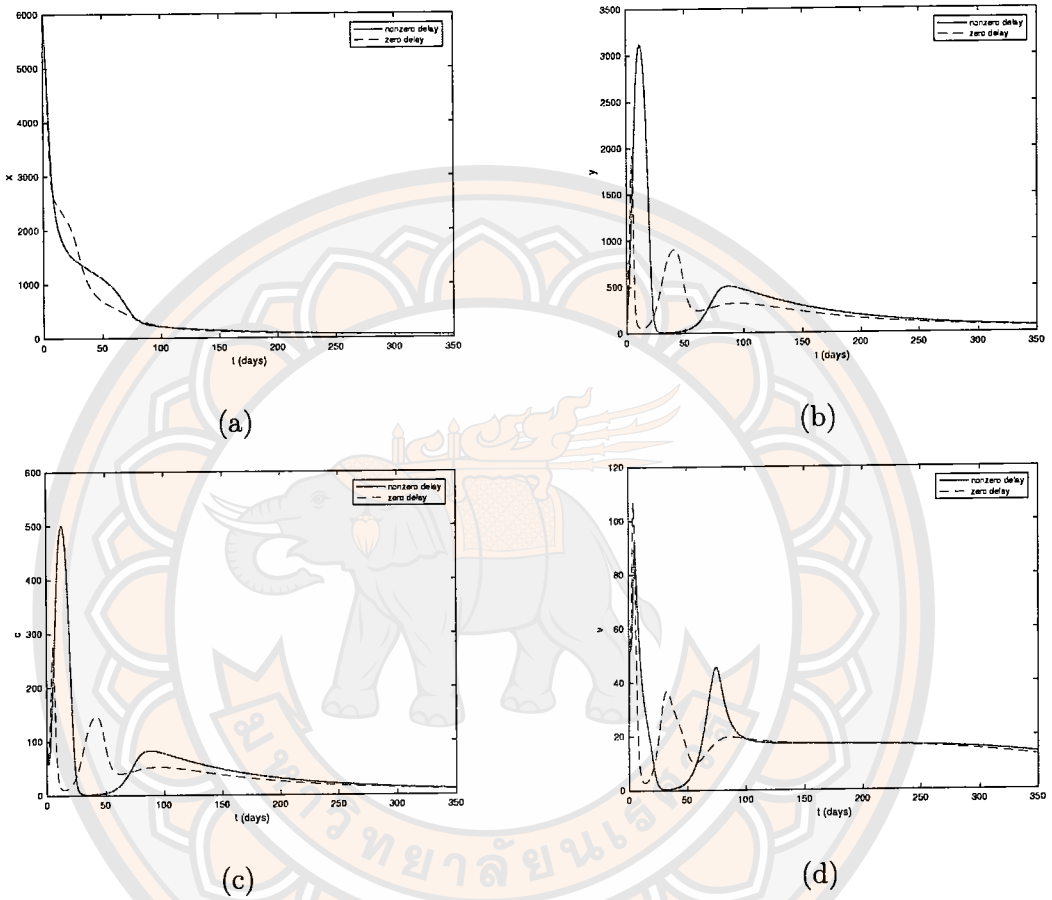

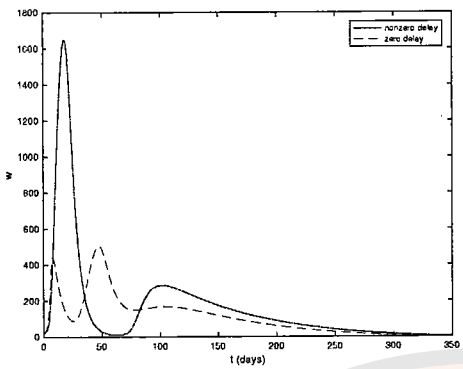

(e)

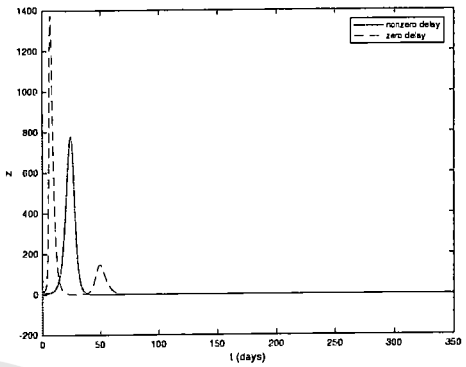

(f)

Figure 20 Dynamics of the HBV model (4.1.1) - (4.1.6) with zero delay (dashed curves) and with nonzero delay (solid curves) for $\tau_1 = 2$ and $\tau_2 = 4$. (a) Concentration of uninfected hepatocytes (x), (b) Concentration of infected hepatocytes (y), (c) Concentration of intracellular HBV DNA-containing capsids (c), (d) Concentration of free viruses (v), (e) Concentration of antibodies (w) and (f) Concentration of CTLs (z).

4.8.2 Case II : optimal control

In the simulations, we computed numerical results for nonzero time delays for the two cases of zero control and optimal nonzero control.

The numerical results for the zero control and optimal control cases are shown in Figures 21(a)–(h) for the time delays $\tau_1 = 2$ days and $\tau_2 = 4$ days. We assumed that control u_1, the efficiency of drug therapy in blocking new infection, and the control u_2, the efficiency of drug therapy in inhibiting viral production, were both in the range $[0, 0.7]$. In all figures, the zero control results are plotted as a blue dashed line and the optimal control results are plotted as a red solid line.

Figures 21(a) and (b) show the optimal control treatment strategies for u_1 and u_2, respectively. For u_1, the optimal strategy is to initially administer the drug at the maximum allowed efficiency level of 70% until day 149 and then gradually reduce the level towards zero by the final day 350. For u_2, the optimal strategy

is to initially administer the drug at the maximum allowed efficiency level of 70% until day 107 and then rapidly reduce the level to zero by day 135.

Figures 21(c)–(h) compare the concentrations of the populations for a period of 350 days for zero control and for the optimal controls shown in Figures 21(a) and (b).

Figure 21(c) shows that for the parameter values considered in this simulation, the effect of applying the two control variables at the optimal efficiency levels shown in Figues 21(a) and (b) is to reduce the rate of infection of the uninfected hepatocytes (x) at a much slower rate than for the zero control case until the rates become approximately equal after 250 days. However, as shown in Figures 21(a) and (b), at 250 days the optimal levels of u_1 and u_2 are both zero.

Figure 21(d) shows that the concentration of infected hepatocytes (y) increases rapidly in the absence of controls u_1 and u_2 to 3100 cells/ml at 11 days and then declines sharply before rising to a small peak of approximately 500 cells/ml at 86 day. A possible explanation for the second peak being smaller is that the high levels of y in the first peak lead to a high concentration of CTLs which can help reduce the concentration of infected hepatocytes in the second peak. For the optimal controls, the concentration reaches a peak at approximately 970 cells/ml at 29 days showing the effectiveness of the therapy. As for the uninfected hepatocytes, the peak in the infected hepatocytes at approximately 200 days shows the increase in infection when the rate at which the drugs are administered is reduced.

Figure 21(e) shows the same dynamical patterns for the concentration of intracellular HBV DNA-containing capsids (c) as the patterns for the infected hepatocytes. That is, for zero controls the concentration increases rapidly to a peak of 500 cells/ml at 12 days, then decreases rapidly to near zero and then rises to a second peak of 80 cells/ml at 86 days. With the optimal controls, the concentration increases more slowly to an initial peak of 44 cells/ml at 30 days and then to a second peak of 60 cells/ml at approximately 140 days. The increase in the second peak for the optimal control can be associated with the reproduction in the drug therapies at 140 days. These results indicate that the control drugs significantly reduce the concentration of intracellular HBV DNA-containing capsids.

Since intracellular HBV DNA-containing capsids play a role in the virus life cycle, as they assemble around viral reverse transcriptase, this reduction in them leads to a reduction in the concentration of free viruses as shown in Figure 21(f).

Figure 21(f) shows similar dynamical patterns for the concentrations of free viruses (v) as for the capsids (c) in Figure 21(e). For zero controls, the concentration increases rapidly to a peak of 90 cells/ml at 6 days, then decreases rapidly to near zero and then rises again to a second peak of 45 cells/ml at 74 days. With the optimal controls, the concentration increases more slowly to an initial peak of 28 cells/ml at 20 days and then to a second peak of 49 cells/ml at 126 days. The increase in the second peak for the optimal control can be associated with the reduction in the drug therapies at 126 days.

Figure 21(g) again shows similar dynamical patterns for the concentrations of antibodies (w). For zero controls, the concentration increases rapidly to a peak of 1640 cells/ml at 16 days, then decreases rapidly to near zero and then rises again to a second peak of 290 cells/ml at 101 days. With the optimal controls, the concentration increases more slowly to an initial peak of 130 cells/ml at 39 days and then to a second peak of 222 cells/ml at 150 days. The increase in the second peak for the optimal control can again be associated with the reduction in the drug therapies at 150 days.

Figure 21(h) again shows similar dynamical patterns for the concentrations of CTLS (z). For zero control, the concentration of CTLs (z) increases rapidly to a peak of 790 cells/ml at 24 days and then decreases rapidly to zero. For the optimal controls, the concentration rises to a small peak of 89 cells/ml at 49 days and then also decreases to zero.

In general, the results show that the therapy greatly reduces the level of infection. This effect can also be seen from the value of the integral for the state variables $\int_0^{350} (x(t) + w(t) + z(t))dt$, which has a value of 393190 cells/ml for the optimal control case and a value of 220630 cells/ml for the zero control case. The results in Figures 21(d)-(h) clearly show the effectiveness of the controls in producing a large reduction in the concentration of infected hepatocytes, intracellular HBV DNA-containing capsids, free viruses, and antibodies and therefore to a re-

duction in the concentration of antibodies and CTLs.

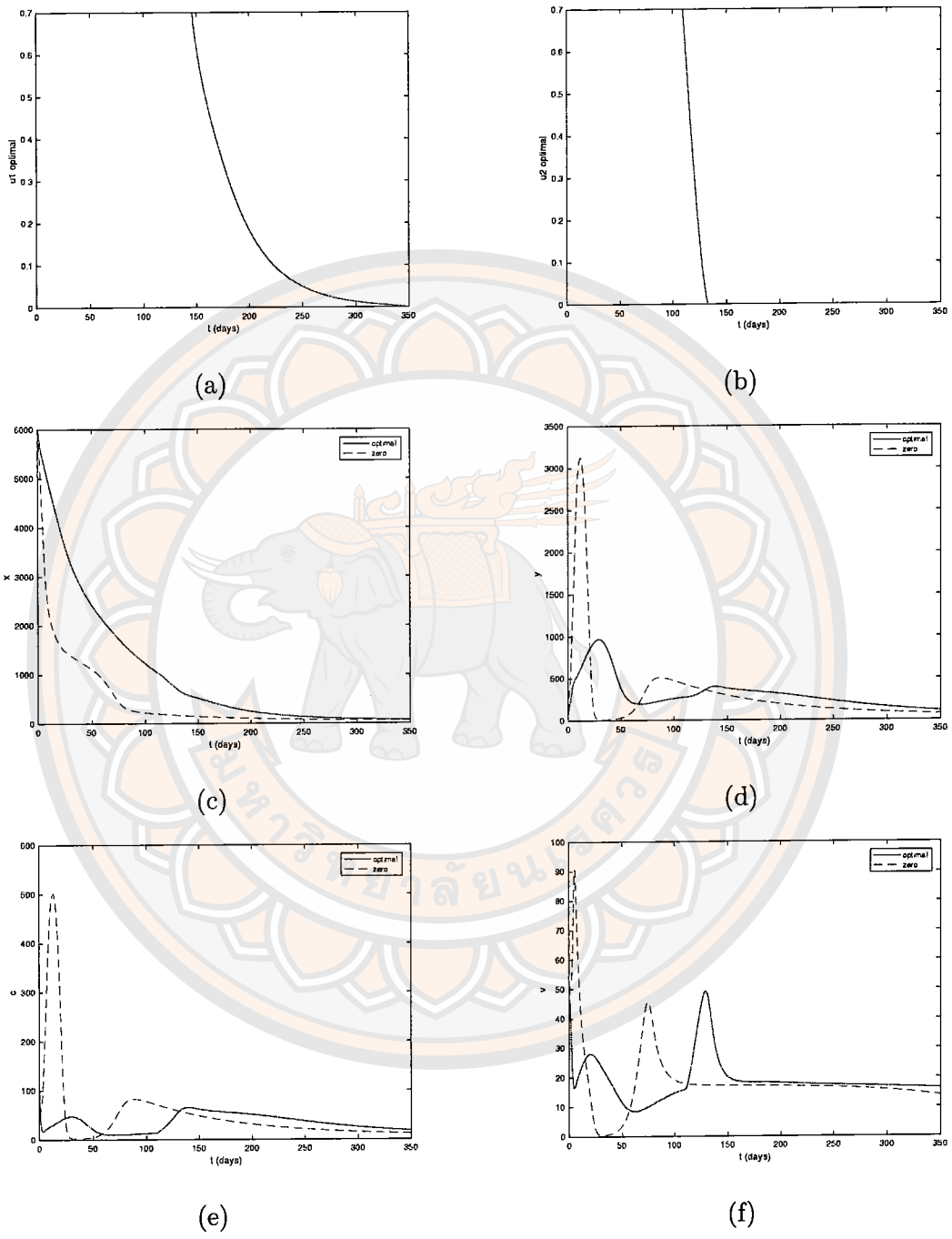

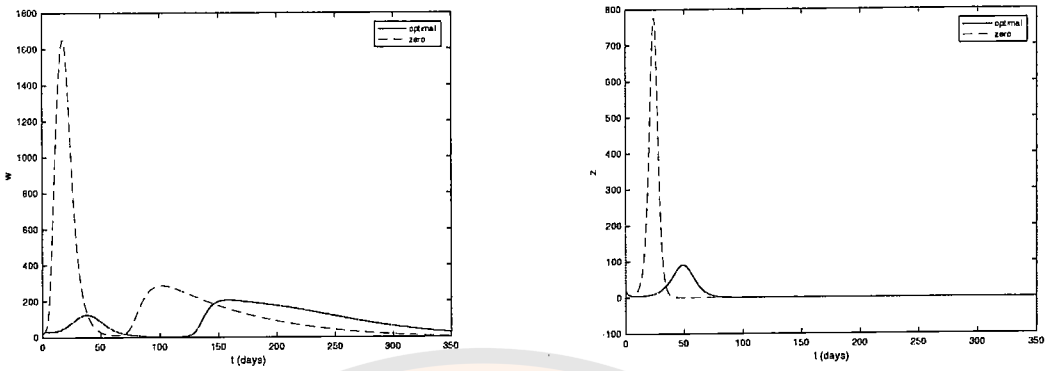

(g) (h)

Figure 21 Dynamics of the HBV model (4.1.1) - (4.1.6) with both controls (solid curves) and without controls (dashed curves) for time delays $\tau_1 = 2$ and $\tau_2 = 4$. (a) Optimal value of u_1, efficiency of drug therapy in blocking new infection, (b) Optimal value of u_2, efficiency of drug therapy in inhibiting viral production, (c) Concentration of uninfected hepatocytes (x), (d) Concentration of infected hepatocytes (y), (e) Concentration of intracellular HBV DNA-containing capsids (c), (f) Concentration of free viruses (v), (g) Concentration of antibodies (w) and (h) Concentration of CTLs (z).

4.8.3 Case III : basic reproduction number against controls

In this section, we show the relationship between the values of the optimal controls and the basic reproduction number for the cases of zero delays and nonzero delays.

Figures 22(a) and (b) show, respectively, the dynamical behavior of R_0 vs time when both controls are in the optimal states shown in Figures 21(a) and (b) for the zero delay case and nonzero delay case. In both cases, it can be seen that when the controls are set at their maximum allowed level of effectiveness ($u_1 = u_2 = 0.7$), the values of R_0 are a minimum and therefore the rate of reduction in the infected populations will be a maximum. However, as the level of the controls is reduced, the value of R_0 increases and the rate of reduction of the infected populations becomes slower. Near the end of the period of 350 days, the control levels are

reduced to zero and R_0 becomes greater than 1 showing that the infection will begin to increase. The results show that the control levels should be maintained at a nonzero minimum level to keep $R_0 < 1$.

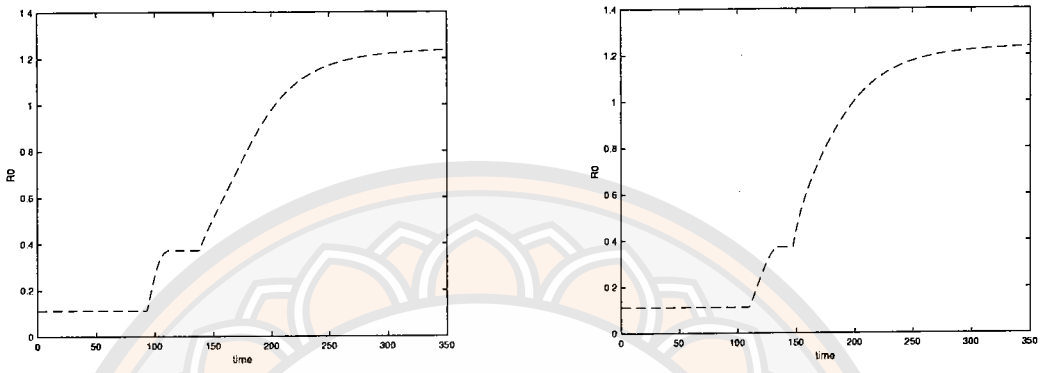

(a) (b)

Figure 22 Plots of basic reproductive number vs time for optimal levels of effectiveness of u_1 and u_2 (see Figures 21(a) and (b)). (a) Zero time delays. (b) Nonzero time delays: $\tau_1 = 2$ days, $\tau_2 = 4$ days.

Figures 23 and 24 show a comparison between the values of the basic reproductive number for zero delay and nonzero delay cases $\tau_1 = 2$ days and $\tau_2 = 4$ days for a range of values of the controls u_1 and u_2. It can be seen that R_0 increases with time slower in the delay case than in the nondelay case. A comparison of Figure 23(a) for zero delay shows that the value of R_0 starts increasing once the control u_1 drops after 138 days, whereas Figure 24(a) for nonzero delay shows R_0 does not start increasing until 150 days which is slower than the zero delay case. A similar pattern can be seen in comparing the zero delay Figure 23(b) with the nonzero delay 24(b) where R_0 starts increasing at approximately 98 days for the zero delay case and 110 days for the nonzero case.

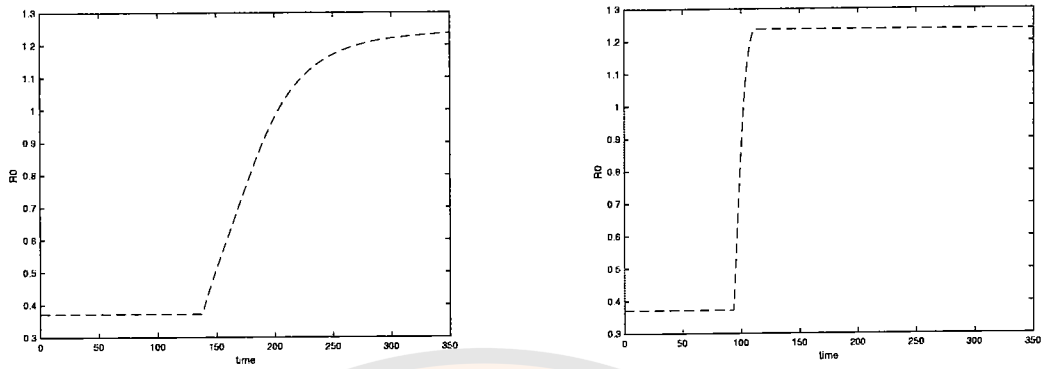

(a) (b)

Figure 23 Plots of basic reproductive number vs time for nondelay case. (a) u_1 optimal and $u_2 = 0$. (b) $u_1 = 0$ and u_2 optimal.

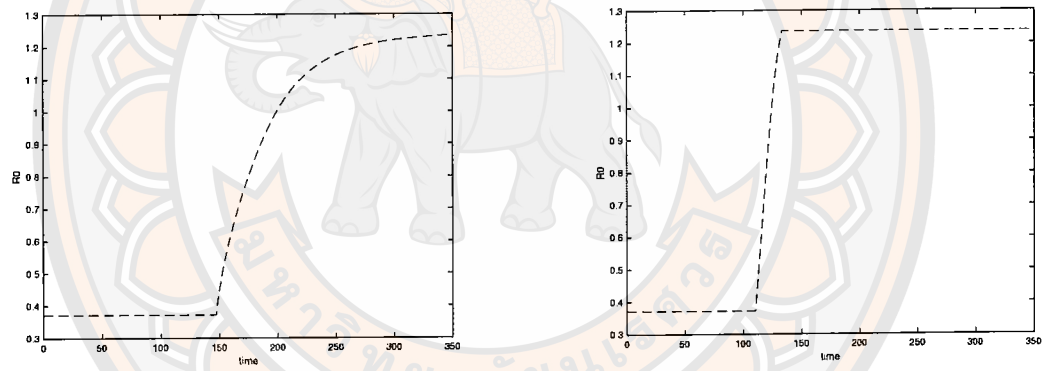

(a) (b)

Figure 24 Plots of basic reproductive number vs time for delay case ($\tau_1 = 2$ days, $\tau_2 = 4$ days). (a) u_1 optimal and $u_2 = 0$. (b) $u_1 = 0$ and u_2 optimal.

Finally, in Figure 25 we show the plots of R_0 vs u_1 and R_0 vs u_2. It can be seen that in both cases a value of approximately 0.2 gives a value of $R_0 = 1$ and could therefore be used, if required, to maintain an infection-free system.

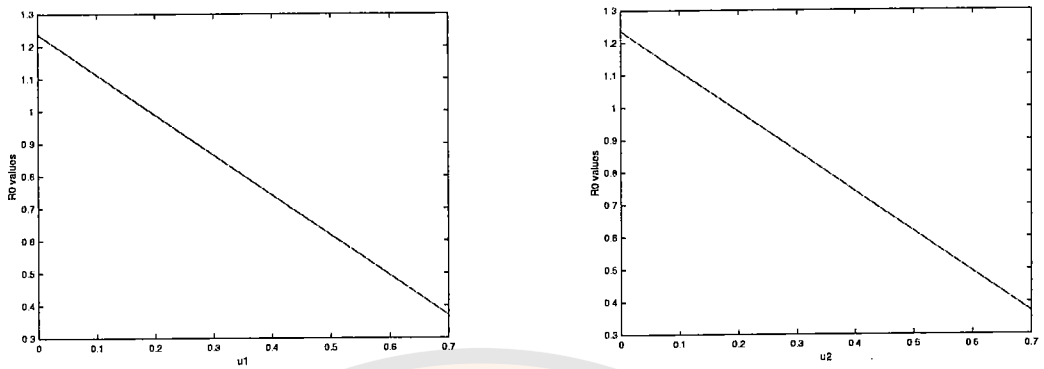

(a) (b)

Figure 25 Plots of basic reproductive number vs optimal control values for zero delay. (a) R_0 vs, u_1. (b) R_0 vs. u_2.

4.9 Conclusion

In this chapter, we have studied an optimal control problem for two drug therapies in a time delay model for HBV infection. The model consists of six populations: uninfected hepatocytes, infected hepatocytes, HBV DNA-containing-capsids, free viruses, antibodies and cytotoxic T-lymphocytes. The two time delays in the model are a delay in virus production after cell infection and a delay in antigenic stimulation generation. The model also includes an adaptive immune response, a cure rate for infected hepatocytes to uninfected hepatocytes and HBV DNA-containing capsids. The two optimal therapies are for blocking new infection of uninfected cells and for inhibiting viral production by infected cells. The solutions of the model are proved to be nonnegative, unique and bounded. The model is shown to have three equilibrium states, namely infection-free, immune-free and immune-activated. The basic reproduction number for the stability of the infection-free equilibrium has been derived and a sensitivity analysis has been carried out to determine the most important parameters to change to control the disease. The Pontryagin maximum principle is used to find the optimal control to maximize the concentrations of uninfected hepatocytes, antibodies and cytotoxic T-lynphocytes at mininmum cost. The existence of optimal control pairs is proved and an algorithm is developed for solution of the state and costate equations for the time

delayed Pontryagin maximum principle. Numerical simulations are then carried out to illustrate the dynamical behavior of the solutions of the time delayed optimal control model of HBV infection. The results show that the effects of the intracellular delays is to slow down the rate of infection. Finally, the results show that the two optimal control therapies considered in this paper can reduce the basic reproductive number to less than one and can significantly reduce the concentration of infected hepatocytes, intracellular HBV DNA-containing capsids, free viruses, antibodies and cytotoxic T-lymphocytes and can also slow down the time of their epidemic peaks. Both control therapies have therefore been shown to be useful measures for reducing HBV infection. In this paper, we have shown examples of the effect of the therapy for a period of 350 days for values of parameters selected from published papers, if available, or that we assumed to be reasonable if published values could not be found.

In this model, we have not considered the possibility of memory or history effects in the state variables of the model. There is now a large literature on fractional derivatives and integrals and their applications to develop models which include these memory or history effects. Extensive reviews of the basic concepts of fractional calculus and its applications can be found in books by Podlubny [90], Hilfer [91], Kilbas et al. [92], Petráš [93], and in the PhD thesis of Kisela [94]. In recent years, there have also been many new definitions of fractional derivatives which have been developed for various purposes including biology. Some examples of useful fractional derivatives include Riemann-Liouville [90], Caputo [90, 95], Hadamard [96], Katugampala [97], Caputo-Fabrizio [98], Atangana-Baleanu [99, 100] and Hattaf [101, 102]. Examples of fractional calculus models related to HBV infection include Bachraoui et al. [103] and Hattaf [101, 102]. Furthermore, spatiotemporal dynamics have not been included in this study. Some works that are related to spatiotemporal dynamics include Hattaf and Yousfi [66], Hattaf [67] and Manna and Hattaf [68]. In future work, it would be interesting to develop further fractional calculus models and spatiotemporal dynamics for HBV infection models.

CHAPTER IV

A DIFFUSIVE MODEL OF HEPATITIS B VIRUS INFECTION

5.1 Model description and formulation

We propose a diffusive model for HBV infection of hepatocytes by modifying the work of Shaoli et al. [57]. We consider the spatial variations of free virus and CTL cells together with two types of drug therapy. The variables D_v and D_z represent the diffusion coefficients for free virus and CTL cells, respectively, with Δ denoting the Laplacian operator. In this model, we assume that both free viruses and CTL cells exhibit Fickian diffusion in their motion. Uninfected hepatocytes are produced at a rate Λ, while σ represents the natural death rate for both infected and uninfected hepatocytes. These uninfected hepatocytes become infected at a rate β, where the infection term is $(1-\phi_1)\beta uv$, with ϕ_1 representing the efficacy of drug therapy in preventing new infections. Infected hepatocytes undergo natural death at a rate of σ and are eliminated by CTL cells at a rate of q. Free viruses are produced at a rate α by infected hepatocytes and the production term is $(1-\phi_2)\alpha y$, where ϕ_2 is the drug therapy efficiency in inhibiting viral production, and free virus are cleared at a rate μ. CTL cells expand in response to viral antigens derived from infected hepatocytes at a rate k, and eventually, they undergo decay at a rate ϵ. The flow chart of the model is presented in Figure 26.

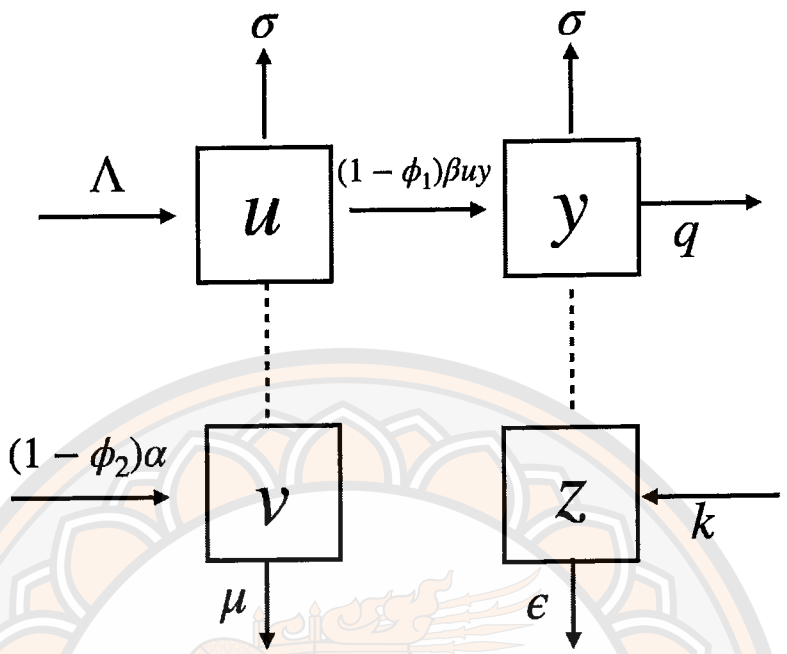

Figure 26 The flow chart of the diffusive model of HBV infection including immune response and drug therapy. The solid lines represent the transferring from one class to another class, whereas the dotted lines represent an involvement or influence of one class on another class.

The model therefore is written as follows

$$\frac{\partial u}{\partial t} = \Lambda - \sigma u(x,t) - (1-\phi_1)\beta u(x,t)v(x,t), \tag{5.1.1}$$

$$\frac{\partial y}{\partial t} = (1-\phi_1)\beta u(x,t)v(x,t) - \sigma y(x,t) - qy(x,t)z(x,t), \tag{5.1.2}$$

$$\frac{\partial v}{\partial t} = D_v \Delta v + (1-\phi_2)\alpha y(x,t) - \mu v(x,t), \tag{5.1.3}$$

$$\frac{\partial z}{\partial t} = D_z \Delta z + ky(x,t)z(x,t) - \epsilon z(x,t), \tag{5.1.4}$$

for $t > 0$, $x \in \Omega$. The initial conditions are

$$\begin{aligned} u(x,0) = \varphi_1(x) \geq 0, y(x,0) = \varphi_2(x) \geq 0, \\ v(x,0) = \varphi_3(x) \geq 0, z(x,0) = \varphi_4(x) \geq 0, \end{aligned} \tag{5.1.5}$$

where Neumann homogeneous boundary condition is

$$\frac{\partial v}{\partial n} = 0, t > 0, x \in \partial\Omega. \tag{5.1.6}$$

A bounded domain in $\mathbb{R}^n$ is represented by Ω with smooth boundary $\partial\Omega$, $\frac{\partial}{\partial n}$ denotes the outward normal derivative on Ω and $u(x,t), y(x,t), v(x,t)$ and $z(x,t)$ are the density of uninfected hepatocytes, infected hepatocytes, free virus and CTL cells at location x and time t, respectively.

5.2 Nonnegativity and boundedness of solutions

In this section, the fact of Lemma 5.2.1 (as shown details in [67]) will be utilized to demonstrate the non-negativity and boundedness of the solution.

Lemma 5.2.1. *Let A, B and D be three constants with $B \neq 0$. Consider the following problem*

$$\begin{aligned} \frac{\partial h}{\partial t} - D\Delta h &\leq A - Bh, x \in \Omega, t > 0, \\ \frac{\partial h}{\partial n} &= 0, x \in \partial\Omega, t > 0 \\ h(x,0) &= h_0(x), x \in \Omega. \end{aligned}$$

Then $h(x,t) \leq \max_{x\in\bar{\Omega}} h_0(x)e^{-Bt} + \frac{A}{B}(1-e^{-Bt})$. *Moreover, if* $B > 0$, *we have* $h(x,t) \leq \max\{\frac{A}{B}, \max_{x\in\bar{\Omega}} h_0\}$ *and* $\limsup_{t\to+\infty} h(x,t) \leq \frac{A}{B}$.

Proof. Let a solution of the following ordinary differential equation be $\tilde{h}(t)$,

$$\frac{d\tilde{h}(t)}{dt} + B\tilde{h}(t) = A, \tag{5.2.1}$$

$$\tilde{h}(0) = \max_{x\in\bar{\Omega}} h_0(x), x \in \Omega. \tag{5.2.2}$$

By integrating factor, we have

$$e^{\int B\ dt} = e^{Bt}, \tag{5.2.3}$$

and multiply both sides of (5.2.1) by the intergrating factor, we have

$$e^{Bt}\tilde{h}(t)\Big|_0^t = \int_0^t e^{Bt}A\ dt \tag{5.2.4}$$

$$e^{Bt}\tilde{h}(t) - \tilde{h}(0) = e^{Bt}\frac{A}{B} - \frac{A}{B} \tag{5.2.5}$$

$$\tilde{h}(t) = \tilde{h}(0)e^{-Bt} + \frac{A}{B}(1 - e^{-Bt}). \tag{5.2.6}$$

Since, $\tilde{h}(0) = \max_{x\in\Omega} h_0(x)$, so we have $\tilde{h}(t) = \max_{x\in\Omega} h_0(x)e^{-Bt} + \frac{A}{B}(1 - e^{-Bt})$. By comparison principle $h(x,t) \leq \tilde{h}(t)$, hence $h(x,t) \leq \max_{x\in\Omega} h_0(x)e^{-Bt} + \frac{A}{B}(1 - e^{-Bt})$.

Hence, if $B > 0$ then $h(x,t) \leq \max\{\frac{A}{B}, \max_{x\in\bar{\Omega}} h_0(x)\}$ and $\limsup_{t\to+\infty} h(x,t) \leq \frac{A}{B}$. □

Theorem 5.2.2. *For any given initial condition $\varphi \in C_H$ where C_H is a Banach space of continuous function, satisfying* (5.1.5)*, problem* (5.1.1)-(5.1.6) *has a unique nonnegative and bounded solution.*

Proof. Define $F = (F_1, F_2, F_3, F_4) : C_H \to X$ by

$$\begin{aligned}
F_1(\varphi)(x) &= \Lambda - \sigma\varphi_1(x,0) - (1-\phi_1)\beta\varphi_1(x,0)\varphi_3(x,0),\\
F_2(\varphi)(x) &= (1-\phi_1)\beta\varphi_1(x,0)\varphi_3(x,0) - \sigma\varphi_2(x,0) - q\varphi_2(x,0)\varphi_4(x,0),\\
F_3(\varphi)(x) &= (1-\phi_2)\alpha\varphi_2(x,0) - \mu\varphi_3(x,0),\\
F_4(\varphi)(x) &= k\varphi_2(x,0)\varphi_4(x,0) - \epsilon\varphi_4(x,0).
\end{aligned}$$

Then problem (5.1.1)-(5.1.5) can be written as the abstract functional equation below

$$w'(t) = Aw + F(w_t), t > 0,\ w(0) = \varphi \in C_H \tag{5.2.7}$$

where $w = (x, y, v, z)^T, \varphi = (\varphi_1, \varphi_2, \varphi_3, \varphi_4)^T$ and $Aw = (D_v\Delta v, D_z\Delta z)^T$.

F is locally Lipschitz in C_H. According to [105–109], we deduce that system (5.2.7) admits a unique local solution on its maximal interval of existence $[0, t_{max})$. Since $0 = (0,0,0,0)$ is a lower-solution of problem (5.1.1)-(5.1.5), we have $u(x,t) \geq 0, y(x,t) \geq 0, v(x,t) \geq 0, z(x,t) \geq 0$.

From Eq. (5.1.1) and Eq. (5.1.2). Let

$$\begin{aligned}
M(x,t) &= u(x,t) + y(x,t)\\
\frac{\partial M(x,t)}{\partial t} &= \Lambda - \sigma(u(x,t) + y(x,t)) - qy(x,t)z(x,t)\\
&\leq \Lambda - \sigma M(x,t).
\end{aligned}$$

Then,

$$\frac{\partial M(x,t)}{\partial t} \leq \Lambda - \sigma M(x,t), x \in \Omega, t > 0$$
$$\frac{\partial M(x,t)}{\partial n} = 0$$
$$M(x,0) = \varphi_1(x,0) + \varphi_2(x,0).$$

With the use of Lemma 5.2.1, we have

$$M(x,t) \leq \max_{x\in\Omega} M_0(x)e^{-\sigma t} + \frac{\Lambda}{\sigma}(1 - e^{-\sigma t})$$
$$M(x,t) \leq \max\left\{\frac{\Lambda}{\sigma}, \max_{x\in\bar{\Omega}}(\varphi_1(x,0) + \varphi_2(x,0))\right\},$$
$$\forall (x,t) \in \bar{\Omega} \times [0, t_{max}) \text{ and } \limsup_{t\to+\infty} M(x,t) \leq \frac{\Lambda}{\sigma}.$$

Therefore, M is bounded, it implies that both u and y are also bounded. From the boundness of y and (5.1.1)-(5.1.4), we deduce that v satisfies the system below

$$\frac{\partial v}{\partial t} = D_v \Delta v + (1 - \phi_2)\alpha y(x,t) - \mu v(x,t).$$

Since, y is bounded, we have

$$\frac{\partial v}{\partial t} \leq D_v \Delta v + \left(\frac{(1-\phi_2)\alpha\Lambda}{\sigma}\right) - \mu v(x,t)$$
$$\frac{\partial v}{\partial t} - D_v \Delta v \leq \left(\frac{(1-\phi_2)\alpha\Lambda}{\sigma}\right) - \mu v(x,t)$$
$$\frac{\partial v(x,t)}{\partial n} = 0$$
$$v(x,0) = \varphi_3(x,0) \geq 0.$$

By Lemma 5.2.1, we obtain
$v(x,t) \leq \max\left\{\frac{(1-\phi_2)\alpha\Lambda}{\sigma\mu}, \max_{x\in\bar{\Omega}} \varphi_3(x,0)\right\}$,
$\forall (x,t) \in \bar{\Omega} \times [0, t_{\max})$ and $\limsup_{t\to+\infty} v(x,t) \leq \frac{(1-\phi_2)\alpha\Lambda}{\sigma\mu}$.
This implies that v is bounded.
From the above, we have proved that $u(x,t), y(x,t)$ and $v(x,t)$ are bounded. Next, let

$$G(x,t) = y(x,t) + \frac{q}{k} z(x,t)$$
$$\frac{\partial G(x,t)}{\partial t} = \frac{\partial y(x,t)}{\partial t} + \frac{q}{k}\frac{\partial z(x,t)}{\partial t}$$

$$= (1-\phi_1)\beta u(x,t)v(x,t) - \sigma y(x,t) + \frac{q}{k}D_z\Delta z - \frac{q\epsilon z(x,t)}{k}.$$

Since, u and v are bounded, we have

$$\begin{aligned}\frac{\partial G(x,t)}{\partial t} &\leq \frac{(1-\phi_1)(1-\phi_2)\beta\alpha\Lambda^2}{\sigma^2\mu} + \frac{q}{k}D_z\Delta z \\ &\quad - \delta(y(x,t) + \frac{q}{k}z(x,t)), \\ &\quad \text{where } \delta = \min\{\sigma, \epsilon\} \\ &= \frac{(1-\phi_1)(1-\phi_2)\beta\alpha\Lambda^2}{\sigma^2\mu} + \frac{q}{k}D_G\Delta G \\ &\quad - \delta G(x,t) \\ \therefore \frac{\partial G(x,t)}{\partial t} - \frac{q}{k}D_G\Delta G &\leq \frac{(1-\phi_1)(1-\phi_2)\beta\alpha\Lambda^2}{\sigma^2\mu} - \delta G(x,t) \\ \frac{\partial G(x,t)}{\partial n} &= 0 \\ G(x,0) &= \varphi_2(x,0) + \frac{q}{k}\varphi_4(x,0) \geq 0.\end{aligned}$$

By Lemma 5.2.1, we then have that
$G(x,t) \leq \max\left\{\frac{(1-\phi_1)(1-\phi_2)\beta\alpha\Lambda^2}{\sigma^2\mu\delta}, \max_{x\in\bar{\Omega}} G(x,0)\right\}$, $\forall (x,t) \in \bar{\Omega} \times [0, t_{max})$ and
$\limsup_{t\to+\infty} G(x,t) \leq \frac{(1-\phi_1)(1-\phi_2)\beta\alpha\Lambda^2}{\sigma^2\mu\delta}$. Therefore, G is bounded. Due to the boundedness of G, it implies that y and z is also bounded. □

5.3 Equilibrium points

Let $D_v = D_z = 0$. In the case of the infection-free, we set $y = v = 0$. Substitute $v = 0$ in Eq.(5.1.1), then

$$\begin{aligned}\Lambda - \sigma u(x,t) &= 0 \\ u(x,t) &= \frac{\Lambda}{\sigma}. \qquad (5.3.1)\end{aligned}$$

And for (5.1.4), we have $z = 0$. Thus, the infection-free equilibrium $(E_0) = (\frac{\Lambda}{\sigma}, 0, 0, 0)$.
Next, in the case of immune-free, i.e., $z = 0$, substitute in (5.1.2), then

$$(1-\phi_1)\beta u(x,t)v(x,t) - \sigma y(x,t) = 0$$

$$y(x,t) = \frac{(1-\phi_1)\beta u(x,t)v(x,t)}{\sigma}. \tag{5.3.2}$$

Next,

$$\frac{\partial v}{\partial t} = (1-\phi_2)\alpha y(x,t) - \mu v(x,t) = 0$$

$$y(x,t) = \frac{\mu v(x,t)}{(1-\phi_2)\alpha}. \tag{5.3.3}$$

Equate (5.3.2) and (5.3.3), we have

$$\frac{(1-\phi_1)\beta u(x,t)v(x,t)}{\sigma} = \frac{\mu v(x,t)}{(1-\phi_2)\alpha}$$

$$u(x,t) = \frac{\sigma\mu}{(1-\phi_1)(1-\phi_2)\beta\alpha}. \tag{5.3.4}$$

Next, we substitute $u(x,t)$ above in (5.1.1), we have

$$\Lambda - \sigma u(x,t) - (1-\phi_1)\beta u(x,t)v(x,t) = 0$$

$$\Lambda - \sigma u(x,t) = (1-\phi_1)\beta u(x,t)v(x,t)$$

$$\frac{\Lambda - \sigma u(x,t)}{(1-\phi_1)\beta u(x,t)} = v(x,t)$$

$$\frac{\Lambda(1-\phi_1)(1-\phi_2)\beta\alpha - \sigma^2\mu}{(1-\phi_1)\beta\sigma\mu} = v(x,t). \tag{5.3.5}$$

The immune-free equilibrium (E_1) is $(u_1(x,t), y_1(x,t), v_1(x,t), z_1(x,t))$, where $u_1(x,t) = \frac{\sigma\mu}{(1-\phi_1)(1-\phi_2)\beta\alpha}, y_1(x,t) = \frac{\mu v_1}{(1-\phi_2)\alpha}$,

$v_1(x,t) = \frac{\Lambda(1-\phi_1)(1-\phi_2)\beta\alpha - \sigma^2\mu}{(1-\phi_1)\beta\sigma\mu}, z_1(x,t) = 0.$

Finally, we calculate for immune-activated equilibrium point. From (5.1.4), since $z \neq 0$, we have $y_2(x,t) = \frac{\epsilon}{k}$. We then substitute $y_2(x,t) = \frac{\epsilon}{k}$ in (5.1.3),

$$\frac{(1-\phi_2)\alpha\epsilon}{k} - \mu v_2(x,t) = 0$$

$$v_2(x,t) = \frac{(1-\phi_2)\alpha\epsilon}{k\mu}. \tag{5.3.6}$$

Next, we substitute $y_2(x,t) = \frac{\epsilon}{k}$ and $v_2(x,t) = \frac{(1-\phi_2)\alpha\epsilon}{k\mu}$ in (5.1.1), we get

$$\Lambda - \sigma u_2(x,t) - \frac{(1-\phi_1)(1-\phi_2)\beta\alpha\epsilon u_2(x,t)}{k\mu} = 0$$

$$\Lambda = \left(\sigma + \frac{(1-\phi_1)(1-\phi_2)\beta\alpha\epsilon}{k\mu}\right)u_2(x,t)$$
$$u_2(x,t) = \frac{\Lambda k\mu}{\sigma k\mu + (1-\phi_1)(1-\phi_2)\beta\alpha\epsilon}. \tag{5.3.7}$$

And by setting (4.1.2) to equal to zero, we have

$$z_2(x,t) = \frac{(1-\phi_1)\beta u_2(x,t)v_2(x,t) - \sigma y_2(x,t)}{q y_2(x,t)}. \tag{5.3.8}$$

The immune-activated equilibrium (E_2) is $(u_2(x,t), y_2(x,t), v_2(x,t), z_2(x,t))$,

where $u_2(x,t) = \dfrac{\Lambda k\mu}{\sigma k\mu + (1-\phi_1)(1-\phi_2)\beta\alpha\epsilon}$, $y_2(x,t) = \dfrac{\epsilon}{k}$, $v_2(x,t) = \dfrac{(1-\phi_2)\alpha\epsilon}{k\mu}$,

$z_2(x,t) = \dfrac{\sigma y_2(x,t)(R_{CTL}-1)}{q y_2(x,t)}$, where $R_{CTL} = \dfrac{(1-\phi_1)\beta u_2(x,t)v_2(x,t)}{\sigma y_2(x,t)}$.

R_{CTL} signifies the CTL immune response reproduction number for the system (5.1.1)-(5.1.4), indicating the average number of the CTL immune cells which are activated by infected hepatocytes when virus infection is completed.

5.4 The basic reproduction number (R_0)

We consider at $D_v = D_z = 0$ (diffusion-free). Taking the derivatives with respect to the stable variables for the transmission and transition terms, the matrices $\mathcal{F}$ and $\mathcal{V}$ can be written by $\mathcal{F} = \begin{bmatrix} (1-\phi_1)\beta uv \\ 0 \end{bmatrix}$ and $\mathcal{V} = \begin{bmatrix} \sigma y + qyz \\ \mu v - (1-\phi_2)\alpha y \end{bmatrix}$.

Hence, the transmisson matrix of $\mathcal{F}$ and $\mathcal{V}$ are

$$F = \begin{bmatrix} 0 & (1-\phi_1)\beta u \\ 0 & 0 \end{bmatrix} \text{ and } V = \begin{bmatrix} \sigma + qz & 0 \\ -(1-\phi_2)\alpha & \mu \end{bmatrix}.$$

By substituting $E_0 = \left(\dfrac{\Lambda}{\sigma}, 0, 0, 0\right)$ in the Jacobian matrices above, we get

$$F(E_0) = \begin{bmatrix} 0 & \dfrac{(1-\phi_1)\beta\Lambda}{\sigma} \\ 0 & 0 \end{bmatrix} \text{ and } V(E_0) = \begin{bmatrix} \sigma & 0 \\ -(1-\phi_2)\alpha & \mu \end{bmatrix}.$$

Find V^{-1} by using $V^{-1} = \frac{1}{\det V}[adjV]$, we have $\det V = \sigma\mu$ and

$$adj(V) = \begin{bmatrix} \mu & 0 \\ (1-\phi_2)\alpha & \sigma \end{bmatrix}.$$

Then, we have $FV^{-1} = \begin{bmatrix} 0 & \frac{(1-\phi_1)\beta\Lambda}{\sigma} \\ 0 & 0 \end{bmatrix} \begin{bmatrix} \frac{1}{\sigma} & 0 \\ \frac{(1-\phi_2)\alpha}{\sigma\mu} & \frac{1}{\mu} \end{bmatrix}$

$$= \begin{bmatrix} \frac{(1-\phi_1)(1-\phi_2)\beta\Lambda\alpha}{\sigma^2\mu} & \frac{(1-\phi_1)\beta\Lambda}{\sigma\mu} \\ 0 & 0 \end{bmatrix}.$$

The reproduction number R_0 is defined by $R_0 = \rho(FV^{-1})$ which is the spectral radius of the matrix FV^{-1}. Hence, $R_0 = \frac{(1-\phi_1)(1-\phi_2)\beta\Lambda\alpha}{\sigma^2\mu}$.

5.5 Stability analysis

For local stability of each equilibrium point, we analyze it from the Jacobian matrix at that equilibrium point of the system of equations (5.1.1)–(5.1.4). The characteristic equation is in the form $\eta_i D + J(E)U$ where $0 = \eta_1 < \eta_2 < ... < \eta_n < ...$ be the eigenvalues of the operator $-\Delta$ on Ω with the homogeneous Neumann boundary condition.

Let $D = diag(0, 0, D_v, D_z)$, $U = (u, y, v, z)$ and $\mathcal{L}U = D\Delta U + J(E)U$, where

$$J(E)U = \begin{pmatrix} -(\sigma + (1-\phi_1)\beta v^*)u - (1-\phi_1)\beta u^* v \\ (1-\phi_1)\beta v^* u - (\sigma + qz^*)y + (1-\phi_1)\beta u^* v - qy^* z \\ (1-\phi_2)\alpha y - \mu v \\ kyz^* + ky^* - \epsilon z \end{pmatrix}$$

and $E(u^*, y^*, v^*, z^*)$ represents any feasible steady state of system of equations (5.1.1)-(5.1.4). The linearization of system of equations (5.1.1)-(5.1.4) at E is of the form $U_t = \mathcal{L}U$. For each $i \geq 1$, $\mathbb{X}_i$ is invariant under the operator $\mathcal{L}$, and λ is an eigenvalue of $\mathcal{L}$ if and only if it is an eigenvalue of the matrix $\eta_i D + J(E)$ for some $i \geq 1$, in which case, there is an eigenvector in $\mathbb{X}_i$. The Jacobian matrix of

equations (5.1.1)-(5.1.4) is

$$J(E) = \begin{bmatrix} -\sigma - (1-\phi_1)\beta v^* & 0 & -(1-\phi_1)\beta u^* & 0 \\ (1-\phi_1)\beta v^* & \sigma - qz^* & (1-\phi_1)\beta u^* & -qy^* \\ 0 & (1-\phi_2)\alpha & -\mu & 0 \\ 0 & kz^* & 0 & ky^* - \epsilon \end{bmatrix}. \quad (5.5.1)$$

5.5.1 Local stability of infection-free equilibrium point

Theorem 5.5.1. *The infection-free equilibrium point (E_0) is locally asymptotically stable if it satisfies the Routh-Hurwitz criteria and $R_0 < 1$.*

Proof. The Jacobian matrix of system of equations (5.1.1)-(5.1.4) at E_0 is

$$J(E_0) = \begin{bmatrix} -\sigma & 0 & \frac{-(1-\phi_1)\beta\Lambda}{\sigma} & 0 \\ 0 & -\sigma & \frac{(1-\phi_1)\beta\Lambda}{\sigma} & 0 \\ 0 & (1-\phi_2)\alpha & -\mu & 0 \\ 0 & 0 & 0 & -\epsilon \end{bmatrix}. \quad (5.5.2)$$

$$\det(J(E_0) - \eta_i DI - \lambda I) = \begin{vmatrix} -\sigma-\lambda & 0 & \frac{-(1-\phi_1)\beta\Lambda}{\sigma} & 0 \\ 0 & -\sigma-\lambda & \frac{(1-\phi_1)\beta\Lambda}{\sigma} & 0 \\ 0 & (1-\phi_2)\alpha & -\mu-\eta_i D_v-\lambda & 0 \\ 0 & 0 & 0 & -\epsilon-\eta_i D_z-\lambda \end{vmatrix} = 0. \quad (5.5.3)$$

The characteristic equation of Jacobian matrix above is

$$(-\sigma-\lambda)(-\epsilon-\eta_i D_z-\lambda)\left(\lambda^2+(\sigma+\mu+\eta_i D_v)\lambda+\sigma(\mu+\eta_i D_v)-\frac{(1-\phi_1)(1-\phi_2)\beta\alpha\Lambda}{\sigma}\right) = 0. \quad (5.5.4)$$

Thus, $\lambda_1 = -\sigma < 0, \lambda_2 = -\epsilon - \eta_i D_z < 0$.

Next, we consider $\lambda^2 + (\sigma+\mu+\eta_i D_v)\lambda + \sigma(\mu+\eta_i D_v) - \frac{(1-\phi_1)(1-\phi_2)\beta\alpha\Lambda}{\sigma} = 0$

in the form $\lambda^2 + a_1\lambda + a_2 = 0$, then $a_1 = \sigma+\mu+\eta_i D_v$,

$a_2 = \sigma(\mu+\eta_i D_v) - \frac{(1-\phi_1)(1-\phi_2)\beta\alpha\Lambda}{\sigma} = \sigma\eta_i D_v + \sigma\mu\left(1 - \frac{(1-\phi_1)(1-\phi_2)\beta\alpha\Lambda}{\sigma^2\mu}\right)$.

From, $R_0 = \frac{(1-\phi_1)(1-\phi_2)\beta\alpha\Lambda}{\sigma^2\mu}$, we have $a_2 = \sigma\eta_i D_v + \sigma\mu\left(1 - R_0\right)$.

Since $0 = \eta_1 < \eta_2 < \ldots < \eta_i < \ldots$ thus $a_1 > 0$ and $a_2 > 0$ when $R_0 < 1$. By Routh-Hurwitz criteria, E_0 is locally asymptotically stable when $R_0 < 1$. □

5.5.2 Global stability of infection-free equilibrium point

Theorem 5.5.2. *The infection-free equilibrium point (E_0) is globally asymptotically stable in Ω when $R_0 < 1$.*

Proof. We use the method of Lyapunov functions to prove the global asymptotic stability of the infection-free equilibrium point. Let

$$L_0(t) = y(t) + \frac{(1-\phi_1)\beta\Lambda v(t)}{\sigma\mu} + \frac{qz(t)}{k} \tag{5.5.5}$$

$$\begin{aligned}
\frac{dL_0(t)}{dt} &= \frac{dy(t)}{dt} + \frac{(1-\phi_1)\beta\Lambda}{\sigma\mu}\frac{dv(t)}{dt} + \frac{q}{k}\frac{dz(t)}{dt} \\
&= (1-\phi_1)\beta u(t)v(t) - \sigma y(t) - qy(t)z(t) + \frac{(1-\phi_1)\beta\Lambda}{\sigma\mu}\Big((1-\phi_2)\alpha y(t) \\
&\quad - \mu v(t)\Big) + \frac{q}{k}\Big(ky(t)z(t) - \epsilon z(t)\Big) \\
&= (1-\phi_1)\beta u(t)v(t) - \sigma y(t) + \frac{(1-\phi_1)(1-\phi_2)\beta\Lambda\alpha y(t)}{\sigma\mu} - \frac{(1-\phi_1)\beta\Lambda v(t)}{\sigma} \\
&\quad - \frac{q\epsilon}{k}z(t) \\
&\leq (1-\phi_1)\beta v(t)\left(u(t) - \frac{\Lambda}{\sigma}\right) + \sigma y(t)\left(\frac{(1-\phi_1)(1-\phi_2)\beta\alpha\Lambda}{\sigma^2\mu} - 1\right) \because u(t) \leq \frac{\Lambda}{\sigma} \\
&= (1-\phi_1)\beta v(t)\left(u(t) - \frac{\Lambda}{\sigma}\right) + \sigma y(t)(R_0 - 1).
\end{aligned}$$

We obtain that $L_0' = 0$, when $v = y = 0$ and $L_0' < 0$ when $R_0 < 1$. Therefore, when $R_0 < 1$ by Lasalle's invariance principle, E_0 is globally asymptotically stable. □

5.5.3 Local stability of immune-free equilibrium point

Theorem 5.5.3. *The immune-free equilibrium point (E_1) is locally asymptotically stable if it satisfies Routh-Hurwitz criteria and $ky_1 < \epsilon + \eta_i D_z$.*

Proof. First, consider the characteristic equation of Jacobain matrix at E_1, we have

$$\det(J(E_1) - \eta_i DI - \lambda I) =$$

$$\begin{vmatrix} -\sigma - (1-\phi_1)\beta v_1 - \lambda & 0 & -(1-\phi_1)\beta u_1 & 0 \\ (1-\phi_1)\beta v_1 & -\sigma - \lambda & (1-\phi_1)\beta u_1 & -qy_1 \\ 0 & (1-\phi_2)\alpha & -\mu - \eta_i D_v - \lambda & 0 \\ 0 & 0 & 0 & ky_1 - \epsilon - \eta_i D_z - \lambda \end{vmatrix} = 0, \tag{5.5.6}$$

$$= (ky_1 - \epsilon - \eta_i D_z - \lambda)\Big[\Big(-\sigma - (1-\phi_1)\beta v_1 - \lambda\Big)\Big((-\sigma - \lambda)(-\mu - \eta_i D_v - \lambda)$$

$$- (1-\phi_1)(1-\phi_2)\beta\alpha u_1\Big) - ((1-\phi_1)\beta)^2(1-\phi_2)\alpha u_1 v_1)\Big]. \tag{5.5.7}$$

Thus, $\lambda_1 = ky_1 - \epsilon - \eta_i D_z$, then we consider

$$\Big[\Big(-\sigma - (1-\phi_1)\beta v_1 - \lambda\Big)\Big((-\sigma - \lambda)(-\mu - \eta_i D_v - \lambda) - (1-\phi_1)(1-\phi_2)\beta\alpha u_1\Big)$$

$$- ((1-\phi_1)\beta)^2(1-\phi_2)\alpha u_1 v_1)\Big] = 0$$

$$= \lambda^3 + (\mu + \eta_i D_v + 2\sigma + (1-\phi_1)\beta v_1)\lambda^2 + \Big(\sigma(\sigma + (1-\phi_1)\beta v_1)$$

$$+ (2\sigma + (1-\phi_1)\beta v_1)(\mu + \eta_i D_v) - (1-\phi_1)(1-\phi_2)\beta\alpha u_1\Big)\lambda$$

$$+ \sigma(\sigma + (1-\phi_1)\beta v_1)(\mu + \eta_i D_v) - (1-\phi_1)(1-\phi_2)\beta\alpha\sigma u_1. \tag{5.5.8}$$

Thus, by considering (5.5.8) in the form $\lambda^3 + a_1\lambda^2 + a_2\lambda + a_3 = 0$, we have

$$a_1 = \mu + \eta_i D_v + 2\sigma + (1-\phi_1)\beta v_1$$

$$a_2 = \sigma(\sigma + (1-\phi_1)\beta v_1) + (2\sigma + (1-\phi_1)\beta v_1)(\mu + \eta_i D_v) - (1-\phi_1)(1-\phi_2)\beta\alpha u_1$$

$$a_3 = \sigma(\sigma + (1-\phi_1)\beta v_1)(\mu + \eta_i D_v) - (1-\phi_1)(1-\phi_2)\beta\alpha\sigma u_1.$$

Since, $u_1 = \dfrac{\sigma\mu}{(1-\phi_1)(1-\phi_2)\beta\alpha}$, we substitute u_1 in a_2 and a_3, then we have

$$a_1 = \mu + \eta_i D_v + 2\sigma + (1-\phi_1)\beta v_1 > 0$$

$$a_2 = \sigma(\sigma + (1-\phi_1)\beta v_1) + (2\sigma + (1-\phi_1)\beta v_1)(\mu + \eta_i D_v) - \sigma^2\mu$$

$$a_3 = \sigma(\sigma + (1-\phi_1)\beta v_1)(\mu + \eta_i D_v) - \sigma^2\mu$$

$$= \sigma^2\eta_i D_v + (1-\phi_1)\beta\sigma v_1(\mu + \eta_i D_v) > 0.$$

Next, we consider $a_1a_2 - a_3$,

$$\begin{aligned}
a_1a_2 - a_3 &= (\mu + \eta_i D_v + 2\sigma + (1-\phi_1)\beta v_1)(\sigma(\sigma + (1-\phi_1)\beta v_1) \\
&\quad + (2\sigma + (1-\phi_1)\beta v_1)(\mu + \eta_i D_v) - \sigma^2\mu) \\
&\quad - \sigma^2\eta_i D_v + (1-\phi_1)\beta\sigma v_1(\mu + \eta_i D_v) \\
&= (\mu + \eta_i D_v + 2\sigma + (1-\phi_1)\beta v_1)\Big[(1-\phi_1)\beta\sigma v_1 + \sigma\eta_i D_v \\
&\quad + (1-\phi_1)\beta v_1(\mu + \eta_i D_v) + \sigma\mu(1-\sigma)\Big] \\
&\quad + (\mu + 2\sigma + (1-\phi_1)\beta v_1)\sigma^2 + \sigma(\mu + \eta_i D_v + 2\sigma)(\mu + \eta_i D_v) > 0.
\end{aligned}$$

Hence, by the Routh-Hurwitz Criterion and $ky_1 < \epsilon + \eta_i D_z$, the immune-free equilibrium point is locally asymptotically stable. This completes the proof. □

5.5.4 Global stability of immune-free equilibrium point

Theorem 5.5.4. *The immune-free equilibrium point (E_1) is globally asymptotically stable in Ω when $R_0 > 1 \geq R_{CTL}$.*

Proof. The method of Lyapunnov functions is used and we define the positive definite Lyapunov function as

$$L_1(t) = \int_\Omega \left\{ \left(u - u_1 \ln\frac{u}{u_1}\right) + \left(y - y_1 \ln\frac{y}{y_1}\right) + \frac{\sigma}{(1-\phi_2)\alpha}\left(v - v_1 \ln\frac{v}{v_1}\right) + \frac{q}{k}z \right\} dx. \quad (5.5.9)$$

Then, the derivative of $L_1(t)$ along the solutions of the model is

$$\frac{dL_1(t)}{dt} = \frac{\partial L_1}{\partial u}\cdot\frac{du}{dt} + \frac{\partial L_1}{\partial y}\cdot\frac{dy}{dt} + \frac{\partial L_1}{\partial v}\cdot\frac{dv}{dt} + \frac{\partial L_1}{\partial z}\cdot\frac{dz}{dt}.$$

Thus, we have

$$\begin{aligned}
\frac{dL_1(t)}{dt} &= \int_\Omega \left\{ \left(\frac{du}{dt} - \frac{u_1}{u}\frac{du}{dt}\right) + \left(\frac{dy}{dt} - \frac{y_1}{y}\frac{dy}{dt}\right) + \frac{\sigma}{(1-\phi_2)\alpha}\left(\frac{dv}{dt} - \frac{v_1}{v}\frac{dv}{dt}\right) \right. \\
&\quad \left. + \frac{q}{k}\frac{dz}{dt} \right\} dx \\
&= \int_\Omega \left\{ \left(1 - \frac{u_1}{u}\right)\left(\Lambda - \sigma u - (1-\phi_1)\beta uv\right) + \left(1 - \frac{y_1}{y}\right)\left((1-\phi_1)\beta uv \right.\right. \\
&\quad \left. - \sigma y - qyz\right) + \frac{\sigma}{(1-\phi_2)\alpha}\left(q - \frac{v_1}{v}\right)\left(D_v\Delta v + (1-\phi_2)\alpha y - \mu v\right) \\
&\quad \left. + \frac{q}{k}\left(D_z\Delta z + kyz - \epsilon z\right)\right\} dx.
\end{aligned}$$

Since, this equilibrium is immune-free, so we have $D_z = 0$ and $\Lambda = \sigma u_1 + (1 - \phi_1)\beta u_1 v_1$.

We get

$$\begin{aligned}
\frac{dL_1(t)}{dt} &= \int_\Omega \left\{ \left(1 - \frac{u_1}{u}\right)\left(\sigma u_1 + (1-\phi_1)\beta u_1 v_1 - \sigma u - (1-\phi_1)\beta uv\right) \right. \\
&\quad + \left(1 - \frac{y_1}{y}\right)\left((1-\phi_1)\beta uv - \sigma y - qyz\right) + qyz - \frac{q\epsilon z}{k} \\
&\quad \left. + \frac{\sigma}{(1-\phi_2)\alpha}\left(q - \frac{v_1}{v}\right)\left(D_v \Delta v + (1-\phi_2)\alpha y - \mu v\right)\right\} dx \\
&= \int_\Omega \left\{ -\frac{\sigma(u-u_1)^2}{u} + (1-\phi_1)\beta u_1 v_1 - (1-\phi_1)\beta u_1 v_1 \frac{u_1}{u} + (1-\phi_1)\beta u_1 v \right. \\
&\quad - (1-\phi_1)\beta uv\frac{y_1}{y} + \sigma y_1 + qy_1 z + \frac{\sigma D_v \Delta v}{(1-\phi_2)\alpha}\left(1 - \frac{v_1}{v}\right) \\
&\quad \left. - \frac{\sigma\mu v}{(1-\phi_2)\alpha} - \frac{\sigma y v_1}{v} + \frac{\sigma\mu v_1}{(1-\phi_2)\alpha} - \frac{q\epsilon z}{k}\right\} dx.
\end{aligned}$$

From the second equation of system of equations (5.1.1)-(5.1.4), we obtain $(1-\phi_1)\beta u_1 = \frac{\sigma y_1}{v_1}$ and $\frac{y_1}{v_1} = \frac{\mu}{(1-\phi_2)\alpha}$, then

$$\begin{aligned}
\frac{dL_1(t)}{dt} &= \int_\Omega \left\{ -\frac{\sigma(u-u_1)^2}{u} + 3\sigma y_1 - \frac{\sigma u_1 y_1}{u} - \frac{\sigma (y_1)^2 uv}{y u_1 v_1} - \sigma y_1 \frac{v_1 y}{y_1 v} \right. \\
&\quad \left. - \frac{\sigma D_v v_1 |\nabla v|^2}{(1-\phi_2)\alpha v^2} + qz\left(\frac{\mu v_1}{(1-\phi_2)\alpha}\right) - \frac{q\epsilon z}{k}\right\} dx
\end{aligned}$$

and since $v_1 = \dfrac{\Lambda(1-\phi_1)(1-\phi_2)\beta\alpha - \sigma^2\mu}{(1-\phi_1)\beta\sigma\mu}$, we have

$$\begin{aligned}
\frac{dL_1(t)}{dt} &= \int_\Omega \left\{ -\frac{\sigma(u-u_1)^2}{u} + 3\sigma y_1 - \frac{\sigma u_1 y_1}{u} - \frac{\sigma (y_1)^2 uv}{y u_1 v_1} - \sigma y_1 \frac{v_1 y}{y_1 v} - \frac{\sigma D_v v_1 |\nabla v|^2}{(1-\phi_2)\alpha v^2} \right. \\
&\quad \left. + qz\left(\frac{\mu}{(1-\phi_2)\alpha}\left(\frac{\Lambda(1-\phi_1)(1-\phi_2)\beta\alpha - \sigma^2\mu}{(1-\phi_1)\beta\sigma\mu}\right) - \frac{\epsilon}{k}\right)\right\} dx \\
&= \int_\Omega \left\{ -\frac{\sigma(u-u_1)^2}{u} + 3\sigma y_1 - \frac{\sigma u_1 y_1}{u} - \frac{\sigma (y_1)^2 uv}{y u_1 v_1} - \sigma y_1 \frac{v_1 y}{y_1 v} - \frac{\sigma D_v v_1 |\nabla v|^2}{(1-\phi_2)\alpha v^2} \right. \\
&\quad \left. + qz\left(\frac{\Lambda}{\sigma} - \frac{k\sigma\mu + (1-\phi_1)(1-\phi_2)\beta\alpha\epsilon}{(1-\phi_1)(1-\phi_2)\beta\alpha k}\right)\right\} dx \\
&= \int_\Omega \left\{ -\frac{\sigma(u-u_1)^2}{u} + 3\sigma y_1 - \frac{\sigma u_1 y_1}{u} - \frac{\sigma (y_1)^2 uv}{y u_1 v_1} - \sigma y_1 \frac{v_1 y}{y_1 v} - \frac{\sigma D_v v_1 |\nabla v|^2}{(1-\phi_2)\alpha v^2} \right. \\
&\quad \left. + \frac{qz\Lambda}{\sigma}\left(1 - \frac{\sigma(k\sigma\mu + (1-\phi_1)(1-\phi_2)\beta\alpha\epsilon)}{(1-\phi_1)(1-\phi_2)\Lambda\beta\alpha k}\right)\right\} dx \\
&= \int_\Omega \left\{ -\frac{\sigma(u-u_1)^2}{u} + \sigma y_1\left(3 - \frac{u_1}{u} - \frac{uvy_1}{u_1 v_1 y} - \frac{v_1 y}{y_1 v}\right) - \frac{\sigma D_v v_1 |\nabla v|^2}{(1-\phi_2)\alpha v^2} \right. \\
&\quad \left. + \frac{qz\Lambda}{\sigma}\left(1 - \frac{1}{R_{CTL}}\right)\right\} dx.
\end{aligned}$$

Since $\frac{-\sigma(u-u_1)^2}{u} \leq 0$ and the function $3-\frac{u_1}{u}-\frac{uvy_1}{u_1v_1y}-\frac{v_1y}{y_1v}$ is negative for all $u, y, v > 0$, this is due to the fact that the arithmetic mean is greater than or equal to the geometric mean. Hence, $R_{CTL} \leq 1$ ensures $\frac{dL_1}{dt} \leq 0$ for all $u, y, v, z > 0$. Thus, the immune-free equilibrium point E_1 is globally asymptotically stable when $R_0 > 1 \geq R_{CTL}$. □

5.5.5 Local stability of immune-activated equilibrium point

Theorem 5.5.5. *The immune-activated equilibrium point (E_2) is locally asymptotically stable if it satisfies the Routh-Hurwitz criteria and $R_0 > 1$.*

Proof. The Jacobian matrix of the immune-activated equilibrium point is as follows

$$J(E_2) = \begin{bmatrix} -\sigma-(1-\phi_1)\beta v_2 & 0 & -(1-\phi_1)\beta u_2 & 0 \\ (1-\phi_1)\beta v_2 & \sigma - qz_2 & (1-\phi_1)\beta u_2 & -qy_2 \\ 0 & (1-\phi_2)\alpha & -\mu & 0 \\ 0 & kz_2 & 0 & ky_2-\epsilon \end{bmatrix}. \tag{5.5.10}$$

Then, the eigenvalues are determined from $\det(J(E_2) - \eta_i DI - \lambda I) = 0$, where $E_2 = (u_2, y_2, v_2, z_2)$,

$\det(J(E_2) - \eta_i DI - \lambda I) =$

$$\begin{vmatrix} -\sigma-(1-\phi_1)\beta v_2-\lambda & 0 & -(1-\phi_1)\beta u_2 & 0 \\ (1-\phi_1)\beta v_2 & \sigma-qz_2-\lambda & (1-\phi_1)\beta u_2 & -qy_2 \\ 0 & (1-\phi_2)\alpha & -\mu-\eta_i D_v-\lambda & 0 \\ 0 & kz_2 & 0 & ky_2-\epsilon-\eta_i D_z-\lambda \end{vmatrix} = 0, \tag{5.5.11}$$

$$= (-\sigma-(1-\phi_1)\beta v_2-\lambda)\begin{vmatrix} -\sigma-qz_2-\lambda & (1-\phi_1)\beta u_2 & -qy_2 \\ (1-\phi_2)\alpha & -\mu-\eta_i D_v-\lambda & 0 \\ kz_2 & 0 & ky_2-\epsilon-\eta_i D_z-\lambda \end{vmatrix}$$

$$-(1-\phi_1)\beta v_2\begin{vmatrix} 0 & -(1-\phi_1)\beta u_2 & 0 \\ (1-\phi_2)\alpha & -\mu-\eta_i D_v-\lambda & 0 \\ kz_2 & 0 & ky_2-\epsilon-\eta_i D_z-\lambda \end{vmatrix} = 0. \tag{5.5.12}$$

From (5.5.12), we have the characteristic equation as

$$\begin{aligned}
&\lambda^4 + (2\sigma + (1-\phi_1)\beta v_2 + \mu + qz_2)\lambda^3 + ((\mu + \epsilon + (1-\phi_1))qz_2 \\
&+ (\sigma + (1-\phi_1)\beta v_2 - \eta_i D_z)\mu + ((1-\phi_1)\beta v_2 - \eta_i D_v)\sigma - (\eta_i)^2 D_v D_z \\
&- (1-\phi_1)(1-\phi_2)\beta\alpha u_2)\lambda^2 + ((\epsilon q z_2 + (\sigma + (1-\phi_1)\beta v_2 - \eta_i D_v)(\sigma + qz_2) \\
&- \eta_i D_z)(\mu + \eta_i D_v) + (\sigma + (1-\phi_1)\beta v_2)(\epsilon q z_2 - \eta_i D_v(\sigma + qz_2)) \\
&- (1-\phi_1)(1-\phi_2)(\sigma + \eta_i D_z)\beta\alpha u_2)\lambda \\
&+ ((\epsilon - \eta_i D_z)qz_2 - \sigma\eta_i D_v)(\sigma + (1-\phi_1)\beta v_2)(\mu + \eta_i D_v) \\
&- \eta_i D_z(1-\phi_1)(1-\phi_2)\beta\alpha\sigma u_2 = 0
\end{aligned} \tag{5.5.13}$$

where

$$\begin{aligned}
a_1 &= 2\sigma + (1-\phi_1)\beta v_2 + \mu + qz_2 > 0, \\
a_2 &= (\mu + \epsilon + (1-\phi_1))qz_2 + (\sigma + (1-\phi_1)\beta v_2 - \eta_i D_z)\mu + ((1-\phi_1)\beta v_2 - \eta_i D_v)\sigma \\
&\quad - (\eta_i)^2 D_v D_z - (1-\phi_1)(1-\phi_2)\beta\alpha u_2, \\
a_3 &= (\epsilon q z_2 + (\sigma + (1-\phi_1)\beta v_2 - \eta_i D_v)(\sigma + qz_2) - \eta_i D_z)(\mu + \eta_i D_v) \\
&\quad + (\sigma + (1-\phi_1)\beta v_2)(\epsilon q z_2 - \eta_i D_v(\sigma + qz_2)) \\
&\quad - (1-\phi_1)(1-\phi_2)(\sigma + \eta_i D_z)\beta\alpha u_2, \\
a_4 &= ((\epsilon - \eta_i D_z)qz_2 - \sigma\eta_i D_v)(\sigma + (1-\phi_1)\beta v_2)(\mu + \eta_i D_v) \\
&\quad - \eta_i D_z(1-\phi_1)(1-\phi_2)\beta\alpha\sigma u_2.
\end{aligned} \tag{5.5.14}$$

Then immune-activated equilibrium point is locally asymptotically stable if it corresponds to the Routh-Hurwitz stability criteria $a_1 > 0$, $a_3 > 0$, $a_4 > 0$ and $a_1 a_2 a_3 > a_3^2 + a_1^2 a_4$. □

5.5.6 Global stability of immune-activated equilibrium point

Theorem 5.5.6. *The immune-activated equilibrium point E_2 is globally asymptotically stable when $R_{CTL} > 1$.*

Proof. The following Lyapunov function is considered

$$L_2(t) = \int_\Omega \left\{ \left(u - u_2 \ln\frac{u}{u_2}\right) + \left(y - y_2 \ln\frac{y}{y_2}\right) + \frac{\sigma + qz_2}{(1-\phi_2)\alpha}\left(v - v_2 \ln\frac{v}{v_2}\right) + \frac{q}{k}\left(z - z_2 \ln\frac{z}{z_2}\right) \right\} dx. \tag{5.5.15}$$

By calculating the time derivative of L_2 along the solution of system of equations (5.1.1) - (5.1.4), then

$$\begin{aligned}\frac{dL_2(t)}{dt} &= \int_\Omega \left\{ \left(\frac{du}{dt} - \frac{u_2}{u}\frac{du}{dt}\right) + \left(\frac{dy}{dt} - \frac{y_2}{y}\frac{dy}{dt}\right) + \frac{\sigma + qz_2}{(1-\phi_2)\alpha}\left(\frac{dv}{dt} - \frac{v_2}{v}\frac{dv}{dt}\right) \right. \\ &\quad \left. + \frac{q}{k}\left(\frac{dz}{dt} - \frac{z_2}{z}\frac{dz}{dt}\right)\right\} dx \\ &= \int_\Omega \left\{ \left(1 - \frac{u_2}{u}\right)\left(\Lambda - \sigma u - (1-\phi_1)\beta uv\right) + \left(1 - \frac{y_2}{y}\right)\left((1-\phi_1)\beta uv \right.\right. \\ &\quad \left. - \sigma y - qyz\right) + \frac{\sigma + qz_2}{(1-\phi_2)\alpha}\left(1 - \frac{v_2}{v}\right)\left(D_v\Delta v + (1-\phi_2)\alpha y - \mu v\right) \\ &\quad \left. + \frac{q}{k}\left(1 - \frac{z_2}{z}\right)\left(D_z\Delta z + kyz - \epsilon z\right)\right\} dx \\ &= \int_\Omega \left\{ -\frac{\sigma(u-u_2)^2}{u} + (1-\phi_1)\beta u_2 v_2 - (1-\phi_1)\beta u_2 v_2 \frac{u_2}{u} + (1-\phi_1)\beta u_2 v \right. \\ &\quad - (1-\phi_1)\beta uv\frac{y_2}{y} + \sigma y_2 - \frac{\sigma\mu v}{(1-\phi_2)\alpha} - \frac{qz_2\mu v}{(1-\phi_2)\alpha} - \sigma v_2\frac{y}{v} - qz_2v_2\frac{y}{v} \\ &\quad + \frac{\sigma\mu v_2}{(1-\phi_2)\alpha} + \frac{\mu q z_2 v_2}{(1-\phi_2)\alpha} + qy_2z_2 + \frac{\sigma + pz_2}{(1-\phi_2)\alpha}\left(1 - \frac{v_2}{v}\right)D_v\Delta v \\ &\quad \left. + \frac{q}{k}\left(1 - \frac{z_2}{z}\right)D_z\Delta z\right\} dx.\end{aligned}$$

From the second equation of system of equations (5.1.1)-(5.1.4), we have $(1-\phi_1)\beta = \dfrac{qy_2z_2 + \sigma y_2}{u_2v_2}$ and positive equilibrium is $u_2(x,t) = \dfrac{\Lambda k\mu}{\sigma k\mu + (1-\phi_1)(1-\phi_2)\beta\alpha\epsilon}$, $y_2(x,t) = \dfrac{\epsilon}{k}, v_2(x,t) = \dfrac{(1-\phi_2)\alpha\epsilon}{k\mu}, z_2(x,t) = \dfrac{(1-\phi_1)\beta u_2(x,t)v_2(x,t) - \sigma y_2(x,t)}{qy_2(x,t)}$.
Then,

$$\begin{aligned}\frac{dL_2(t)}{dt} &= \int_\Omega \left\{ -\frac{\sigma(u-u_2)^2}{u} + \sigma y_2\left(3 - \frac{u_2}{u} - \frac{uvy_2}{u_2v_2y} - \frac{v_2y}{vy_2}\right) + qy_2z_2\left(3 - \frac{u_2}{u}\right.\right. \\ &\quad \left.\left. - \frac{uvy_2}{u_2v_2y} - \frac{v_2y}{vy_2}\right) - \frac{\sigma + qz_2D_vv_2|\nabla v|^2}{(1-\phi_2)\alpha v^2} - \frac{qD_zz_2|\nabla z|^2}{kz^2}\right\} dx.\end{aligned}$$

By the similar discussion as in Theorem 5.5.4, the immune-activated equilibrium point E_2 is globally asymptotically stable. □

5.6 Numerical simulations

In this section, the numerical simulation of an HBV infection with a CTL immune response and spatial diffusion of the virus and CTL by finite difference method is performed to confirm the global stability of all three equilibrium points, i.e. the

infection-free equilibrium point (E_0), the immune-free equilibrium point (E_1), and the immune-activated equilibrium point (E_2). The existence and global stability of the equilibrium points determined by two threshold parameters and they are the basic reproduction number (R_0) and the CTL immune response reproduction number (R_{CTL}). More specifically, the infection-free equilibrium point is globally asymptotically stable when $R_0 < 1$, which biologically denotes that the HBV is eliminated and the infection is eradicated. The immune-free equilibrium point is globally asymptotically stable if $R_0 > 1 \geq R_{CTL}$, but it becomes unstable at $R_{CTL} > 1$. The immune-activated equilibrium point is stable when $R_{CTL} > 1$. In numerical simulation, we use parameters values from Table 4 and let the diffusion coefficient $D_v = 0.1$ and $D_z = 0.1$. We divide our results into four cases.

Table 4 Parameters used in the model of equations (5.1.1)-(5.1.4)

Parameter	Description	Value	Unit	Ref
Λ	The production rate of the uninfected hepatocytes.	4.0551	$day^{-1}mm^{-3}$	[45]
σ	The natural death rate of hepatocytes.	0.011	day^{-1}	[41]
ϕ_1	The efficiency of drug therapy in blocking new infection.	0.7	-	assume
ϕ_2	The efficiency of drug therapy in inhibiting viral production.	0.7	-	assume
β	The infection rate of uninfected hepatocytes by the free virus.	0.0014	$mm^3virion^{-1}day^{-1}$	[33]
q	The death rate of infected hepatocytes by the CTLs response.	0.001	mm^3day^{-1}	[18]
α	The growth rate of virions in blood.	0.0693	day^{-1}	[29]
μ	The death rate of free viruses.	0.693	day^{-1}	[41]
k	The expansion rate of CTLs in response to viral antigen derived from infected hepatocytes.	0.001	mm^3day^{-1}	assume
ϵ	The decay rate of CTLs in the absence of antigenic stimulation.	0.5	day^{-1}	[112]

5.6.1 Case I: when $R_0 < 1$

Some numerical simulations of the system of equations (5.1.1) - (5.1.4) is performed to guarantee the theoretical results and show the spatiotemporal behaviour of the solutions. Here we choose $\beta = 3 \times 10^{-13}$, which leads to $R_0 = 2.8013 \times 10^{-9} < 1$. In this case, the solutions of system of equations (5.1.1)-(5.1.4) converge to the infection-free equilibrium $E_0 = (90.9091, 0, 0, 0)$ as shown in Fig 27a - 27d, which support the results in Theorem 5.5.2.

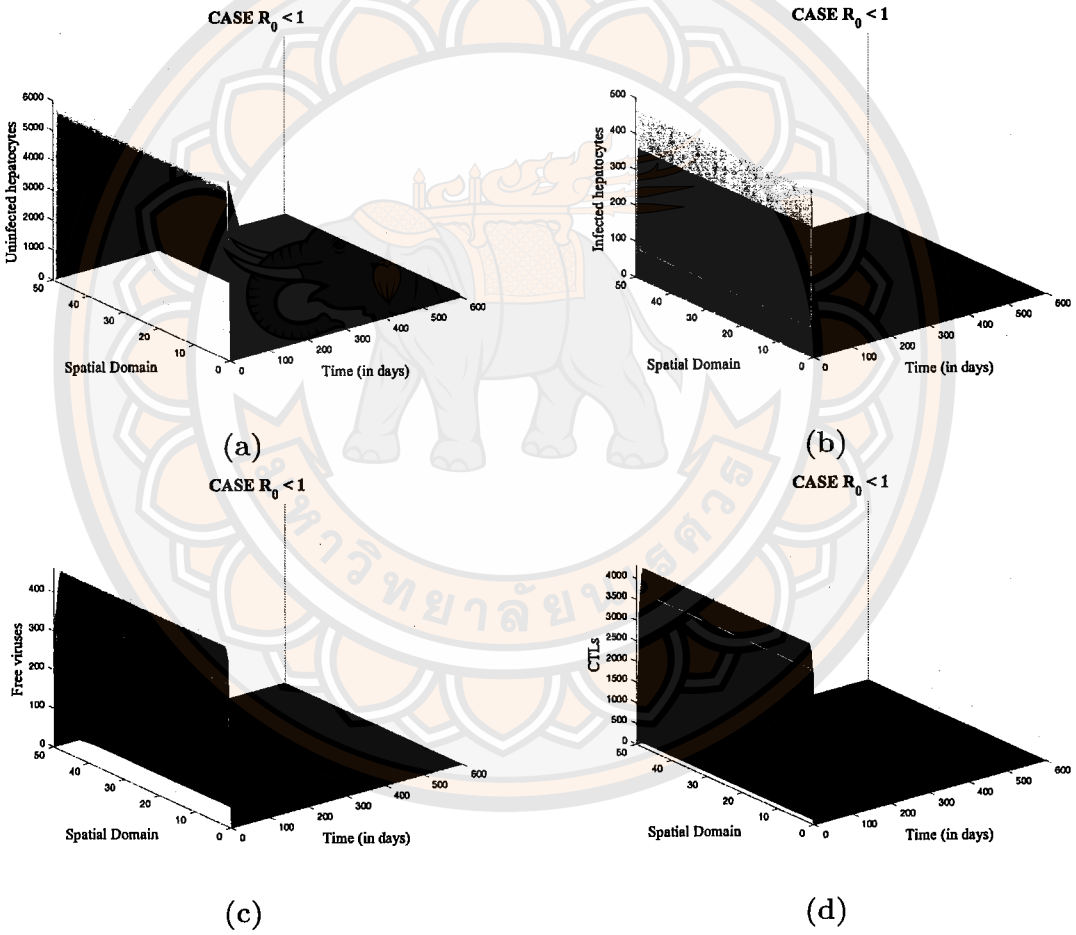

Figure 27 The numerical simulation of system of equations (5.1.1)-(5.1.4) when $R_0 < 1$ with parameters $\Lambda = 1, \phi_1 = 0.7, \phi_2 = 0.7, \sigma = 0.011, \beta = 3 \times 10^{-13}, \alpha = 0.87, \mu = 0.0693, k = 0.01, \epsilon = 0.5, q = 0.001, D_v = 0.1, D_z = 0.1$, showing that the infection-free equilibrium point E_0 is globally asymptotically stable. The sub-figures show the spatiotemporal behaviours of (a) uninfected hepatocytes, (b) infected hepatocytes, (c) free viruses and (d) CTL.

5.6.2 Case II: when $R_0 > 1 \geq R_{CTL}$

Here we set $\Lambda = 0.5$ and $\beta = 0.0014$, we have $6.5364 = R_0 > 1 > R_{CTL} = 0.7981$. This set of thresholds guarantees the global stability of the immune-free equilibrium point because the solution of the system converges to the immune-free equilibrium point $E_1 = (6.9540, 38.5005, 145.0020, 0)$, which supports the result of Theorem 5.5.4. The concentration of uninfected hepatocytes in Fig 28a decreases faster than that in Fig 27a with HVB infection when $R_0 > 1 > R_{CTL}$ and the immune system is inactive.

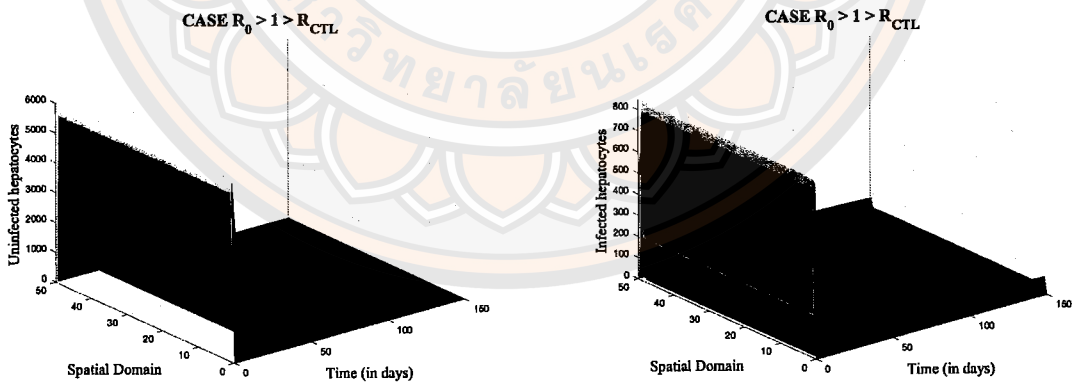

(a) (b)

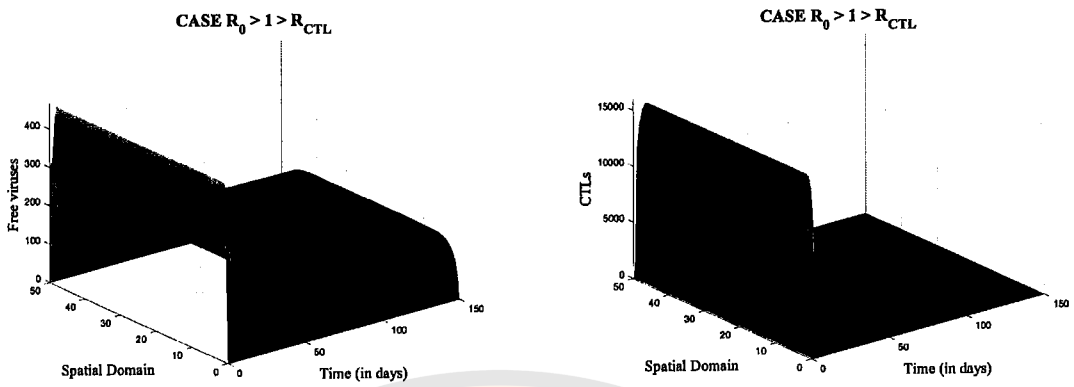

(c) (d)

Figure 28 The numerical simulation of system of equations (5.1.1)-(5.1.4) when $R_0 > 1 > R_{CTL}$ with parameters $\Lambda = 0.5, \phi_1 = 0.7, \phi_2 = 0.7, \sigma = 0.011, \beta = 0.0014, \alpha = 0.87, \mu = 0.0693, k = 0.01, \epsilon = 0.5, q = 0.001, D_v = 0.1, D_z = 0.1$, showing that the immune-free equilibrium point E_1 is globally asymptotically stable. The subfigures show the spatiotemporal behaviours of (a) uninfected hepatocytes, (b) infected hepatocytes, (c) free viruses and (d) CTL.

5.6.3 Case III: when $R_{CTL} > 1$

We set $\Lambda = 4.0551$ and $\beta = 0.0014$, then $R_{CTL} = 6.4727 > 1$. Fig 29a - 29d shows the dynamic curve converges to equilibrium $E_2(u_2, y_2, v_2, z_2) = (45.0112, 50, 188.3117, 60.1995)$. Thus, it is consistent with Theorem 5.5.6.

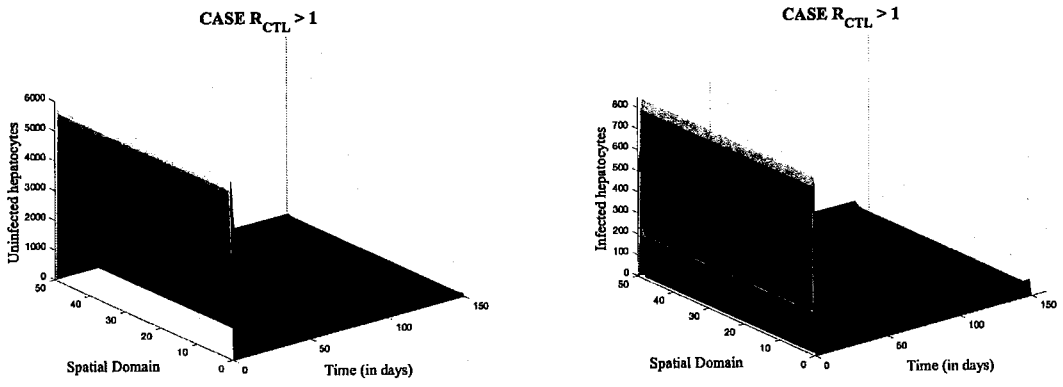

(a) (b)

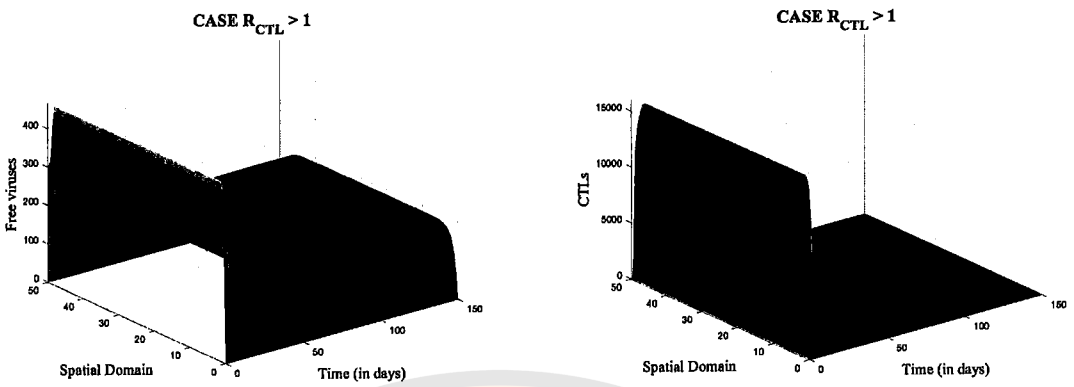

(c) (d)

Figure 29 The numerical simulation of system of equations (5.1.1)-(5.1.4) when $6.4727 = R_{CTL} > 1$ with parameters $\Lambda = 4.0551, \phi_1 = 0.7, \phi_2 = 0.7, \sigma = 0.011, \beta = 0.0014, \alpha = 0.87, \mu = 0.0693, k = 0.01, \epsilon = 0.5, q = 0.001, D_v = 0.1, D_z = 0.1$, showing that the immune-activated equilibrium point E_2 is globally asymptotically stable. The sub-figures show the spatiotemporal behaviours of (a) uninfected hepatocytes, (b) infected hepatocytes, (c) free viruses and (d) CTL.

5.6.4 Case IV: Different diffusion coefficients

Furthermore, a different set of values of D_v and D_z are used to investigate the dynamics of free virus as shown in Figure 30a - 30d. Here we choose parameter values in order for $R_{CTL} > 1$. We can observe from this figure that over the long period, all four situations of (D_v, D_z), which are four different cases, i.e., (0.1,0.1), (0.1,0.4), (0.4,0.1), and (0.4,0.4) present very similar dynamics for the concentration of free viruses. This indicates that the diffusion of virus and CTL do not affect the equilibria's asymptotic properties. Further, it can be noticed from Figure 30a - 30d that the greater the diffusion cofficient of free virus and CTL cells, the slower the time for virus to reach the equilibrium value.

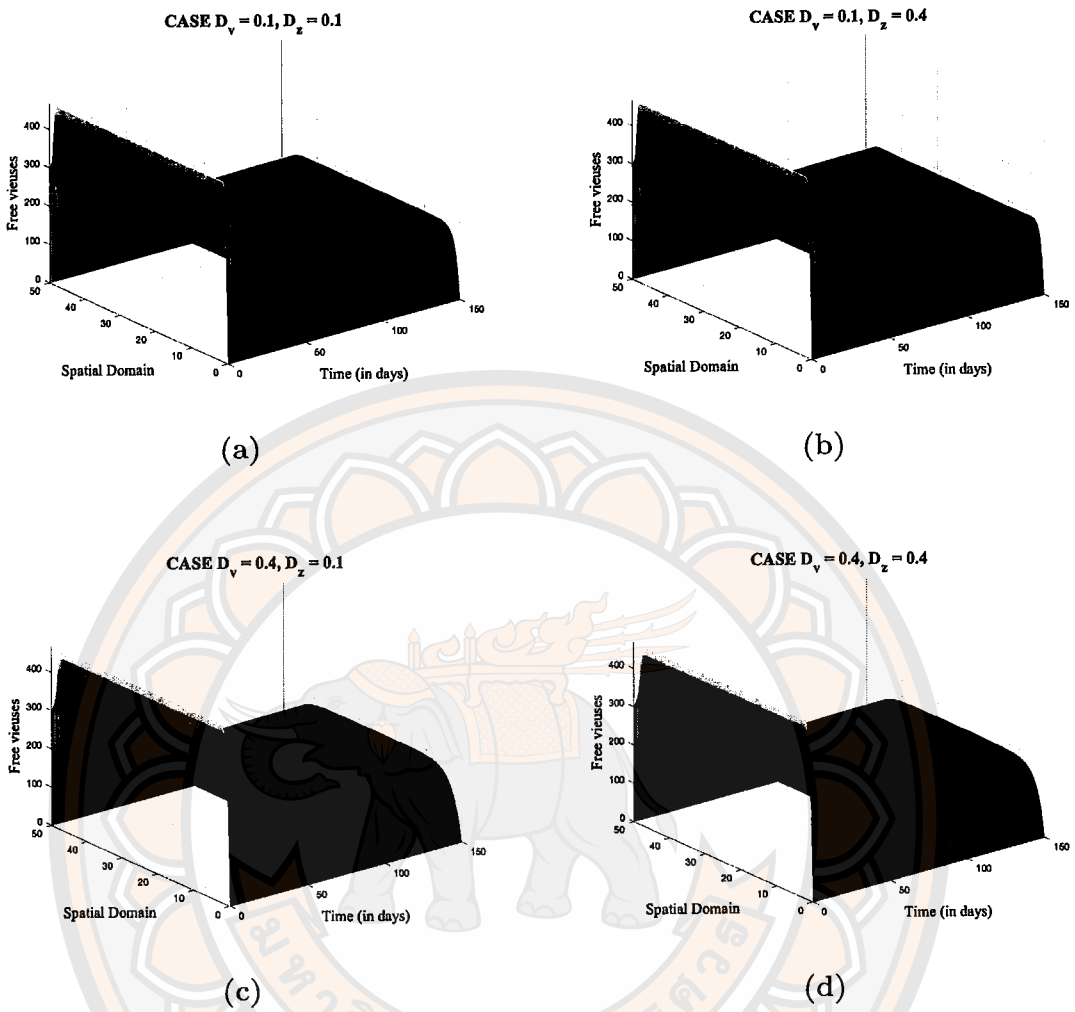

Figure 30 Distribution of virus under different diffusion coefficients. (a) $D_v = 0.1$, $D_z = 0.1$, (b) $D_v = 0.1$, $D_z = 0.4$, (c) $D_v = 0.4$, $D_z = 0.1$, and (d) $D_v = 0.4$, $D_z = 0.4$

5.7 Conclusion

We propose s a model of hepatitis B viral infection (HBV) of hepatocytes with diffusion to better understand the mechanisms and dynamics of the infection. The model incorporates the spatial variations of cytotoxic T lymphocytes (CTL) and viruses, the adaptive immune response exerted by CTL, and two types of drug therapy. It consists of four variables and they are uninfected hepatocytes (u), infected hepatocytes (y), free virus (v) and CTL (z). Nonnegativity and boundedness of model solutions are verified. Three equilibrium states, i.e., infection-free,

immune-free and immune-activated are obtained. The basic reproduction number (R_0) and the CTL immune response reproduction number (R_{CTL}) are calculated, and they become the threshold indicating the existence and global stability of each equilibrium point. When $R_0 < 1$, the infection-free equilibrium point is globally stable, indicating biological meaning that the infection is cleared and the HBV infection dies out eventually. When $R_{CTL} \leq 1 < R_0$, the immune-free equilibrium point is globally stable, i.e., immune response would not be activated in this condition eventually. Further, the immune-activated equilibrium point is globally stable when $R_{CTL} > 1$, this indicates that the existence of CTL cells cannot eliminate all infected hepatocytes and viruses, however, it could reduce the amount of them. Numerical simulation of the model is performed. By the results in section 5.6, we obtain that with the conditions set as Theorem 5.5.2 - 5.5.6, our numerical solutions converge to infection-free, immune-free and immune-activated equilibrium points, respectively, confirming global stability of all equilibrium points. This supports the theoretical findings. Finally, different diffusions of virus and CTL are used to investigate the HBV dynamics. Our results demonstrate that the diffusion has no effect on the global dynamics of the HBV infection. These results match the results of Shaoli et al. [57], Bachraoui et al. [113], Yang et al. [114], and Manna and Chakrabarty [58]. Further, our results show that the greater diffusion coefficient of free virus and CTL cells would cause the density of free virus to reach equilibrium state slower. Overall, our model that includes the spatial diffusion of CTL cells has shown that the mobility of CTL cells would not affect the global dynamics of HBV infection.

CHAPTER VI

CONCLUSION

In this thesis, we presented three mathematical models to study the dynamics of hepatitis B virus (HBV) infection. There are 5 chapters in total. We introduced hepatitis B virus infection and the scope of the study in Chapter 1, whereas the theories and literature reviews are in Chapter 2. In Chapter 3 we propose relevant a model which expanded the work of Danane et al. [20] by incorporating a delay in the immune response activation, specifically the generation of cytotoxic T-lymphocytes (CTLs) denoted by τ_2. This delay model is represented by a system of delay differential equations (3.1.1)-(3.1.6) and contains six variables: uninfected hepatocytes $x(t)$, infected hepatocytes $y(t)$, intracellular HBV DNA-containing capsids $c(t)$, free viruses $v(t)$, antibodies $w(t)$, and CTLs $z(t)$. This model describes the hepatitis B virus (HBV) dynamics, considering both immune response dynamics and two drug therapies. The parameter u_1 represents drug therapy that prevents new infections, while u_2 represents drug therapy that inhibits the replication of viruses. We have analyzed the local and global stability for each equilibrium state, deriving conditions for stability in terms of the basic reproduction number R_0. Our numerical simulations demonstrate that both drug therapies significantly contribute to the reduction of overall HBV infection.

In Chapter 4, we extended the two-time delays model in Chapter 3 by incorporating a non-cytolytic cure process, which explains the recovery of infected hepatocytes to the uninfected state. We analyzed a sensitivity analysis of the parameters to identify the most effective strategies for reducing HBV infection, calculating the sensitivity indices of the basic reproduction number R_0. The analysis in section 4.6 demonstrates that increasing the values of the virus death rate (μ) and the rate of curing infected hepatocytes to the uninfected state (p), while simultaneously decreasing the parameters related to hepatocyte infection (β), intracellular capsid production rate (a), and virus growth rate, contributes to the reduction of Hepatitis B virus (HBV) infection. Additionally, we consider time-dependent drug effectiveness and optimal control problem. We verified

the existence of optimal control and employed Pontryagin's maximum principle for analysis. Numerical simulations demonstrate that the two effective control interventions can decrease the concentrations of intracellular HBV DNA-containing capsids, free viruses, cytotoxic T-lymphocytes, and infected hepatocytes. Furthermore, these control strategies contribute to slowing down the time of their epidemic peaks.

In Chapter 5, we studied the spread of Hepatitis B virus (HBV) infection within hepatocytes, considering the assumption that hepatocytes remain stationary while free viruses and cytotoxic T lymphocytes (CTLs) can move freely within the liver. We extended the work of Shaoli et al. in 2011 [57]. The model includes four variables: uninfected hepatocytes, infected hepatocytes, free viruses, and CTLs. In this model, we calculated the basic reproduction number (R_0) at the infection-free equilibrium and the average number of the CTLs immune cells (R_{CTL}) as conditions for analyzing the stability of local and global equilibria. Our results demonstrate that the greater diffusion coefficient of free virus and CTL cells would cause the density of free virus to reach equilibrium state slower. In conclusion, our model that includes the spatial diffusion of CTL cells has shown that the mobility of CTL cells would not affect the global dynamics of HBV infection.

In this thesis, we have not considered the possibility of a diffusive HBV model with delay. There is now a several of literature works on the delay and diffusion of HBV infection, as seen in the works by Wang et al. [43], Yang et al. [115], and Manna, K. [68]. However, these studies have not yet incorporated the diffusion of cytotoxic T lymphocytes (CTLs). Therefore, we are interested in addressing this element in future research works.

REFERENCES

REFERENCES

1. Ribeiro RM, Lo A, Perelson AS. Dynamics of hepatitis B virus infection. Microbes and Infection. 2002;4(8):829-35.

2. Hepatitis B [Internet]. 2020. [cited 2023 Nov 6].
Available from: http://www.who.int/mediacentre/factsheets/fs204/en/

3. Tsui LV, Guidotti LG, Ishikawa T, Chisari FV. Posttranscriptional clearance of hepatitis B virus RNA by cytotoxic T lymphocyte-activated hepatocytes. Proceedings of the National Academy of Sciences. 1995;92(26): 12398-402.

4. Guidotti LG, Ishikawa T, Hobbs MV, Matzke B, Schreiber R, Chisari FV. Intracellular inactivation of the hepatitis B virus by cytotoxic T lymphocytes. Immunity. 1996;4(1):25-36.

5. Guidotti LG, Chisari FV. To kill or to cure: options in host defense against viral infection. Current opinion in immunology. 1996;8(4):478-83.

6. Guidotti LG, Rochford R, Chung J, Shapiro M, Purcell R, Chisari FV. Viral clearance without destruction of infected cells during acute HBV infection. Science. 1999;284(5415):825-9.

7. Iannacone M, Sitia G, Guidotti LG. Pathogenetic and antiviral immune responses against hepatitis B virus. Future Virology. 2006;1(2):189–96.

8. Long C, Qi H, Huang SH. Mathematical Modeling of Cytotoxic Lymphocyte-Mediated Immune Response to Hepatitis B Virus Infection. Journal of Biomedicine and Biotechnology. 2008(2008):1–9.

9. Phillips SM, Chokshi S, Riva A, Evans A, Williams R, Naoumov NV. CD8+ T Cell Control of Hepatitis B Virus Replication: Direct Comparison between Cytolytic and Noncytolytic Functions. Journal of Immunology. 2009;184(1):287–95.

10. Chisari FV, Isogawa M, Wieland. SF. Pathogenesis of hepatitis B virus infection. Pathologie Biologie. 2010;58(4):258–66.

11. Busca A, Kumar A. Innate immune responses in hepatitis B virus (HBV) infection. Virology Journal. 2014;11(1).

12. Elaiw AM, Alshamrani NH. Global analysis for a delay-distributed viral infection model with antibodies and general nonlinear incidence rate. Journal of the Korea Society for Industrial and Applied Mathematics. 2014;18(4):317–35.

13. Wang Y, Zhou Y, Wu J, Heffernan J. Oscillatory viral dynamics in a delayed HIV pathogenesis model. Mathematical Biosciences. 2009;219(2): 104–12.

14. Wang S, Song X, Ge Z. Dynamics analysis of a delayed viral infection model with immune impairment. Applied Mathematical Modelling. 2011;35(10):4877–85.

15. Bairagi N, Adak D. Global analysis of HIV-1 dynamics with Hill type infection rate and intracellular delay. Applied Mathematical Modelling. 2014;38 (21-22):5047–66.

16. Guo B, Cai L. A note for the global stability of a delay differential equation of hepatitis B virus infection. Mathematical Biosciences and Engineering. 2011;8(3):689–94.

17. Song H, Jiang W, Liu S. Virus dynamics model with intracellular delays and immune response. Mathematical Biosciences and Engineering. 2015;12(1):185–208.

18. Adil Meskaf, Karam Allali, Tabit Y. Optimal control of a delayed hepatitis B viral infection model with cytotoxic T-lymphocyte and antibody responses. International Journal of Dynamics and Control. 2016;5(3):893–902.

19. Manna K, Chakrabarty SP. Global stability of one and two discrete delay models for chronic hepatitis B infection with HBV DNA-containing capsids. Computational and Applied Mathematics. 2017;36:525-36.

20. Danane J, Allali K. Mathematical analysis and treatment for a delayed hepatitis B viral infection model with the adaptive immune response and DNA-containing capsids. High-Throughput. 2018;7(4):35.

21. Bertoletti A, Maini MK, Ferrari C. The host–pathogen interaction during HBV infection: immunological controversies. Antiviral Therapy. 2010;15 (Suppl 3):15–24.

22. Hadziyannis SJ, Tassopoulos NC, Heathcote EJ, Chang T-T, Kitis G, Rizzetto M, et al. Adefovir dipivoxil for the treatment of hepatitis B e

antigen–negative chronic hepatitis B. New England Journal of Medicine. 2003;348(9):800–7.

23. Stein L, Loomba R. Drug targets in hepatitis B virus infection. Infectious Disorders–Drug Targets. 2009;9(2):105–16.

24. Hagiwara S, Nishida N, Kudo M. Antiviral therapy for chronic hepatitis B: combination of nucleoside analogs and interferon. World Journal of Hepatology. 2015;7(23):2427–31.

25. van den Berg F, Limani SW, Mnyandu N, Maepa MB, Ely A, Arbuthnot P. Advances with RNAi-Based Therapy for Hepatitis B Virus Infection. Viruses. 2020;12(8):851.

26. Nayagam JS, Cargill ZC, Agarwal K. The Role of RNA interference in functional cure strategies for chronic hepatitis B. Current Hepatology Reports. 2020;19(4):362–9.

27. De Clercq E, Férir G, Kaptein S, Neyts J. Antiviral treatment of chronic hepatitis B virus (HBV) infections. Viruses. 2010;2(6):1279–305.

28. Lau GK, Piratvisuth T, Luo KX, Marcellin P, Thongsawat S, Cooksley G, Gane E, Fried MW, Chow WC, Paik SW, Chang WY. Peginterferon Alfa-2a, lamivudine, and the combination for HBeAg-positive chronic hepatitis B. New England Journal of Medicine. 2005;352(26):2682-95.

29. Nowak MA, Bonhoeffer S, Hill AM, Boehme R, Thomas HC, McDade H. Viral dynamics in hepatitis B virus infection. Proceedings of the National Academy of Sciences. 1996;93(9):4398-402.

30. Goyal A, Ribeiro RM, Perelson AS. The role of infected cell proliferation in the clearance of acute HBV infection in humans. Viruses. 2017;9(11):350.

31. Ciupe SM, Ribeiro RM, Nelson PW, Dusheiko G, Perelson AS. The role of cells refractory to productive infection in acute hepatitis B viral dynamics. Proceedings of the National Academy of Sciences. 2007;104(12):5050-5.

32. Ciupe SM, Ribeiro RM, Nelson PW, Perelson AS. Modeling the mechanisms of acute hepatitis B virus infection. Journal of theoretical biology. 2007;247(1):23-35.

33. Hews S, Eikenberry S, Nagy JD, Kuang Y. Rich dynamics of a hepatitis B viral infection model with logistic hepatocyte growth. Journal of Mathematical Biology. 2010;60:573-90.

34. Yousfi N, Hattaf K, Tridane A. Modeling the adaptive immune response in HBV infection. Journal of mathematical biology. 2011;63:933-57.

35. Elaiw AM, Almuallem NA. Global properties of delayed-HIV dynamics models with differential drug efficacy in cocirculating target cells. Applied Mathematics and Computation. 2015;265:1067-89.

36. Mboya K, Makinde DO, Massawe ES. Cytotoxic cells and control strategies are effective in reducing the HBV infection through a mathematical modelling. International Journal of Prevention and Treatment. 2015;4(3):48-57.

37. Tridane A, Hattaf K, Yafia R, Rihan FA. Mathematical modeling of HBV with the antiviral therapy for the immunocompromised patients. Commun. Math. Biol. Neurosci. 2016.

38. Yosyingyong P, Viriyapong R. Global stability and optimal control for a hepatitis B virus infection model with immune response and drug therapy. Journal of Applied Mathematics and Computing. 2019;60:537-65.

39. Lewin SR, Ribeiro RM, Walters T, Lau GK, Bowden S, Locarnini S, Perelson AS. Analysis of hepatitis B viral load decline under potent therapy: complex decay profiles observed. Hepatology. 2001;34(5):1012-20.

40. Eikenberry S, Hews S, Nagy JD, Kuang Y. The dynamics of a delay model of hepatitis B virus infection with logistic hepatocyte growth. Mathematical Biosciences and Engineering. 2009;6(2):283-99.

41. Gourley SA, Kuang Y, Nagy JD. Dynamics of a delay differential equation model of hepatitis B virus infection. Journal of Biological Dynamics. 2008;2(2):140-53.

42. Xie Q, Huang D, Zhang S, Cao J. Analysis of a viral infection model with delayed immune response. Applied Mathematical Modelling. 2010;34(9): 2388-95.

43. Wang K, Wang W, Song S. Dynamics of an HBV model with diffusion and delay. Journal of Theoretical Biology. 2008;253(1):36-44.

44. Fisicaro P, Valdatta C, Boni C, Massari M, Mori C, Zerbini A, Orlandini A, Sacchelli L, Missale G, Ferrari C. Early kinetics of innate and adaptive immune responses during hepatitis B virus infection. Gut. 2009;58(7): 974–82.

45. Sun D, Liu F. Analysis of a new delayed HBV model with exposed state and immune response to infected cells and viruses. BioMed Research International. 2017; 2017:7805675.

46. Manna K, Chakrabarty SP. Chronic hepatitis B infection and HBV DNA-containing capsids: modeling and analysis. Communications in Nonlinear Science and Numerical Simulation. 2015;22(1-3):383-95.

47. Guo T, Liu H, Xu C, Yan F. Global stability of a diffusive and delayed HBV infection model with HBV DNA-containing capsids and general incidence rate. Discrete and Continuous Dynamical Systems-B. 2018;23(10):4223-42.

48. Aniji M, Kavitha N, Balamuralitharan S. Mathematical modeling of hepatitis B virus infection for antiviral therapy using LHAM. Advances in Difference Equations. 2020;2020(1):408.

49. Allali K, Meskaf A, Tridane A. Mathematical modeling of the adaptive immune responses in the early stage of the HBV infection. International Journal of Differential Equations. 2018;2018:1-3.

50. Hattaf K, Rachik M, Saadi S, Yousfi N. Optimal control of treatment in a basic virus infection model. Applied Mathematical Sciences. 2009;3(17-20): 949-58.

51. Manna K, Chakrabarty SP. Combination therapy of pegylated interferon and lamivudine and optimal controls for chronic hepatitis B infection. International Journal of Dynamics and Control. 2018;6:354-68.

52. Forde J, Ciupe S, Cintron-Arias A, Lenhart S. Optimal control of drug therapy in a hepatitis B model. Applied Sciences. 2016;6(8):219.

53. Danane J, Meskaf A, Allali K. Optimal control of a delayed hepatitis B viral infection model with HBV DNA-containing capsids and CTL immune response. Optimal Control Applications and Methods. 2018;39(3):1262–72.

54. Meskaf A. Optimal control of a delayed hepatitis b viral infection model with dna-containing capsids, the adaptive immune response and cure rate. Int. J. Open Problems Compt. Math. 2019;12(3).

55. Khatun MS, Biswas MH. Optimal control strategies for preventing hepatitis B infection and reducing chronic liver cirrhosis incidence. Infectious Disease Modelling. 2020;5:91-110.

56. Wang K, Wang W, Pang H, Liu X. Complex dynamic behavior in a viral model with delayed immune response. Physica D: Nonlinear Phenomena. 2007;226(2):197-208.

57. Wang S, Feng X, He Y. Global asymptotical properties for a diffused HBV infection model with CTL immune response and nonlinear incidence. Acta Mathematica Scientia. 2011;31(5):1959–67.

58. Manna K, Chakrabarty SP. Global stability and a non-standard finite difference scheme for a diffusion driven HBV model with capsids. Journal of Difference Equations and Applications. 2015;21(10):918-33.

59. Elaiw AM, Al Agha AD. Global dynamics of a general diffusive HBV infection model with capsids and adaptive immune response. Advances in Difference Equations. 2019;2019(1):1-31.

60. Huang KS, Shyu YC, Lin CL, Wang FB. Mathematical analysis of an HBV model with antibody and spatial heterogeneity. Math. Biosci. Eng. 2019;17(2):1820-37.

61. Elaiw AM, AlShamrani NH. Analysis of an HTLV/HIV dual infection model with diffusion. Mathematical Biosciences and Engineering. 2021;18(6):9430-73.

62. AlShamrani NH, Elaiw A, Raezah AA, Hattaf K. Global dynamics of a diffusive within-host HTLV/HIV co-Infection model with latency. Mathematics. 2023;11(6):1523.

63. Xu R, Ma Z. An HBV model with diffusion and time delay. Journal of Theoretical Biology. 2009;257(3):499-509.

64. Chan Chí N, AvilaVales E, García Almeida G. Analysis of a HBV model with diffusion and time delay. Journal of Applied Mathematics. 2012.

65. Zhang Y, Xu Z. Dynamics of a diffusive HBV model with delayed Beddington–DeAngelis response. Nonlinear Analysis: Real World Applications. 2014;15:118-39.

66. Hattaf K, Yousfi N. A generalized HBV model with diffusion and two delays. Computers & Mathematics with Applications. 2015;69(1):31-40.

67. Manna K, Hattaf K. Spatiotemporal dynamics of a generalized HBV infection model with capsids and adaptive immunity. International Journal of Applied and Computational Mathematics. 2019;5(3):65.

68. Manna K. Dynamics of a delayed diffusive HBV Infection model with capsids and CTL immune response. International Journal of Applied and Computational Mathematics. 2018;4(5).

69. Lepschy A, Mian GA, Viaro U. A stability test for continuous systems. Systems & control letters. 1988;10(3):175-9.

70. Hu H, Wang Z, Schaechter DB. Dynamics of controlled mechanical systems with delayed feedback. Appl. Mech. Rev. 2003;56(3):B37.

71. Kuang Y, editor. Delay differential equations: with applications in population dynamics. United States:Academic press; 1993.

72. Marshall JE. Time-delay systems: stability and performance criteria with applications. New York: E. Horwood; 1992.

73. Van, Watmough J. Reproduction numbers and sub-threshold endemic equilibria for compartmental models of disease transmission. Mathematical biosciences. 2002;180:29–48.

74. Samsuzzoha MD, Singh M, Lucy D. Uncertainty and sensitivity analysis of the basic reproduction number of a vaccinated epidemic model of influenza. Applied Mathematical Modelling. 2013;37(3):903-15.

75. Ngoteya FN, Gyekye YN. Sensitivity analysis of parameters in a competition model. Appl. Comput. Math. 2015;4(5):363-408.

76. Luenberger DG. Introduction to dynamic systems. New York: John Wiley & Sons; 1979.

77. Lenhart S, Workman JT. Optimal control applied to biological models. New York: Chapman and Hall/CRC; 2007.

78. Pontryagin LS. Mathematical theory of optimal processes. Abingdon-on-Thames: Routledge; 2018.

79. Zhuang K. Dynamical analysis of a delayed hepatitis B virus model with immune responses. WSEAS Transactions on Mathematics. 2016;15:325-34.

80. Manna K, Hattaf K. Spatiotemporal dynamics of a generalized HBV infection model with capsids and adaptive immunity. International Journal of Applied and Computational Mathematics. 2019;5(3):65.

81. Harroudi S, Meskaf A, Allali K. Modelling the adaptive immune response in HBV infection model with HBV DNA-containing capsids. Differential Equations and Dynamical Systems. 2020:1-23.

82. Birkhoff G, Rota GC. Ordinary differential equations. 4th ed. New York: John Wiley & Sons; 1989.

83. Driver RD. Ordinary and delay differential equations. New York: Springer-Verlag; 1977.

84. Anton H, Rorres C, Kaul A. Elementary linear algebra : applications version. Hoboken, Nj: Wiley; 2019.

85. Fleming WH, Rishel RW. Deterministic and stochastic optimal control. New York: Springer Science & Business Media; 2012.

86. Cesari L. Existence theorems for weak and usual optimal solutions in Lagrange problems with unilateral constraints. I. Transactions of the American Mathematical Society. 1966;124(3):369-412.

87. Kharatishvili GL. Maximum principle in the theory of optimum time-delay processes. Moscow: Russian Academy of Sciences; 1961.

88. Göllmann L, Maurer H. Theory and applications of optimal control problems with multiple time-delays. Journal of Industrial & Management Optimization. 2014;10(2).

89. Ibrahim F, Hattaf K, Rihan FA, Turek S. Numerical method based on extended one-step schemes for optimal control problem with time-lags. International Journal of Dynamics and Control. 2017;5(4):1172-81.

90. Podlubny I. Fractional differential equations: an introduction to fractional derivatives, fractional differential equations, to methods of their solution and some of their applications. Elsevier; 1998.

91. Hilfer R, editor. Applications of fractional calculus in physics. Singapore: World scientific; 2000.

92. Kilbas AA, Srivastava HM, Trujillo JJ. Theory and applications of fractional differential equations. Elsevier; 2006.

93. Petráš I. Fractional-order nonlinear systems: modeling, analysis and simulation. Heidelberg: Springer Science & Business Media; 2011.

94. Kisela T. Fractional differential equations and their applications. Faculty of Mechanical Engineering Institute of Mathematics. 2008.

95. Caputo M. Linear models of dissipation whose Q is almost frequency independent—II. Geophysical Journal International. 1967;13(5):529-39.

96. Kilbas AA. Hadamard-type fractional calculus. J. Korean Math. Soc. 2001;38(6):1191-204.

97. Katugampola UN. A new approach to generalized fractional derivatives. arXiv preprint arXiv:1106.0965. 2011.

98. Caputo M, Fabrizio M. A new definition of fractional derivative without singular kernel. Progress in Fractional Differentiation & Applications. 2015;1(2):73-85.

99. 107.Atangana A, Baleanu D. New fractional derivatives with nonlocal and non-singular kernel: Theory and application to heat transfer model. Thermal Science. 2016;20(2):763–809.

100. Atangana A, Gómez-Aguilar JF. A new derivative with normal distribution kernel: Theory, methods and applications. Physica A: Statistical mechanics and its applications. 2017;476:1-4.

101. Hattaf K. On the stability and numerical scheme of fractional differential equations with application to biology. Computation. 2022;10(6):97.

102. Hattaf K. A new class of generalized fractal and fractal-fractional derivatives with non-singular kernels. Fractal and Fractional. 2023;7(5):395.

103. Bachraoui M, Hattaf K, Yousfi N. Qualitative analysis of a fractional model for HBV infection with capsids and adaptive immunity. International Journal of Dynamical Systems and Differential Equations. 2022;12(2):146-62.

104. Wang W, Ma W. Global dynamics of a reaction and diffusion model for an HTLV-I infection with mitotic division of actively infected cells. J. Appl. Anal. Comput. 2017;7(3):899-930.

105. Travis CC, Webb G. Existence and stability for partial functional differential equations. Transactions of the American Mathematical Society. 1974;200:395-418.

106. Fitzgibbon WE. Semilinear functional differential equations in Banach space. Journal of Differential Equations. 1978;29(1):1-4.

107. Martin RH, Smith HL. Abstract functional-differential equations and reaction-diffusion systems. Transactions of the American Mathematical Society. 1990;321(1):1-44.

108. Smith H, Martin R. Reaction-diffusion systems with time delays: monotonicity, invariance, comparison and convergence. Journal für die reine und angewandte Mathematik. 1991;1991(413):1-35.

109. Wu J. Theory and applications of partial functional differential equations. New York: Springer Science & Business Media; 1996.

110. Zhou X, Song X, Shi X. A differential equation model of HIV infection of CD4+ T-cells with cure rate. Journal of Mathematical Analysis and Applications. 2008;342(2):1342-55.

111. Ciupe SM, Ribeiro RM, Perelson AS. Antibody responses during hepatitis B viral infection. PLoS computational biology. 2014;10(7):e1003730.

112. Ahmed R, Gray D. Immunological memory and protective immunity: understanding their relation. Science. 1996;272(5258):54-60.

113. Bachraoui M, Ichou MA, Hattaf K, Yousfi N. Spatiotemporal dynamics of a fractional model for hepatitis B virus infection with cellular immunity. Mathematical Modelling of Natural Phenomena. 2021;16.

114. Yang J, Zheng F, Wang X, Li X. An hbv model with diffusion and age of infection. Asian-European Journal of Mathematics. 2010;3(4):731-9.

115. Yang Y, Xu Y. Global stability of a diffusive and delayed virus dynamics model with Beddington–DeAngelis incidence function and CTL immune response. Computers & Mathematics with Applications. 2016;71(4): 922-30.